IDENTIFYING PATHOGENIC EPITOPES AND AUTOREACTIVE CELLS IN ANCA VASCULITIS

Katherine G. Stember

A dissertation submitted to the faculty at the University of North Carolina at Chapel Hill in partial fulfillment of the requirements for the degree of Doctor in Philosophy in Pathobiology and Translational Science in the Department of Pathology and Laboratory Medicine in the School of Medicine.

Chapel Hill
2018

Approved by:

Maureen A. Su

Ronald J. Falk

J. Charles Jennette

Donald N. Cook

Meghan E. Free

ABSTRACT

Katherine G. Stember: Identifying Pathogenic Epitopes and Autoreactive Cells in ANCA Vasculitis
(Under the direction of Ronald J. Falk)

This dissertation is focused on the interaction between the humoral (B cell) and cellular (T cell) arms of the adaptive immune system, and known autoantigens in patients with anti-neutrophil cytoplasmic autoantibody (ANCA) vasculitis. ANCA vasculitis is characterized by vascular inflammation that leads to organ damage. Current treatment involves medications designed to induce disease remission, but many patients suffer from side effects including severe infection. We hypothesized that elucidating specific interactions between autoreactive lymphocytes and known autoantigens in patients would reveal targets for novel therapies that could halt the autoimmune response without side effects.

In Chapter 1, I use high-resolution human leukocyte antigen (HLA) typing to identify alleles prevalent in our patients and demonstrate using Kaplan Meier estimates that carriage of HLA-DPB1*04:01 does not increase risk of relapse, contrary to previous results (*1*). Based on our independent serotype analysis, we hypothesize that carriage of HLA-DPB1*04:01 is a risk factor for patients with PR3-ANCA vasculitis (not MPO-ANCA vasculitis). Also addressed are significant differences between patients with MPO- and PR3-ANCA vasculitis, to clarify the rationale for focusing exclusively on MPO-ANCA vasculitis for the remainder of this dissertation.

Chapter 2 focuses on potentially immunopathogenic regions of MPO. Patient autoantibody reactivity was assessed by enzyme-linked immunosorbent assay (ELISA) and anti-

$MPO_{447\text{-}461}$ antibodies were detected in 53% of patients. Epitopes were characterized using alanine scanning, circular dichroism, and solvent exposure experiments. Finally, *in silico* and *in vitro* binding studies confirmed the ability of MPO epitopes to bind patient HLA.

In Chapter 3, I assess patient $CD4^+$ T cell recognition of MPO epitopes. MHC II tetramers were created with patient HLA alleles and MPO epitopes, and used to stain patient cells. Patients demonstrated specific $CD4^+CD25^{intermediate}$ T cell binding to tetramers and these cells secreted the pro-inflammatory cytokine IL-17A. TCR sequencing studies revealed clonally expanded autoreactive cells compared to controls, and some public TCR clones. Elucidation of these specific immune interactions will allow for new antigen-specific treatments using a variety of emerging techniques including chimeric antigen receptor (CAR) T cells, tolerogenic dendritic cells (DC), nanoparticle presentation of antigens, gene therapy, or removal of pathogenic T cells by apheresis.

To all of the women and people of color
who have been excluded from the scientific enterprise for generations
because of their identities and despite their capabilities,
and to those who have made it, and been discriminated against from within
I will never stop fighting for equality and inclusivity in science.

ACKNOWLEDGEMENTS

In 2002 at a Defense Department briefing, Donald Rumsfeld stated that “There are known knowns. There are things we know that we know. There are known unknowns. That is to say, there are things that we now know we don't know. But there are also unknown unknowns. There are things we do not know we don't know.” I’ve found that what I love so much about being a scientist and creating new knowledge is that we are able to pursue both the known unknowns (the only way to get a grant funded these days), and the unknown unknowns through our failures in pursuit of the known unknowns. I think the most important lesson I have learned during my time in graduate school is how to fail repeatedly, thoroughly, dramatically, and somehow muster the courage to come back and try again the next day. It is in these failures that we learn what to do next, because each wrong path narrows it down to the correct one. Even beyond that, sometimes our failures reveal those unknown unknowns because there is another explanation for our failure that we had not considered yet. Despite extensive practice, I continue to struggle with failure, so I would be remiss not to mention the many people who have helped to pick me up and dust me off so that I could try again. To all of you, I am eternally grateful.

First and most importantly, this body of work would not exist without numerous scientific mentors and collaborators. To Dr. Ron Falk, who agreed to take in an ambitious young student determined to finish a PhD in four years, despite knowing that she had no concept of the struggle and discomfort accomplishing that goal would require, thank you. Thank you for forgiving my missteps and for always giving me the advice I did not fully appreciate at the time, but now realize was exactly what I needed to hear. To Dr. Meghan Free, thank you for showing

me the heights a young female scientist can reach if she puts her mind to it. You are a brilliant, accomplished scientist and I have been lucky to learn from you and work alongside you over the last four years. To Dr. Dominic Ciavatta, thank you for your patience with my often-limited understanding of the complicated sequencing methods we used for these experiments. Your constant kindness, despite repeated questions and late Thursday nights in the lab, was not overlooked; in fact, it often got me through. To Dr. Donna Bunch, thank you for always putting aside the more important things you could have been doing to make time for me whenever I asked. Thank you especially for sharing in both my celebrations and frustrations over the years. To Dr. Susan Hogan, thank you for being a friend, a sounding board, and a mentor, in addition to being the rock star statistician every scientist wishes they had easy access to. To Dr. Charles Jennette, thank you for always reminding me to look at the cells, and to question everything I think I know if there is a piece of evidence that doesn't fit the current story. I cannot imagine a person to better complement Dr. Falk or co-advise the Falk lab. To Dr. Maureen Su, thank you for taking time out of your impossibly busy schedule to be my committee chair and a personal mentor when I needed advice on various graduate student challenges. To Dr. Jon Homeister, thank you for being a DGS who goes above and beyond for his students, exemplified by the time you personally escorted me to Campus Health Services during student seminar. To Dr. Don Cook, thank you for agreeing to be a member of my thesis committee and a mentor. Your intellectual contributions to this work are greatly appreciated. To Dr. James Meigs, who gave me a chance and started my research career, and to Dr. Susan Slaugenhaupt who helped me grow into a scientist worthy of graduate school, thank you. Finally, to Beka Layton, Josh Hall, Ashalla Freeman, Jeff Steinbach, Patrick Brandt and all of the other amazingly supportive staff in the

Office of Graduate Education, thank you for the numerous professional development opportunities and personal support in all of my endeavors.

Being a member of the Falk lab has given me the opportunity to be part of an incredible team of people who are working tirelessly toward new cures for patients with ANCA vasculitis and other kidney diseases. I consider myself lucky to have worked alongside every one of you. To Candace Henderson, this document would not exist without your constant dedication to getting me the samples I needed for these crazy experiments. To Yichun Hu, this document similarly would not exist without all of your hard work compiling and analyzing the data that was beyond my statistical analysis skills. To Caroline Poulton and Lauren Blazek, thank you for always answering my frantic emails with whatever patient demographic data I needed pulled, and for working with me to figure out the nuances of our patient cohort. To Dr. Britta Jones, thank you for your experimental support/advice and for demystifying the dissertation by willingly answering my seemingly endless questions about the process. To Jacob Hess and Andrew Le, thank you for being my lab-bay buddies, which meant entertaining me when I wanted to be social and working quietly when I was trying to focus. You guys are the best lab neighbors I could have asked for. Thank you to Carmen Mendoza and Liz McInnis for always asking how my projects were going or if there was anything you could do to help, and for always showing me where to find hidden lab supplies during my panicked searches. To Karen Apperson, thank you for your friendship, the lunches, the laughs, and for always managing to squeeze me in to Dr. Falk's crazy schedule. Trina Pugh, Rochelle Moser, and Sheri Kremer – thank you for your constant willingness to assist me with everything from computer setup, to reimbursements, to paying my tuition with smiles on your faces. To everyone else, thank you for making me

laugh, for eating candy with me, and for discussing new exciting science with me during research journal club.

I would also like to acknowledge all of the scientists outside of my lab who helped with various parts of this work. To all of the staff at the UNC Flow Core, thank you for all of your support with the flow experiments. To Evan especially, thank you for never making me feel guilty for showing up 30 minutes late for my sort time (every time!), despite knowing you would have to stay 30 minutes later that day. Thank you to our collaborators Bjoern Peters, Simon Mallal, Eddie James, Ben Vincent, and Jon Serodi and all of the members of their labs who worked on this project for deciding it was worth doing and for doing it well.

Throughout the last four years, I have had the opportunity to participate in the UNC community outside of my research. Being a member of The Graduate and Professional Student Federation was a highlight of my time as a student. To Madelyn Percy and the rest of the incredible, talented, motivated students who I had the opportunity to work with – WE DID IT. Because of our hard work and dedication, graduate and professional students have a stronger voice than ever at this university and I am confident that the foundation we laid together is just the start of everything The GPSF will accomplish. I am grateful to have been a part of such a remarkable team of passionate people. To those of you writing a dissertation at some point in the future, I can assure you that the process is nothing compared to trying to write a new Constitution with stubborn undergraduates – you totally got this.

To my Yesteryears family, thank you for giving me a home away from home to meet up with good friends and drink good beer. I cherish the memories I have of our special place, and look forward to making many new memories at Vecino Brewing. To Rachel Dee, Jamie Byrnes, and Sravya Kattula (my Pathology family) thank you for supporting me from the very beginning.

Graduate school is HARD and having friends to commiserate with over classes, qualifying exams, and student seminar made it all that much easier to get through. I also want to thank Brenda Brock and Angel Truesdale for making sure I always had my ducks in a row. To Karissa Sciacca and Oyin Kolawole, I never could have dreamed that two random roommates freshman year of college would come to be the best friends a girl could ask for. Living across the country from the two of you has been challenging, but knowing that you are never more than a phone call or text away, ready to share advice and perspective on whatever disaster I find myself in, makes it slightly more bearable. I look forward to our days terrorizing a retirement home together, though I hope we will find a way to live closer before then.

To Fabio Urbina, I am exceedingly grateful for your friendship these last four years. Your ability to live with a type A, occasionally neurotic roommate is nothing short of extraordinary. Thank you for being a second parent to my ridiculous cats (that you helped pick out) and for going along with most of my crazy plans as though they were perfectly reasonable. We have had a lot of fun and consumed a lot of beer and I look forward to our future commune shenanigans. To Alex Guseman, I am not sure I have adequate words to thank you for loving me in the remarkably patient and kind way that you have over the years. You are an inspiring human being, a talented scientist, and I consider myself lucky to call you my partner. I know that you are going to do incredible things and I look forward to cheering you on in all of your future endeavors. To my cats, who have added stress and unconditional love in equal measure to my life over the last four years, I adore you and I can't imagine having it any other way.

None of this is possible without my family. I am blessed with an enormous family, so for brevity sake I will limit this section, but know that I am grateful to every single one of you for the support. To my three living grandparents, thank you for challenging me and cheering for me

always. Jules, every day you inspire me with your uncompromising commitment to being exactly who you are – no more and no less. Being true to yourself is a challenging thing to do in a society that is constantly making snap judgments about those who do not fit into boxes. You own your identity with such grace that I often find myself wishing I were more like you. Dad, your unwavering support of everything I have ever pursued has made it possible for me to take big risks, knowing you would be there to catch me no matter the outcome. You are kind and open in a way that I have not encountered much in my life, while also being strong and determined. I aspire to be more like you. Mom, you have worked unbelievably hard your entire life to ensure that Jules and I want for nothing, and it has not gone unnoticed. Despite our inability to communicate effectively sometimes, I am grateful to be so much like you. To me, being like you means being tenacious, motivated, and brave. Those characteristics are what got me to this point, completing my dissertation in just four short years.

I've heard it said
That people come into our lives
For a reason
Bringing something we must learn
And we are led to those
Who help us most to grow
If we let them
And we help them in return.
Well I don't know if I believe that's true
But I know I'm who I am today
Because I knew you.

- Steven Schwartz

Sincerely, thank you.

TABLE OF CONTENTS

LIST OF TABLES xv

LIST OF FIGURES xvi

LIST OF ABBREVIATIONS xviii

PROLOGUE: ADAPTIVE IMMUNITY IN AUTOIMMUNE DISEASE 1

ANCA Vasculitis Pathogenesis 3

Major Autoantigens in ANCA Vasculitis 5

Genetics of Autoimmunity and ANCA Vasculitis 6

B Cells and T Cells in Autoimmunity and ANCA Vasculitis 8

New Therapeutic Strategies 10

Central Hypothesis 12

CHAPTER 1: CARRIAGE OF HLA-DPB1*04:01 DOES NOT INCREASE RELAPSE RISK IN PATIENTS WITH ANCA-VASCULITIS 14

Introduction 14

Materials and Methods 15

Study Design 15

Patient Cohort 16

HLA Sequencing 16

Statistical Analysis 17

Results 18

HLA allele prevalence differs between MPO- and PR3-ANCA vasculitis 18

Homozygous carriers of HLA-DPB1*04:01 are white and most have PR3-ANCA vasculitis 19

Carriage of HLA-DPB1*04:01 Does Not Increase Relapse Risk in a Combined Cohort 20

Carriage of HLA-DPB1*04:01 May Influence Risk in Patients with PR3-ANCA Vasculitis 20

Discussion 24

CHAPTER 2: PATIENT ANCA AND HLA ALLELES BIND MPO EPITOPES 27

Introduction 27

Materials and Methods 28

Study Design 28

Patient Cohort 29

ELISA Studies 29

Alanine Scanning 30

Circular Dichroism 31

Solvent Exposure 31

In Silico Predictions 31

In Vitro Binding Studies 31

Statistical Analysis 32

Results 33

Patient ANCA bind $MPO_{447-461}$ most often at disease onset 33

$MPO_{447-461}$ is buried and $MPO_{435-454}$ is exposed to solvent 37

$Lysine_{448}$ and $Isoleucine_{456}$ are required for ANCA binding to $MPO_{447-461}$ 39

The alpha helix structure of $MPO_{447-461}$ is required for ANCA binding 40

Patient HLA alleles are predicted to bind regions of MPO 41

HLA-DPB1*04:01 and HLA-DRB4*01:01 bind $MPO_{447-461}$ and $MPO_{435-454}$ *in vitro* 42

Discussion 44

CHAPTER 3: AUTOREACTIVE $CD4^+$ T CELLS ARE PRO-INFLAMMATORY MEMORY CELLS THAT BIND MPO 47

Introduction 47

Materials and Methods 50

Patient Cohort 50

MHC II Tetramer Studies 53

Cytokine Capture for IL-17A 55

Flow Sorting 56

RNA Isolation 57

TCR Sequencing 57

Statistical Analysis 57

Results 58

MHC II tetramers identify patient autoreactive $CD4^+$ T cells 58

Autoreactive $CD4^+$ T cells are enriched for $CD25^{intermediate}$ memory effector cells 61

Autoreactive $CD4^+$ T cells secrete IL-17A 63

Autoreactive $CD4^+$ T cells are clonally restricted compared to controls 64

TCR sequencing reveals some public TCR clones 66

Discussion 69

Summary 71

EPILOGUE: RESTRICTED EPITOPE RECOGNITION IN PATIENTS WITH MPO-ANCA VASCULITIS 74

Future Directions 76

Conclusions 79

REFERENCES 80

LIST OF TABLES

Table 1.1 HLA allele prevalence in MPO-ANCA vasculitis. 18

Table 1.2 HLA allele prevalence in PR3-ANCA vasculitis. 19

Table 1.3. Cohort demographics by HLA-DPB1*04:01 carrier status. 21

Table 1.4. Characteristics of ANCA vasculitis cohort according to relapse status. 24

Table 2.1. Demographics summary for Patient ELISA cohort. 30

Table 2.2. Comparison of ELISA Study Patient Demographics by anti-$MPO_{447-461}$ reactivity. 35

Table 2.3. MPO epitopes and *in silico* predicted HLA binding partners. 42

Table 2.4. MPO epitopes and *in vitro* HLA binding partners. 43

Table 3.1. Demographics summary for tetramer studies cohort. 52

Table 3.2. Non-HLA-DPB1*04:01 alleles in tetramer studies cohort. 53

LIST OF FIGURES

Figure 1.1. Kaplan Meier curve of relapse by HLA-DBP1*04:01 carrier status..... 22

Figure 1.2. Kaplan Meier curves of relapse by HLA-DBP1*04:01 carrier status and ANCA serotype..... 23

Figure 2.1. Anti-$MPO_{447-461}$ autoantibody is detectable in 53% of patients by ELISA most often at onset..... 34

Figure 2.2. Anti-$MPO_{447-461}$ reactivity correlates with disease activity or disease onset in patients..... 36

Figure 2.3. Anti-$MPO_{447-461}$ reactivity to $MPO_{447-461}$ does not correlate with reactivity to whole MPO..... 37

Figure 2.4. $MPO_{435-461}$ is located on an alpha helix that is mostly buried within MPO..... 38

Figure 2.5. Sphere model demonstrating exposed portions of region $MPO_{435-459}$ based on crystal structure..... 39

Figure 2.6. Alanine scanning of $MPO_{447-461}$ reveals $Lysine_{448}$ or $Isoleucine_{456}$ are required for binding to patient ANCA..... 40

Figure 2.7. Circular dichroism experiments reveal loss of alpha helical structure with alanine substitutions at K_{448} or I_{456}..... 41

Figure 2.8. Human myeloperoxidase model based on crystal structure..... 45

Figure 3.1. Amino acid sequence alignment of mouse and human myeloperoxidase..... 53

Figure 3.2. Strategy for gating $tetramer^+$ $CD4^+$ lymphocytes..... 55

Figure 3.3. Gating strategy for IL-17A positivity..... 56

Figure 3.4. Patients demonstrate HLA and epitope specific tetramer recognition by $CD4^+$ T cells..... 59

Figure 3.5. Epitope specificity of Patient $CD4^+$ tetramer binding..... 60

Figure 3.6. Dual staining reveals dual binding ability of patient $CD4^+$ T cells..... 61

Figure 3.7. Patient $CD4^+$ T cells that bind tetramers are enriched for $CD25^{intermediate}$ cells..... 62

Figure 3.8. Patient $CD4^+$ T cells that bind tetramers are enriched for memory marker CD45RO..... 62

Figure 3.9. Patient $CD4^+$ T cells that bind tetramers are pro-inflammatory cells that secrete IL-17A. 63

Figure 3.10. Patient tetramer positive cells demonstrate decreased TCR diversity compared to controls. 65

Figure 3.11. Clonotype population comparison reveals $CD25^-$ naive and $CD25^{intermediate}$ memory T cell clones shared between two patients. 67

Figure 3.12. TRBV usage analysis reveals differences in TRBV-6 subunit usage between tetramer positive cells and control T cell populations. 68

Figure 3.13. TRBJ usage analysis reveals no differences in joining subunit usage between tetramer positive cells and control T cell populations. 69

Figure E.1. $MPO_{435-461}$ in relation to the active site of MPO. 74

LIST OF ABBREVIATIONS

Aire	autoimmune regulator (transcription factor)
ANCA	anti-neutrophil cytoplasmic autoantibody
APC	antigen presenting cell
AUC	area under the curve
AZA	azathioprine
BCR	B cell receptor
Bmem	memory B cell
Breg	regulatory B cell
BVAS	Birmingham vasculitis activity score
CAAR	chimeric autoantibody receptor
CAR	chimeric antigen receptor
CD	cluster of differentiation
CDR3	complementarity-determining region 3
CI	confidence interval
CLIP	class II-associated Ii peptide
cPR3	complementary proteinase 3
CPT	cell preparation tube
DB	database
DC	dendritic cell
DNA	deoxyribose nucleic acid
DPB1	DP beta 1
DRB1	D related beta 1
DRB4	D related beta 4
DSG3	desmoglein 3

d50	diversity 50 index
eGFR	estimated glomerular filtration rate
EGPA	eosinophilic granulomatosis with polyangiitis
ELISA	enzyme-linked immune-absorbent assay
FBS	fetal bovine serum
FDR	false discovery rate
GI	gastrointestinal
GMB	glomerular basement membrane
GFR	glomerular filtration rate
GPA	granulomatosis with polyangiitis
GWAS	genome wide association study
HC	healthy control
HLA	human leukocyte antigen
HLA-DM	human leukocyte antigen DM
HLA-DP	human leukocyte antigen DP
HLA-DR	human leukocyte antigen DR
Hom	homozygous
Hz	heterozygous
H3K27	histone H3 lysine 27 trimethylation
IBD	inflammatory bowel disease
IC50	inhibitor concentration where response is reduced by half
IFN-γ	interferon gamma
Ig	immunoglobulin
IL-2	interleukin 2
IL-4	interleukin 4

IL-17	interleukin 17
IMGT	ImMunoGeneTics information system
IQR	interquartile range
LPS	lipopolysaccharide
MALDI-TOF	matrix assisted laser desorption/ionization time-of-flight
MCP-1	monocyte chemoattractant protein 1
MHC	major histocompatibility receptor
MHC I	major histocompatibility receptor class I
MHC II	major histocompatibility receptor class II
MID	multiplex identifier
mL	mililiter
MMF	mycophenolate mofetil
MPA	microscopic polyangiitis
MPO	myeloperoxidase
MPO-ANCA	myeloperoxidase specific anti-neutrophil cytoplasmic autoantibodies
MS	multiple sclerosis
mTECs	medullary thymic epithelial cells
PBMCs	peripheral blood mononuclear cells
PBS	phosphate buffered saline
PCR	polymerase chain reaction
PDB	protein database
PDBID	protein database identification
PE	phycoerythrin
PECy5	phycoerythrin-cyanine 5 conjugate
PR3	proteinase 3

PR3-ANCA	proteinase 3 specific anti-neutrophil cytoplasmic autoantibodies
qPCR	quantitative polymerase chain reaction
RA	rheumatoid arthritis
Rag	recombination-activating gene
RNA	ribonucleic acid
RPMI	Roswell Park Memorial Institute medium
SD	standard deviation
SLE	systemic lupus erythymatosus
TCR	T cell receptor
TOF-MS	time-of-flight mass spectrometry
Th17	T helper 17 cells
TRB	T cell receptor beta
TRBJ	T cell receptor beta joining
TRBV	T cell receptor beta variable
TReg	regulatory T cell
T1D	type 1 diabetes
UNC	University of North Carolina

PROLOGUE: ADAPTIVE IMMUNITY IN AUTOIMMUNE DISEASE

Autoimmune diseases occur when the immune system misidentifies self as foreign and attacks, leading to inflammation and damage of healthy tissues. Since the 1950s when immune reactivity to self-proteins was first confirmed in patients with rheumatoid arthritis and later in systemic lupus erythematosus (*2, 3*), we have made enormous strides toward understanding the pathology of autoimmunity. However, many questions remain including the contributions of genetics vs. environment, why certain antigens are targeted by the immune system, and the pathogenic role of numerous immune cell subsets in these diseases. Most chronic diseases are determined by complex interactions between genetics and environmental influences (*4*), though the precise cause remains elusive.

Leading hypotheses include a role for both genetics and environment in autoimmune disease etiology. One hypothesis proposes that sequence similarity between infectious agents and self-proteins (molecular mimicry) leads to misidentification by the immune system, though identifying microbial and self-peptide pairs has proved challenging (*5*). Another hypothesis is based on the temporal correlation between decreased infectious disease (due to improved hygiene), and the rising incidence of autoimmune diseases. The "hygiene hypothesis" proposes that a lack of childhood exposure to infectious agents, microorganisms, and parasites causes allergy and autoimmunity. This hypothesis is strongly supported by epidemiological data, and specific T cell responses (T helper 1 and T helper 2) have been implicated, though the underlying mechanisms remain unclear (*6*). In contradiction to the hygiene hypothesis is the "old friends" hypothesis that implicates the microbiome in allergy and autoimmunity, and suggests the need

for early exposure to a range of "friendly" microbes, not infectious pathogens to train the immune system (*7*). Diet, sanitation, antibiotic use, and parasite infection have been shown to alter human microbe exposure, and changes to these factors correlate with the rise in autoimmune prevalence. Epigenetic dysregulation has also been proposed as an explanation for autoimmunity because loss of epigenetic homeostasis leads to aberrant gene expression and immune dysfunction (*8*). Finally, it has been proposed that glycans in the immune system discriminate self from non-self and that altered glycosylation may explain autoimmunity, though analysis of the glycome has proven technically difficult (*9*).

Autoimmune diseases have a significant impact on the United States in terms of individuals affected and healthcare costs. The National Institutes of Health estimates that 25-50 million Americans suffer from more than one hundred distinct autoimmune diseases, costing nearly $100 billion in direct healthcare costs (*10*). Current treatments target the whole immune system, inflammation, or total T cell or B cell populations, rather than using antigen specific approaches to the immune response (*11*). Although existing treatments can be effective, autoimmune disease carries an extremely high cost to society including decreased quality of life, co-morbidities including depression and anxiety, lost productivity, and familial disruption due to the increased risk for women of childbearing age (*12*). Additionally, side effects of these medications include life-threatening opportunistic infections, long-term risk of malignancy, osteoporosis, diabetes mellitus, and cardiovascular disease (*13*, *14*). Considering that the incidence of autoimmune disease is increasing over time (*15*), patients affected by these devastating diseases desperately need new, more effective treatments.

This dissertation focuses on a group of autoimmune diseases collectively called ANCA vasculitis. A 2015 epidemiological report estimates the annual incidence at approximately 46-

184/million with peak onset between 55 and 75 years of age (*16*). Though rare, this disease has been investigated for more than thirty years, and therapeutic breakthroughs for ANCA vasculitis may be adapted for efficacy in other autoimmune diseases. Additionally, ANCA vasculitis research has the advantage of exquisite autoantigen specificity compared to other autoimmune diseases. While type 1 diabetes (T1D), multiple sclerosis (MS), rheumatoid arthritis (RA), and systemic lupus erythematosus (SLE) have four or more identified autoantigens (*17*), most patients with ANCA vasculitis have autoantibody reactivity to one main autoantigen, MPO or PR3. This autoantigen specificity facilitates development of antigen-specific immunotherapy with increased probability of success compared to the other diseases.

ANCA Vasculitis Pathogenesis

Per the 2012 Chapel Hill Consensus Conference, ANCA vasculitis describes necrotizing small-vessel (arteries, arterioles, venules, veins) vasculitis with few or no immune deposits and the presence of myeloperoxidase specific anti-neutrophil cytoplasmic autoantibodies (MPO-ANCA) or proteinase 3 specific anti-neutrophil cytoplasmic autoantibodies (PR3-ANCA) (*18*). These vasculitides are sub-classified into microscopic polyangiitis (MPA), granulomatosis with polyangiitis (GPA; formerly Wegener's granulomatosis), and eosinophilic granulomatosis with polyangiitis (EGPA; formerly Churg-Strauss syndrome), (*19*). Depending on the location and severity, this blood vessel damage can lead to pulmonary hemorrhage, kidney glomerulonephritis, and eventually kidney failure, among many other symptoms (*20*). Untreated, patients with ANCA vasculitis develop severe organ damage most often in the lungs and/or kidneys (*20*). Even with existing therapies, patients are at serious risk for complications from disease relapse (*21*), the immunosuppressive therapy itself (*22*), and comorbidities including cardiovascular disease (*23*), diabetes, and malignancy (*24*). Consistent with other autoimmune diseases, the etiology and pathogenesis of ANCA vasculitis are influenced by a combination of

genetic factors and environmental exposures including infection, which also determine the characteristics of the innate and adaptive immune system for each patient.

The vascular inflammation that is characteristic of ANCA vasculitis stems from inappropriate monocyte and neutrophil activation by patient ANCA binding to antigens such as MPO and PR3 at the surface of primed neutrophils (*25*, *26*). Although the origin of the ANCA autoimmune response remains unclear, we know that ANCA are predominantly immunoglobulin G (IgG) autoantibodies secreted by plasma cells after their precursor B cells receive T cell help (*27*, *28*). In the active injury phase, ANCA activated neutrophils degranulate, releasing toxic reactive oxygen species, enzymes, and factors that activate the complement system (*26*, *29*). This begins an inflammatory amplification loop that results in destructive necrotizing lesions and endothelial injury (*26*, *30*-*32*). In the next response-to-injury phase, neutrophil induced damage attracts monocytes that transform into macrophages and recruit T cells, ultimately leading to granulomatous inflammation (*29*, *33*). Monocytes can also be activated directly by ANCA and produce cytokines including interleukin 8 (IL-8) and monocyte chemoattractant protein 1 (MCP-1) that further recruit and activate immune system players (*34*-*36*). The consequence of this process is acute necrotizing injury to the vessel wall that either resolves or, in the case of severe injury or repeat antigen exposure, progresses to fibrosis and sclerosis of blood vessels (*33*). In patients with ANCA vasculitis, this pathogenic process occurs asynchronously in multiple organs, with each cycle taking approximately one to two weeks (*29*).

ANCA vasculitis can also be sub-classified based on autoantibody reactivity to target autoantigens MPO or PR3 (*37*, *38*). ANCA binding to either of these self-antigens on circulating neutrophils and monocytes leads to blood vessel inflammation and damage as described above (*39*-*42*). It has been demonstrated that B cell secretion of ANCA induces

vascular damage, but autoantibody titers do not always correlate with disease activity (*43*), some healthy controls harbor naturally occurring anti-MPO antibodies (*44*), and some patients with identical disease symptoms do not have detectable levels of circulating ANCA (*45*). It follows that there must be additional immune dysfunction beyond the presence of autoreactive B cells and ANCA to fully explain onset and pathogenesis of disease in ANCA vasculitis. Possible explanations include T cell dysregulation, epitope specificity, avidity of the autoreactive cells, and/or dysregulation of antigen expressing cells.

Major Autoantigens in ANCA Vasculitis

The two major target antigens in patients with ANCA vasculitis are MPO and PR3. Currently, IgG reactivity to MPO or PR3 measured by ELISA is the gold standard for diagnosing ANCA vasculitis (*46, 47*). Historically, ANCA vasculitis has also been diagnosed using an indirect immunofluorescence assay (*46*). It remains unclear which specific regions of these autoantigens are being targeted by the immune system in patients, though this information is important because it may reveal information about disease etiology. If the molecular mimicry hypothesis is correct, regions of the autoantigen identified by the immune system may share significant homology with a known pathogen and implicate that pathogen in disease onset. Additionally, knowledge of antigenic MPO and PR3 epitopes will inform the development of new immunotherapies, through re-introduction of immune tolerance to the epitopes.

MPO is a peroxidase enzyme with antimicrobial properties synthesized in both neutrophils and monocytes and stored in granules and lysosomes respectively. MPO is released into the extracellular space during neutrophil degranulation (*48*). Myeloperoxidase is both microbicidal and damaging to normal tissue upon release, which implicates MPO in disease pathogenesis. Numerous studies have investigated epitope specificity of the autoimmune response to MPO using patient samples, mouse models of disease, and some *in vitro* models (*49-*

56). PR3 is a serine protease enzyme with antimicrobial properties that is also expressed in neutrophil granulocytes. Previous work in our lab showed that patients have ANCA that bind not only to PR3 epitopes, but also to complementary PR3 (cPR3) (*57*). This finding is explained by the autoantigen complementarity theory that proposes the inciting antigen is not the self-antigen or a mimic, but a protein with complementary structure to the autoantigen (*58*). This finding was confirmed by another group who showed minimal patient PBMC response to PR3 peptide and a clear T cell response to the cPR3 peptide that was not present in healthy controls or with control peptide (*59*).

One possible explanation for ANCA reactivity to MPO and PR3 is aberrant expression in patient neutrophils and therefore increased antigen availability. Indeed, studies have shown that both MPO and PR3, normally silenced in healthy controls, are expressed in mature neutrophils of ANCA patients (*60, 61*). Further investigation revealed that this dysregulation may be due to perturbed gene silencing, specifically via depleted chromatin modification histone H3 lysine 27 trimethylation (H3K27) at both MPO- and PR3-encoding genes (*62, 63*). Recently, our group reported hypomethylation of genes that encode MPO and PR3 and increased autoantigen expression in patients with active disease (*64*). Additionally, increased deoxyribose nucleic acid (DNA) methylation at a specific CpG within PRTN3 (the gene that encodes PR3) was a predictor of sustained remission independent of serotype. Although the trigger for failed epigenetic gene silencing of MPO and PR3 remains unknown, these results implicate aberrant autoantigen expression in the pathogenesis and potentially onset of disease.

Genetics of Autoimmunity and ANCA Vasculitis

Genome wide association (GWAS) studies have implicated genetics in autoimmune disease by repeatedly identifying variants in the region of the genome that encodes HLA. The identification of HLA as a genetic risk factor specifically implicates the adaptive arm of the

immune system in disease, because HLA genes encode MHC receptors that play a key role in antigen presentation to T cells. MHC molecules are split up into two classes, MHC class I (MHC I) and MHC class II (MHC II) that share a similar function in that they present peptides to CD8+ and $CD4^+$ T cells respectively (*65*). Generally, the presented peptides originate intracellularly for MHC I and exogenously for MHC II, however occasionally cross-presentation occurs; MHC I molecules presenting exogenous antigens, or MHC II molecules presenting degraded cytosolic proteins (*66, 67*). It is possible that MHC II molecules have access to intracellular antigen (MPO and PR3) peptides via macroautophagy, and therefore could present them to $CD4^+$ T cells (*68*).

In ANCA vasculitis specifically, GWAS studies have identified HLA-DP and HLA-DQ alleles that encode MHC II receptors (*59, 69, 70*). Additionally, HLA-DPB1*04:01 has been implicated in risk of relapse for ANCA vasculitis patients. For this reason, the T cell studies herein focus exclusively on $CD4^+$ T cells and their interaction with MHC II-peptide complexes. MHC II molecules are primarily expressed by DCs, macrophages, and B cells, are assembled in the endoplasmic reticulum, and are loaded with class II-associated Ii peptide (CLIP). In order to present antigen to $CD4^+$ T cells, HLA-DM facilitates exchange of the CLIP fragment for epitopes from proteins degraded in the endosomal pathway, and then the MHC molecule is transported to the plasma membrane (*71*).

GWAS studies in ANCA vasculitis have also revealed genetic associations with the SERPINA1 (the gene for α(1)-antitrypsin) and PTPN22 (the gene for protein tyrosine phosphatase, non-receptor type 22) loci, with PRTN3, and with a single SNP near SEMA6A (the gene for semaphorin 6A) (*59, 69, 70*). It is possible that any of these variants directly influence the pathogenesis of ANCA vasculitis, though the mechanisms and extent of this influence remain to be elucidated.

B Cells and T Cells in Autoimmunity and ANCA Vasculitis

The adaptive immune system consists of B and T lymphocytes (B and T cells) that identify and react to specific antigens (toxic or foreign molecules capable of inducing an immune response) via their surface antigen receptors called B cell receptors (BCR) and TCRs. BCRs and TCRs are encoded by random gene recombination: this process allows for broad recognition of extremely diverse pathogens, but occasionally results in the development of cells that recognize self-antigens (autoreactive cells). Rare autoreactive cells are usually controlled by intrinsic regulatory mechanisms, but there are documented cases where these safeguards fail and autoreactive cells persist (*72-74*).

Tolerance describes the ability of the immune system to distinguish self from non-self and can be categorized into central and peripheral tolerance. Central tolerance is determined in the thymus and bone marrow, where naïve T cells and B cells are presented self-antigens and deleted based on inappropriate responses to those self-antigens before release into the periphery (*108*). Peripheral tolerance mechanisms include anergy (lack of functional response), deletion (apoptosis), or suppression by regulatory cells (*109*). Autoimmune disease occurs with failure of both central and peripheral tolerance mechanisms, as autoreactive cells have been repeatedly identified in the periphery of healthy individuals (*110-113*).

One intrinsic mechanism regulates central T cell tolerance by determining the presentation of self-antigens to T cells during development in the thymus (*75*). Central T cell tolerance is mediated by the autoimmune regulator (Aire) transcription factor, which promotes promiscuous expression of self-antigens by medullary thymic epithelial cells (mTECs) (*76-79*). T cells that bind self-peptide MHC complexes with high-affinity are deleted in the thymus, preventing them from entering the periphery. However, some autoreactive cells escape this selection process and are managed by peripheral tolerance mechanisms including suppression by

naturally arising regulatory Tregs via a contact-dependent, cytokine-independent mechanism (*80*). One study looked specifically at Aire regulation of thymic MPO expression in mice and revealed that both Aire-dependent central deletion and regulatory T cell-mediated peripheral tolerance were important for establishing and maintaining tolerance to MPO (*81*). Mechanisms of autoreactive B cell regulation include deletion, receptor editing, and anergy induction (*74*).

TCRs interact with antigens presented in a specific manner by MHC receptors on antigen presenting cells (APCs). In contrast, BCRs are composed of immunoglobulin (Ig) molecules that directly acquire and react to antigens in their environment. Importantly, autoreactive B cells and T cells have been implicated in the pathogenesis of autoimmune diseases (*82*) including SLE (*83, 84*), T1D (*85, 86*), and RA (*87, 88*).

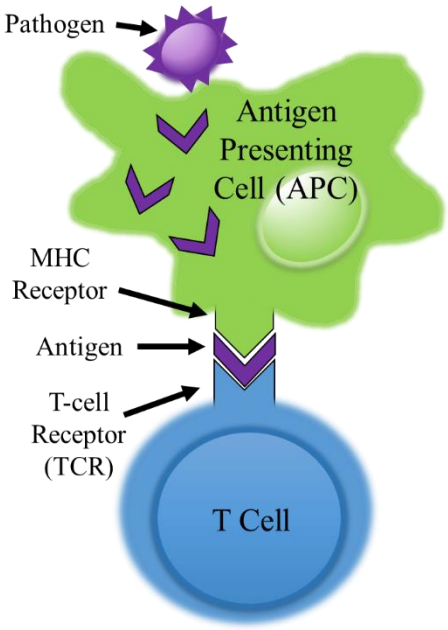

APCs present antigens to T cells to activate them via MHC receptor and T cell receptor interaction.

In ANCA vasculitis, B cells are implicated in disease pathogenesis by the presence of anti-MPO or anti-PR3 antibodies and by the ability of Rituximab (anti-B cell therapy) to ameliorate disease in patients (*89*). Our group demonstrated the importance of regulatory B cells (Bregs) by showing that after B cell depletion by Rituximab, patients on low maintenance immunosuppression who repopulated their CD5+ Bregs (*90*) with low or decreasing percentage had a shorter time to relapse compared to patients with normalized CD5+ B cells or higher immunosuppression (*91*). Additionally, we showed that in active disease CD5+ Bregs that produce anti-inflammatory cytokine IL-10 are decreased, and that the presence of more Bregs (as in disease remission)

correlates with decreased ANCA titer (*90*). Another group reported that peripheral B cells in patients with ANCA vasculitis display higher expression of CD38 and lower expression of CD5 during disease activity, compared to increased CD25 and CD86 expression in remission (*92*). Other B cell defects include a numerical deficiency of Bregs and a reduction of memory B cells (Bmem) during active disease (*93*). Additionally, mouse models of ANCA vasculitis have demonstrated that ANCA alone can cause disease (*41, 94*).

T cells have been implicated in ANCA vasculitis pathogenesis based on their presence at sites of inflammation (*95-98*), and the discovery that $CD4^+$ T cell help is required to produce ANCA (*99*). Reported T cell defects in patients include persistent $CD4^+$ T cell activation (*100-102*), dysfunctional regulatory T cells (*103-105*), and an expansion of a suppression resistant, proinflammatory, antigen experienced T cell population (*105*). Chapter 3 includes a detailed discussion of the existing literature describing T cell defects in ANCA vasculitis.

New Therapeutic Strategies

Despite the basic understanding that autoimmune diseases are caused by inappropriate adaptive immune responses to self-antigens, decades of extensive research, and development of new targeted therapies (ex. Rituximab), we are still unable to clinically predict who will enter stable remission off therapy or cure patients with these diseases (*106*). Currently the most effective therapies for patients with ANCA vasculitis and other autoimmune conditions are immunosuppressive agents that destroy entire populations of immune cells and put patients at high risk for severe complications (*107*). There is a dire need for antigen-specific therapies that halt autoimmune reactivity in patients without depleting the cells necessary to fight infection. As mentioned previously, ANCA vasculitis is a model disease for the development of new antigen-specific treatments due to the specificity of the autoimmune response (to MPO or PR3) compared to the numerous antigens that have been identified in other diseases.

Antigen-specific immunotherapy involves reintroducing immune tolerance that is lost in autoimmunity. Proposed methods to reintroduce tolerance are similar to allergen specific immunotherapies used to desensitize the immune system to allergens (*17*). One method involves nasal administration of antigen directly; another delivers antigenic epitopes bound to nanoparticles. Researchers have attempted to reintroduce lost immune tolerance in mouse models of numerous autoimmune conditions using both of these methods (*114-116*), and with nasal administration in type 1 diabetes patients (*117*) with varied success. If we can elucidate the specific interactions between autoreactive lymphocytes and the autoantigens in ANCA vasculitis, we may be able to harness these methods to reintroduce immune tolerance to MPO and PR3.

Another category of antigen-specific immunotherapy involves selectively deleting autoreactive cells, inducing anergy in those cells, or generating regulatory cells to suppress the autoimmune response. One of these methods involves designing CAR T cells with TCRs that target autoreactive cells. One group designed chimeric autoantibody receptor (CAAR) T cells to treat the autoimmune blistering disease pemphigus vulgaris. These CAAR-T cells exhibited cytotoxicity against autoreactive B cells expressing anti-DSG3 BCRs on their surface and specifically eliminated these cells *in vivo* (*118*). If a specific marker of autoreactivity for patient B and/or $CD4^+$ T cells can be identified in ANCA vasculitis, CAR T cells can be designed to selectively target cells with that marker. Alternatively, several methods have been developed to generate antigen specific regulatory T cells, which may be harnessed to replace the faulty Tregs in patients with ANCA vasculitis (*119*). One method modifies the TCR to target specific peptides presented by HLA, though these cells are HLA restricted. Alternatively, chimeric antigen receptor modified Tregs are HLA unrestricted but can exhibit bystander suppression.

Tolerogenic dendritic cell therapy has also been proposed as a method to reintroduce T cell tolerance in autoimmunity. Antigen presentation by DCs without proper co-stimulation leads to T cell anergy, and may be used to halt autoreactive T cell responses. Phase 1 clinical trials in rheumatoid arthritis and type 1 diabetes have confirmed the safety of dendritic cell immunotherapy and are paving the way for development of these new treatments (*120, 121*). If we can identify pathogenic T and B cell epitopes within the known ANCA vasculitis autoantigens, these epitopes will inform development of these antigen-specific immunotherapies for patients.

Central Hypothesis

B cells and T cells have been repeatedly implicated in autoimmunity broadly and ANCA vasculitis specifically. However, the specific interactions between these cells and known autoantigens largely remain poorly understood. The central hypothesis of this body of work is that specific interactions between B cells, T cells, and known autoantigens MPO and PR3 play an important role in both onset and pathogenesis of disease. If we can identify and understand these interactions, we can harness them to develop new therapies for patients with ANCA vasculitis. This hypothesis can be broken down into several sub-hypotheses. The first, addressed in Chapter 1, is that patients with ANCA vasculitis are carriers of specific HLA alleles that put them at increased risk for disease onset and increase relapse rates. In this chapter I identify HLA-DPB1 and HLA-DRB4 alleles that are more prevalent in patients than controls, though we do not see any increase in relapse rate for carriers of HLA-DPB1*04:01, contrary to previous reports (*1*). This is the only sub-hypothesis and chapter that includes PR3-ANCA patients, due to significant differences between disease serotypes and the merits of studying MPO-ANCA patients independently.

The second sub-hypothesis, addressed in Chapter 2, is that previously identified pathogenic MPO epitopes are exposed to solvent, bound by patient autoantibodies and MHC II receptors, and that binding will be dependent on secondary structure and specific residues of the epitope. These studies demonstrate that 53% of patients have anti-$MPO_{447-461}$ antibodies and that binding is dependent on both the alpha helix structure of the epitope and two specific amino acids $Lysine_{488}$ and $Isoleucine_{456}$. Interestingly, these studies also reveal that one end of the T cell epitope $MPO_{435-454}$ is exposed to solvent but B cell epitope $MPO_{447-459}$ is buried within MPO. Finally, *in silico* and *in vitro* binding studies confirm binding of $MPO_{447-459}$ and $MPO_{435-454}$ to patient HLA.

The third sub-hypothesis, addressed in Chapter 3, is that patient $CD4^+$ T cells will bind previously identified pathogenic MPO epitopes. These autoreactive $CD4^+$ T cells will be $CD25^{intermediate}$, pro-inflammatory, memory cells with decreased TCR diversity (indicating clonal expansion) compared to controls, and some TCRs may be shared between patients. In this chapter, I demonstrate that patients with MPO-ANCA vasculitis who are carriers of HLA-DBP1*04:01 and/or HLA-DRB4*01:01 have $CD4^+$ T cells that bind both T cell epitope $MPO_{435-454}$ and B cell epitope $MPO_{447-461}$. These cells are $CD25^{intermediate}$, pro-inflammatory (IL-17A secretion), memory cells (CD45RO expression), that are clonally expanded compared to control naïve ($CD25^-$), memory ($CD25^{intermediate}$), and regulatory ($CD25^+$, $CD127^-$) $CD4^+$ T cell populations.

CHAPTER 1: CARRIAGE OF HLA-DPB1*04:01 DOES NOT INCREASE RELAPSE RISK IN PATIENTS WITH ANCA-VASCULITIS

Introduction

GWAS studies in ANCA vasculitis have consistently shown an association between HLA and disease (*59, 69, 70*). More specifically, three separate GWAS studies identified HLA-DP as a risk allele in ANCA vasculitis (*59, 69, 70*). Additional studies have described associations between specific HLA alleles (HLA-DPB1*04:01 and HLA-DRB1*15) and disease (*1, 122*). Hilhorst et al. investigated carriage of HLA-DPB1 and risk of relapse in a cohort of European patients and found that carriage of HLA-DPB1*04:01 was associated with an increased risk of relapse regardless of disease serotype (*1*). Cao et al. reported that Caucasians with PR3-ANCA had 2.2-fold higher odds of carrying DRB1*1501 than controls, that African Americans with PR3-ANCA had a 73.3-fold higher odds of having HLA-DRB1*15 alleles than community based controls, and that many carry the HLA-DRB1*15:01 allelic variant of Caucasian descent, rather than the HLA-DRB1*15:03 allelic variant of African descent (*122*).

It is not surprising that associations have been found between specific HLA alleles and disease in patients with ANCA vasculitis because HLA alleles encode the shape and charge of the MHC peptide-binding pocket and therefore determine the size, shape, and charge of antigens that can be recognized, bound, and presented to T cells by APCs. Additionally, HLA has been previously associated with numerous other autoimmune diseases including T1D (*123*), celiac disease (*124*) and SLE (*125*). This association between HLA and disease further supports a role for T cells in the pathogenesis of ANCA vasculitis.

In addition to the need for new therapies, there remains a need for prognostic indicators for patients with ANCA vasculitis. Given the severe side effects of current immunosuppressive therapy, a biomarker that identifies patients at increased risk for relapse would aid clinicians in determining which patients to treat and which to monitor. The rituximab versus cyclophosphamide/azathioprine for AAV (RAVE) trial was one of several studies that found serial PR3-ANCA titers to be useful in anticipation of severe relapses in a subset of patients (*126*), but prognosis indicators that are useful for all patients with ANCA vasculitis have yet to be identified. It is possible that carriage of specific HLA alleles may be used to predict risk of relapse in patients with ANCA vasculitis (*1*).

In this chapter, I investigated the prevalence of specific HLA alleles in our cohort of patients, and the influence of HLA-DPB1*04:01 carriage on risk of disease relapse. We hypothesized that carriers of HLA-DPB1*04:01 would be at increased risk of relapse in a combined cohort of MPO- and PR3-ANCA vasculitis patients. Despite numerous phenotypic similarities between European and North American patient populations, it is possible that there are enough regional differences to yield a dissimilar result in our cohort compared to the Hilhorst et al. cohort (*1*). Contrary to the previous study, we found no increased risk of relapse for carriers of HLA-DPB1 when including patients with both MPO- and PR3-ANCA vasculitis. When assessing patients by serotype we determined that carriage of HLA-DPB1*04:01 may incur some risk for patients with PR3-ANCA vasculitis, but appears to have no effect on those with MPO-ANCA vasculitis.

Materials and Methods

Study Design

The objective of this study was to delve further into the strong association between HLA and ANCA vasculitis (*59, 69, 70*) by performing high-resolution, sequence-based HLA typing in

a large population of patients with ANCA vasculitis. Patients with ANCA vasculitis were enrolled at University of North Carolina at Chapel Hill clinics and followed in the Glomerular Disease Collaborative Network (*127, 128*). Patients were recruited according to the guidelines of the Institutional Review Board (study no. 97–0523) by the University of North Carolina Office of Human Research Ethics. Study subjects gave informed, written consent and participated according to University review board guidelines.

Patient Cohort

Patients were diagnosed according to the Chapel Hill Consensus Conference (*18, 129*). Patient charts were reviewed by clinicians to confirm disease activity status, periods of relapse, periods of remission, and serotype, prior to analysis. ANCA serotypes were assessed by indirect immunofluorescence and antigen-specific PR3 and MPO ELISAs (*130*). Disease activity was determined by the 2003 Birmingham Vasculitis Activity Score (BVAS) in conjunction with clinical signs of activity. In this study, patients with a BVAS of 0 and no clinical or laboratory evidence of active disease were considered to be in remission. Active disease was defined as a BVAS >0 with clinical and/or laboratory evidence of disease (*131*). Patients were excluded from the study if they were ANCA negative by ELISA, had suspected or confirmed drug-induced forms of ANCA vasculitis, or had overlapping diseases. Patients were selected for this study based on availability of DNA samples for HLA sequencing.

HLA Sequencing

High-resolution HLA typing was performed by our collaborators at the Institute for Immunology and Infectious Diseases (IIID) in Perth, Western Australia, which is accredited by the American Society for Histocompatibility and Immunogenetics (ASHI) and the National Association of Testing Authorities (NATA). All the steps in the pipeline from sample prep to the reporting were quality assessed and tracked using an accredited Laboratory Information and

Management System (ELab). Automated liquid handlers and data analysis were performed using accredited proprietary software applications HLA allele caller and HLA Analysis Suite (Murdoch University, Western Australia). Briefly, HLA loci were PCR amplified for Class I (A, B, C Exons 2 and 3) and Class II (DQB1, Exons 2 and 3; DRB, DQA1 and DPB1, Exon 2) MHC genes using MID tagged primers were optimised to minimize allele dropouts and primer bias. Amplified DNA products from unique MID tagged products were pooled in equimolar ratios and prepared for Illumina sequencing. Libraries were quantified by qPCR and quality assessed on the Agilent Bio analyser or Tape Station. Normalized libraries were then sequenced using Illumina MiSeq platform (MiSeq V3 600-cycle kit, 2X300bp paired end reads). The quality filtered data was demultiplexed by MID tags, merged, and the alleles were called using an HLA allele caller software that minimises the influence of sequencing errors. Alleles were called using the latest IMGT HLA allele database as the allele reference library. The HLA analysis reporting software, performed comprehensive allele balance checks, and assigned putative allele calls for ambiguous results and contamination checks on the final dataset.

Statistical Analysis

Categorical measures were summarized as number and percent, and continuous measures were reported as mean and standard deviation or median and interquartile range, if not normally distributed. Comparison of demographics and clinical parameters between groups by HLA-DPB1*04:01 genotype status (null, heterozygous, or homozygous) were done using Fisher Exact tests for categorical variables and Kruskal-Wallis tests for continuous variables. Kaplan-Meier estimates and log rank test were used to assess differences in time to relapse of HLA-DPB1*04:01 genotypes in all ANCA vasculitis patients and in ANCA serotypes independently. Proportional hazards models with each variable of interest were used to assess differences between relapsing and non-relapsing patients, with hazards ratios, p-values, and 95% confidence

intervals reported. Cohort allele prevalence was calculated by number of patient alleles over total possible alleles and presented as a percent. Patient prevalence was calculated as the number heterozygous and homozygous patients for alleles of interest, over total number of patients and presented as a percent.

Results

HLA allele prevalence differs between MPO- and PR3-ANCA vasculitis

One way to assess HLA prevalence in a cohort of patients is to consider the frequency of each allele compared to the total number of possible alleles (2 per patient). To unambiguously identify specific HLA variants, we performed HLA typing for our cohort of ANCA vasculitis patients (n=249) and found that the two most prevalent class II alleles in our cohort of ANCA vasculitis patients were HLA-DPB1*04:01 (n=260, 52%) and HLA-DRB4*01:01 (n=176, 35%). These alleles are slightly overrepresented in our patient cohort compared to the general population of Caucasians in the United States (41% for HLA-DPB1*04:01 and 32% for HLA-DRB4*01:01 based on data from the Allele Frequency Net Database www.allelefrequencies.net). In MPO-ANCA patients alone, HLA-DPB1*04:01 (n=110, 42%), HLA-DRB4*01:01 (n=108, 41%), HLA-A 02:01 (n=88, 33%), and HLA-DQA1*03:01 (n=79, 30%) were the most prevalent alleles (Table 1.1).

HLA-A n(%)	HLA-B n(%)	HLA-C n(%)	HLA-DPB1 n(%)	HLA-DQA1 n(%)	HLA-DQB1 n(%)	HLA-DRB1 n(%)	HLA-DRB3 n(%)	HLA-DRB4 n(%)	HLA-DRB5 n(%)
02:01 88(33%)	07:02 40(15%)	07:02 41(16%)	04:01 110(42%)	03:01 79(30%)	03:02 56(21%)	04:04 36(14%)	02:02 34(13%)	01:01 108(41%)	01:01 37(14%)
01:01 31(12%)	08:01 26(10%)	07:01 35(13%)	04:02 39(15%)	05:01 52(20%)	03:01 49(19%)	07:01 30(11%)	01:01 30(11%)	N/A	02:02 6(2%)
03:01 30(11%)	44:02 24(9%)	04:01 29(11%)	02:01 28(11%)	01:02 49(19%)	06:02 35(13%)	15:01 30(11%)	03:01 10(4%)	N/A	01:02 2(1%)

Table 1.1 HLA allele prevalence in MPO-ANCA vasculitis. Top three most prevalent alleles for each HLA gene in our cohort of MPO-ANCA vasculitis patients (n=132) including number of alleles (n) and percent (%) of total alleles (n=264) for each.

In PR3-ANCA patients, HLA-DPB1*04:01 (n=150, 64%), HLA-DRB4*01:01 (n=68, 29%), HLA-A*02:01 (n=66, 28%), and HLA-DQA1*01:02 (63, 27%) were the most prevalent alleles (Table 1.2). Interestingly, of the HLA genes with more than three identified alleles, the top three most prevalent alleles are consistent between MPO- and PR3-ANCA vasculitis patients for HLA-A and HLA-B (encode MHC I receptors), as well as HLA-DPB1 and HLA-DRB3 (encode MHC II receptors). For others, like HLA-DQA1 the same three top alleles are the same but in a different order of prevalence.

HLA-A n(%)	HLA-B n(%)	HLA-C n(%)	HLA-DPB1 n(%)	HLA-DQA1 n(%)	HLA-DQB1 n(%)	HLA-DRB1 n(%)	HLA-DRB3 n(%)	HLA-DRB4 n(%)	HLA-DRB5 n(%)
02:01 66(28%)	07:02 46(20%)	07:02 48(21%)	04:01 150(64%)	01:02 63(27%)	03:01 51(22%)	15:01 38(16%)	02:02 42(18%)	01:01 68(29%)	01:01 47(20%)
01:01 37(16%)	08:01 32(14%)	07:01 43(18%)	04:02 44(19%)	05:01 58(25%)	06:02 51(22%)	03:01 29(12%)	01:01 33(14%)	N/A	02:02 1(0.5%)
03:01 35(15%)	44:02 20(9%)	05:01 23(10%)	02:01 16(7%)	03:01 41(18%)	02:01 27(12%)	07:01 27(12%)	03:01 10(4%)	N/A	N/A

Table 1.2 HLA allele prevalence in PR3-ANCA vasculitis. Top three most prevalent alleles for each HLA gene in our cohort of PR3-ANCA vasculitis patients (n=117) including number of patients (n) and percent (%) of total alleles (n=234) for each.

Homozygous carriers of HLA-DPB1*04:01 are white and most have PR3-ANCA vasculitis

Based on previous GWAS studies in ANCA vasculitis and the Hilhorst et al. report on HLA-DPB1 carrier risk (*1*), we investigated carrier frequency of the HLA-DPB1*04:01 allele in our cohort. This analysis revealed that of 117 PR3-ANCA vasculitis patients included in the analysis, 96 patients or 82% were heterozygous or homozygous carriers of HLA-DPB1*04:01. In contrast, only 85 of 132 MPO-ANCA vasculitis patients (64%) were carriers of HLA-DPB1*04:01. Our patient carrier frequencies were similar to the Hilhorst et al. cohort of 174 patients (90% PR3 carriers, 63% MPO carriers), though our carrier frequency in PR3-ANCA vasculitis patients was lower.

Table 1.3 shows patient cohort characteristics by HLA-DPB1*04:01 carrier status. Homozygous carriers of HLA-DPB1*04:01 differed from heterozygous carriers and/or non-carriers by race, follow-up time, ANCA serotype, diagnosis, estimated glomerular filtration rate (eGFR), and organ involvement. Homozygous carriers of HLA-DPB1*04:01 were most often white and were more likely to have PR3-ANCA vasculitis. Homozygous carriers also had the longest follow up time, highest prevalence of GPA diagnosis, and highest eGFR. Additionally, they were more likely to have upper respiratory, joint, and neurological disease involvement compared to heterozygous and non-carriers.

Carriage of HLA-DPB1*04:01 Does Not Increase Relapse Risk in a Combined Cohort

In our combined cohort of 117 PR3-ANCA and 132 MPO-ANCA patients, we do not see an increased risk in time to relapse when stratified by HLA-DBP1*04:01 carrier status (p=0.27, Figure 1.1). This result is in direct contradiction to the Hilhorst et al. study, which reported a stepwise effect of HLA-DPB1*04:01 carriage in a cohort of 344 MPO- and PR3-ANCA vasculitis patients (*1*). They showed in their combined cohort of European patients (Dutch and German) that homozygous carriers were at the highest risk for relapse, followed by heterozygous carriers, and then non-carriers.

Carriage of HLA-DPB1*04:01 May Influence Risk in Patients with PR3-ANCA Vasculitis

When stratified by ANCA subtype, MPO-ANCA vasculitis patients showed no difference in risk of relapse (Figure 1.2A), regardless of HLA-DPB1*04:01 carrier status (p=0.63). In contrast, PR3-ANCA vasculitis patients showed a trend toward increased risk of relapse in homozygous HLA-DPB1*04:01 carriers as compared to heterozygous carriers and non-carriers (Figure 1.2B, p=0.07). This PR3-ANCA vasculitis result closely resembles the Hilhorst et al. German cohort relapse analysis, likely explained by their cohort composition (80% PR3-ANCA vasculitis and 12% MPO-ANCA vasculitis patients) (*1*).

	All patients (n=249)	Non-Carrier (n=68)	Heterozygous (n=104)	Homozygous (n=77)	P values
Age, median(IQR) Years	59.4(44.6, 69.2)	60.4(48.1, 69.2)	60.4(43.8, 71.4)	57.9(43.5, 67.5)	0.6196
Male	133(53.4%)	33(48.5%)	54(51.9%)	46(59.7%)	0.3864
Race (non-white)	47(18.9%)	24(35.3%)	17(16.3%)	6(7.8%)	<0.0001
Follow-up time median(IQR) Years	4.9(1.8, 9.1)	4.0(1.8, 8.6)	4.2(1.3, 7.6)	7.0(2.9, 12.8)	0.0041
ANCA Serotype					
MPO	132(53.0%)	47(69.1%)	61(58.7%)	24(31.2%)	<0.0001
PR3	117(47.0%)	21(30.9%)	43(41.3%)	53(68.8%)	
Diagnosis					
GPA	88(35.3%)	24(35.3%)	28(26.9%)	36(46.8%)	0.0358
MPA	112(45.0%)	29(42.6%)	49(47.1%)	34(44.2%)	
EGPA	5(2.0%)	2(2.9%)	3(2.9%)	0(0.0%)	
Lim	44(17.7%)	13(19.1%)	24(23.1%)	7(9.1%)	
Estimated GFR, median(IQR) (n=199)	27.2(14.4, 60.0)	26.7(15.8, 63.0)	21.3(11.5, 45.5)	36.0(18.9, 63.2)	0.0041
Highest BVAS, median(IQR) (n=171)	11.0(6.0, 15.0)	10.5(6.0, 14.5)	12.0(6.5, 15.5)	10.0(6.5, 15.5)	0.8482
Organ Involvement					
Lung	131(52.6%)	34(50.0%)	51(49.0%)	46(59.7%)	0.3246
Upper Resp	103(41.37%)	29(42.6%)	32(30.8%)	42(54.5%)	0.0055
Joints	120(48.2%)	30(44.1%)	41(39.4%)	49(63.6%)	0.0042
Neuro	37(14.9%)	5(7.4%)	12(11.5%)	20(26.0%)	0.0043
Derm	59(23.7%)	15(22.1%)	23(22.1%)	21(27.3%)	0.6757
Kidney	228(91.6%)	61(89.7%)	95(91.3%)	72(93.5%)	0.7412

Table 1.3. Cohort demographics by HLA-DPB1*04:01 carrier status. Characteristics of the UNC ANCA vasculitis cohort overall and according to HLA-DPB1*04:01 status. Differences between the three groups were evalulated using Fisher Exact test for categorical variables and Kruskal-Wallis test for continuous variables.

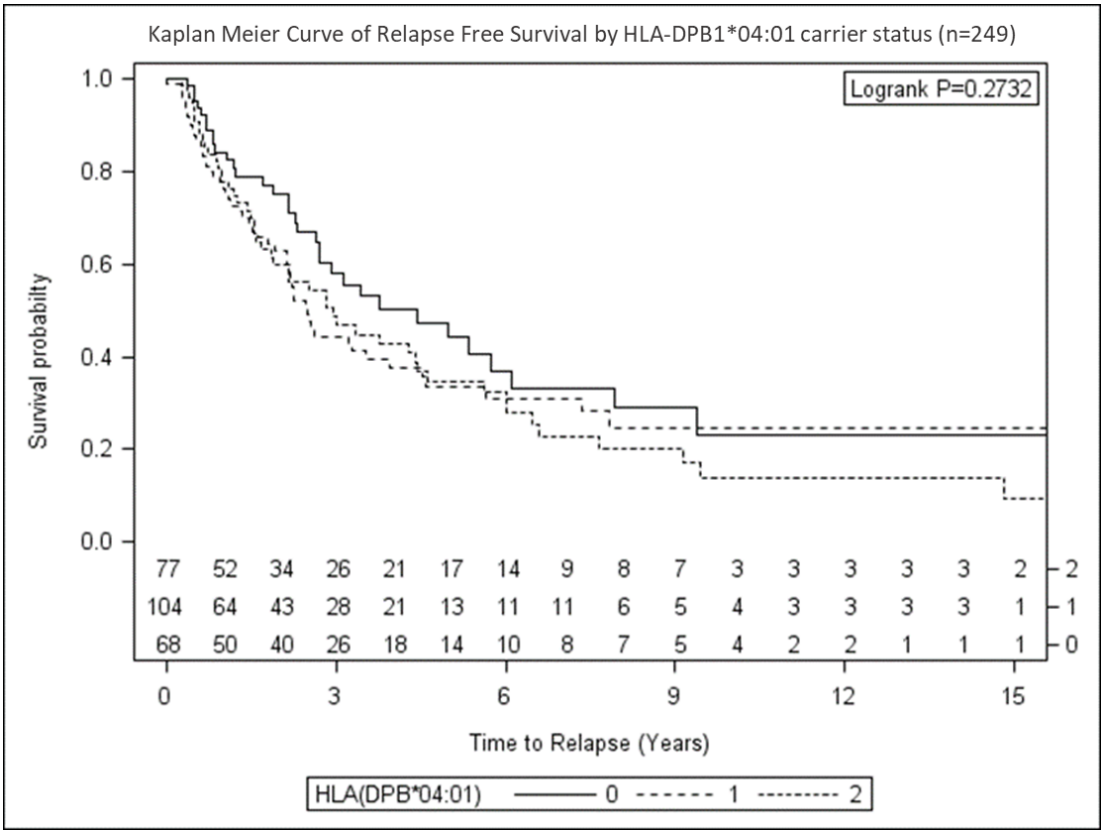

Figure 1.1. Kaplan Meier curve of relapse by HLA-DBP1*04:01 carrier status. Cohort (n=249, log-rank test=0.2732) includes both MPO- and PR3-ANCA patients. Patients are null (0, solid line), heterozygous (1, dashed line) or homozygous (2, dotted line) for HLA-DPB1*04:01.

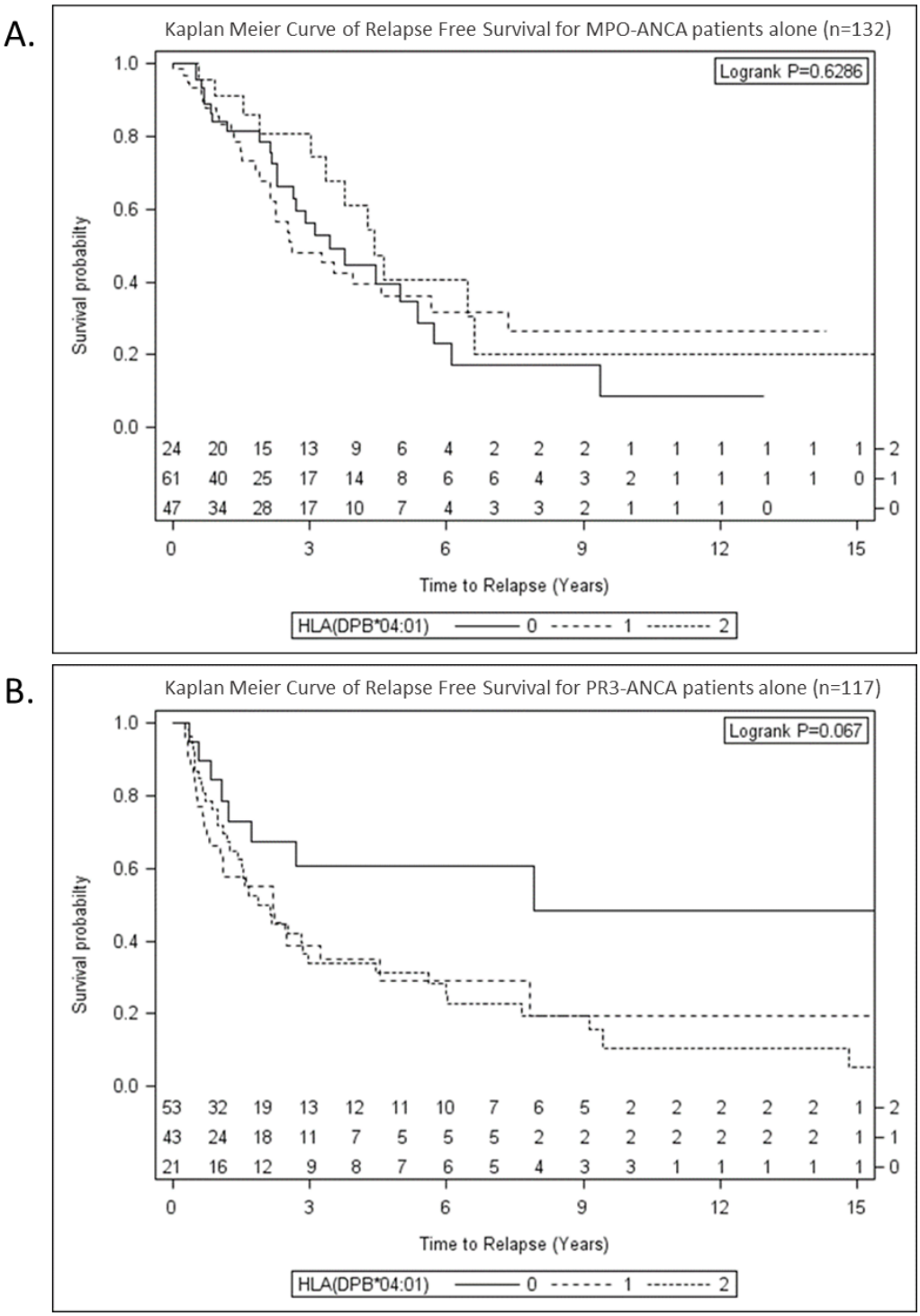

Figure 1.2. Kaplan Meier curves of relapse by HLA-DBP1*04:01 carrier status and ANCA serotype. (A) Kaplan Meier curve of relapse for MPO-ANCA patients alone n=132 (B) Kaplan Meier curve of relapse for PR3-ANCA patients alone n=117. Patients are null (0, solid line), heterozygous (1, dashed line) or homozygous (2, dotted line) for HLA-DPB1*04:01.

We also evaluated characteristics of patients who relapsed compared to those who did not relapse over a period of 15 years, and assessed the influence of these characteristics on the time to relapse by HLA-DPB1*04:01 status (Table 1.4). We did not find statistically significant predictors of relapse when assessing age, gender, eGFR, race, highest BVAS, HLA-DPB1*04:01 status, ANCA serotype (MPO or PR3), or diagnosis (MPA, GPA, or Renal Limited disease).

Characteristics of relapsing vs. non-relapsing AAV Patients (n=207)			
Characteristic	No Relapse (n=79)	Relapse (n=128)	Hazard Ratio
Age, mean ± SD Years	56.95 ± 17.72	56.57 ± 18.36	1.00 (0.99, 1.01)
Male	49(62.0%)	61(47.7%)	0.80(0.56, 1.13)
eGFR, mean ± SD	35.07 ± 33.08 (n=78)	46.44 ± 31.82(n=124)	1.00(1.996, 1.01)
Race (non-white)	18(22.8%)	21(16.4%)	0.77(0.48, 1.23)
Highest BVAS, mean ± SD	11.78 ± 6.50 (n=49)	11.44 ± 6.26 (n=116)	1.03(1.00, 1.06)
HLA-DPB1*04:01 Status			
Homozygous (n=67)	21(26.6%)	46(35.9%)	1.21(0.77, 1.91)
Heterozygous (n=82)	32(40.5%)	50(39.1%)	1.37(0.88, 2.13)
Noncarrier (n=58)	26(32.9%)	32(25.0%)	ref
ANCA Serotype			
PR3-ANCA (n=98)	34(43.0%)	64(50.0%)	ref
MPO-ANCA (n=109)	45(57.0%)	64(50.0%)	0.82(0.58, 1.17)
Diagnosis			
Lim (n=33)	18(22.8%)	15(11.7%)	ref
GPA (n=79)	24(30.4%)	55(43.0%)	1.51(0.85, 2.68)
EGPA(n=5)	3(3.8%)	2(1.6%)	1.04(0.24, 4.56)
MPA (n=90)	34(43.0%)	56(43.8%)	1.48(0.83, 2.61)

Table 1.4. Characteristics of ANCA vasculitis cohort according to relapse status. n=207 patients went into complete remission (on or off therapy) and were eligible to relapse. A proportional Hazards models for each variable were used with hazards ratios and 95% confidence intervals (CI) reported.

Discussion

Contrary to previous work, in our cohort of MPO- and PR3-ANCA vasculitis patients, carriers of the DPB1*04:01 allele did not have an increased probability of relapse compared to non-carriers. This contradictory result is likely explained by cohort composition, as our cohort consisted of 53% MPO-ANCA compared to 22% in the previous study's combined cohort (*1*). Based independent serotype analyses, we conclude that HLA-DPB1*04:01 carrier status may be informative for PR3-ANCA patients, but is not predictive of relapse in a combined or MPO-ANCA only cohort. This finding is consistent with previous GWAS results that HLA-DPB1 is a

risk factor for patients with PR3-ANCA only (*59*). Less likely explanations for this contradictory result include differences in race (18% non-white patients in our cohort vs. 0% previously), baseline eGFR (lower in our cohort), or presence of renal involvement (90% in our cohort vs. 50% previously) in our cohort compared to Hilhorst et al. (*1*). Additionally, there may be geographical differences in disease phenotype between our cohorts that are not captured by measures included in the analysis. Although carriage of HLA-DPB1*04:01 did not predict risk of relapse in our cohort, it is possible that there are additional risk alleles carried by our patients that either independently, or in combination with HLA-DPB1*04:01, provide prognostic value for our patients. Future studies should investigate the value of additional HLA alleles as a biomarker of disease.

Despite similarities in the pathogenesis of MPO- and PR3-ANCA vasculitis, there are significant differences between the two serotypes at every level, from autoantigen recognition (*37*, *38*) to genetics (*59*) and frequency of disease relapse (*21*). This suggests that evaluation of MPO- and PR3-ANCA vasculitis patients together may mask important differences between the two groups, especially at the level of T cell autoantigen interaction. Indeed, the difference in risk of relapse conferred by carriage of HLA-DPB1*04:01 between MPO-ANCA and PR3-ANCA patients was hidden in our combined cohort analysis and only revealed with independent serotype analyses. Additional reported differences between MPO- and PR3-ANCA vasculitis include autoantibody class (IgG in MPO, IgG and IgA in PR3) (*132*), prevalence of MPA and GPA (PR3 commonly GPA, MPO commonly MPA or EGPA) (*133*), geographic location (PR3 in northern areas, MPO in southern areas) (*134*), and environmental risk factors (PR3 Ross River virus and *staphylococcus aureus*, MPO silica and hydralazine) (*135*-*137*).

Unlike MPO-ANCA vasculitis, investigation of PR3-ANCA vasculitis pathology has been hindered by the lack of reproducible animal models of disease, in part due to differences between human and murine neutrophil PR3 expression (*138*). Therefore, much of what we know about PR3-ANCA vasculitis comes from *in vitro* experiments and human studies. This has prevented investigation into specific cell-epitope interactions that have been thoroughly studied using mouse models of MPO-ANCA vasculitis. Given how much more we know about MPO epitope specificity and the significant differences in disease pathogenesis between disease serotypes, the remainder of this dissertation will focus solely on MPO-ANCA vasculitis. Ideally, successful methods used to elucidate cell-epitope interactions in MPO-ANCA vasculitis will be amenable to future PR3-ANCA vasculitis studies.

CHAPTER 2: PATIENT ANCA AND HLA ALLELES BIND MPO EPITOPES

Introduction

While B cells and their secretion of ANCA undoubtedly play a role in vascular damage, some observations from patients complicate our understanding of their specific role in the induction of immune dysregulation. These observations include: autoantibody titers that do not always correlate with disease activity (*43*), healthy controls which harbor naturally occurring anti-MPO antibodies (*44*), and some patients with disease symptoms without detectable levels of circulating ANCA (*45*). One possible explanation for these observations is that epitope specificity of ANCA determines their pathogenicity.

To address this, previous work in our lab used a highly sensitive epitope excision/mass spectrometry approach (MALDI-TOF/TOF-MS) to determine epitope specificity of anti-MPO antibodies in ANCA vasculitis patients and healthy controls (*49*). This study identified a linear epitope, $MPO_{447-459,}$ that was of particular interest due to the presence of patient anti-$MPO_{447-459}$ ANCA reactivity during periods of disease activity that declined upon clinical remission, and was not identified in healthy controls (*49*). In mice, Ooi et al. screened overlapping MPO peptides of 20 amino acids and identified $MPO_{409-428}$ as an immunodominant MPO T-cell epitope based on its ability to induce focal necrotizing glomerulonephritis upon immunization in C57BL/6 mice (*50*). The human homolog of this epitope ($MPO_{435-454}$) overlaps our previously identified linear MPO epitope ($MPO_{447-459}$) by eight amino acids. Additionally, they found that transfer of $MPO_{409-428}$ specific $CD4^+$ T cell clones into $Rag1^{-/-}$ mice in combination with LPS or anti-GBM antibodies induced disease (*50*). Recently, Chang et al. also identified $MPO_{431-439}$ as a

pathogenic $CD8^+$ T cell MPO epitope and demonstrated that co-transfer of $MPO_{431-439}$ specific $CD8^+$ T cells into $Rag1^{-/-}$ mice exacerbated disease (*139*). This epitope is just a few amino acids downstream from the $CD4^+$ T cell epitope identified in mice, and our B cell epitope identified in humans, which suggests that we may have collectively identified an immunodominant region of MPO.

In this chapter, we set out to further investigate the properties of this region of MPO for its potential role in disease pathogenesis. Our hypothesis was that previously identified pathogenic MPO epitopes ($MPO_{447-459}$ and $MPO_{435-454}$) are exposed to solvent, bound by patient autoantibodies and MHC II receptors, and that binding will be dependent on secondary structure and specific residues of the epitope. ELISA studies, alanine scanning, solvent exposure studies, and MHC binding assessments were used to determine structure, location, exposure, and binding capabilities of this region to inform future cellular experiments.

Materials and Methods

Study Design

The objective of these experiments was to understand the immunogenic potential and biochemical properties of previously identified MPO epitopes $MPO_{447-459}$ and $MPO_{435-454}$. Patients with ANCA vasculitis were enrolled at University of North Carolina at Chapel Hill clinics and followed in the Glomerular Disease Collaborative Network (*127, 128*). Patients, healthy controls, and disease controls (SLE and PR3-ANCA) were recruited according to the guidelines of the Institutional Review Board (study no. 97–0523) by the University of North Carolina Office of Human Research Ethics. Study subjects gave informed, written consent and participated according to University review board guidelines. Patients were chosen for ELISA studies based on availability of repeat serum samples.

Patient Cohort

Patients were diagnosed according to the Chapel Hill Consensus Conference (*18, 129*). Patient charts were reviewed by clinicians to confirm disease activity status, periods of relapse, periods of remission, and serotype. ANCA serotypes were assessed by indirect immunofluorescence and antigen-specific PR3 and MPO enzyme-linked immune-absorbent assays (ELISA) (*130*). Disease activity was determined by the 2003 Birmingham Vasculitis Activity Score (BVAS) in conjunction with clinical signs of activity. In this study, patients with a BVAS of 0 and no clinical or laboratory evidence of active disease were considered to be in remission. Active disease was defined as a BVAS >0 with clinical and/or laboratory evidence of disease (*131*). Patients were excluded from the study if they were ANCA negative by ELISA, had suspected or confirmed drug-induced forms of ANCA vasculitis, or had overlapping diseases. Patients with systemic lupus erythematosus (SLE) and healthy controls (HC) were used as comparator groups.

ELISA Studies

Demographic features of the study subjects are shown in Table 2.1. A total of 979 serum samples were tested by ELISA for reactivity to native MPO and $MPO_{447-461}$ (Biomatik). Control samples included serum from 93 healthy controls, 24 patients with systemic lupus erythematosus, and 48 patients with PR3-ANCA with half in disease remission. The remaining serum samples were acquired from 66 patients with MPO-ANCA at multiple time points spanning disease course (>4 samples n=45, >3 samples n=50) as determined by clinical manifestations of disease and conventional assays. In addition, longitudinal autoantibody responses to the B cell epitope $MPO_{447-461}$ were measured in 51 patients over time (average follow-up time of cohort was 3.86 years) by ELISA.

	MPO ANCA	PR3 ANCA	Healthy Control	SLE
n	51	48	93	24
Average age at time of sample	55	55	37	36
Gender (% female)	29/51 (57%)	22/48 (46%)	57/93 (61%)	17/24 (71%)
Ethnicity (% white)	34/51 (67%)	43/48 (90%)	69/93 (74%)	5/24 (21%)

Table 2.1. Demographics summary for Patient ELISA cohort.

ELISA studies utilized a peptide with the addition of two amino acids ($MPO_{447-461}$ instead of $MPO_{447-459}$) to increase solubility of the peptide. Solid white ELISA plates (Grenier) were coated with 0.01mM peptide coating solution made in 0.5M carbonate-bicarbonate buffer at pH 9.3 and incubated overnight at 4° C. Plates were blocked in Dulbeccos's PBS (Gibco) with 1% goat serum (Gibco) and 0.5% Tween20 (Fisher Scientific) for 2 hours at 37° C. The serum samples were diluted in blocking buffer (1:100) and incubated at 37° C for 1 hour. Goat anti-human with alkaline phosphatase conjugate secondary antibody specific to Ig (H+L) (Millipore) (1:10,000) was also diluted in blocking buffer then incubated for 1 hour at room temperature and detected using CDP-Star substrate in Roche Detection Buffer with enhancer in a Tecan Infinite M200 Pro plate reader programmed for luminescence. For cross-sectional studies, the peak value is represented from each patient (Figure 2.1A).

MPO ANCA serum samples were screened for MPO titers regardless of disease activity or previously reported titers. The MPO ANCA kits were purchased from INOVA and all the samples were run in duplicate, following the recommended protocol. Absorbance values were measured by a Tecan Infinite M200 Pro plate reader (Life Sciences).

Alanine Scanning

To determine the residues required for binding peptide binding to patient IgG, each amino acid in $MPO_{447-461}$ (RKIVGAMVQIITYRD) was replaced with an alanine. All peptides were run in triplicate with positive (known positive patient for RKIV) and negative (healthy

serum and secondary alone) controls consistent across plates, with one patient per plate. Chemiluminescence was measured using a Tecan Infinite M200 Pro plate reader (Life Sciences).

Circular Dichroism

The spectra were the average of four scans obtained by collecting data at 0.2 nm intervals from 260 to 190 nm, with a response time of 2s and a bandwidth of 1 nm. The raw CD data were adjusted by subtracting a buffer blank. Peptide concentration in all samples was 100 uM in 10 mM phosphate buffer, pH 7.4 containing 150 mM NaCl.

Solvent Exposure

The atomic coordinates were obtained from the Protein Data Bank (entry 1CXP). Solvent accessibility was calculated using the 'rolling ball' algorithm and the GETAREA software (*140*). This algorithm uses a sphere (of solvent) of a particular radius (typically 1.4 Å) to 'probe' the surface of the molecule. Residues are considered to be solvent exposed if the ratio value exceeds 50% and to be buried if the ratio is less than 20%.

In Silico Predictions

In silico predictions were made by the Immune Epitope Database (www.iedb.org) to identify antigen candidates (15 amino acid length maximum based on algorithm limits) for the HLA alleles carried by our patients.

In Vitro Binding Studies

Assays to quantitatively measure peptide binding to HLA-DRB4*01:01 and HLA-DPB1*0401 (class II) MHC molecules are based on the inhibition of binding of a high affinity radiolabeled peptide to purified MHC molecules, and were performed essentially as described elsewhere (*141-143*). In brief, 0.1-1 nM of radiolabeled peptide was co-incubated at room temperature with 1 nM to 1 µM of purified MHC in the presence of a cocktail of protease inhibitors. Following a two day incubation, MHC bound radioactivity was determined by

capturing the MHC/peptide complexes on L243 (anti HLA-DR) or B7/21 (anti HLA-DP) antibody coated Lumitrac 600 plates (Greiner Bio-one, Frickenhausen, Germany), and measuring bound cpm using the TopCount (Packard Instrument Co., Meriden, CT) microscintillation counter. In the case of competitive assays, the concentration of peptide yielding 50% inhibition of the binding of the radiolabeled peptide was calculated. Under the conditions utilized, where [label]<[MHC] and IC50 ≥ [MHC], the measured IC50 values are reasonable approximations of the true Kd values (*144, 145*). IC50 values under 100 are indicative of high affinity binding to HLA, values between 100 and 1000 represent good binding pairs, and values greater than 1000 indicate lack of binding to the HLA. Each competitor peptide was tested at six concentrations covering a 100,000-fold dose range. As a positive control, the unlabeled version of the radiolabeled probe was also tested in each experiment.

Human Myeloperoxidase structure was obtained from the Protein database using PDB code 5FIW and visualized using PyMOL by Schrödinger.

Statistical Analysis

Descriptive statistics included number with percentage, mean with standard deviation, and/or median with interquartile range. Differences between groups were compared using Fisher's exact tests for categorical measures. T tests, Wilcoxon rank sum tests, or Kruskal-Wallis tests were used for continuous measures, based on the number of groups being compared and whether or not the data was normally distributed. Sign rank tests were used for paired comparisons. GraphPad Prism was used to generate figures (Version 7, GraphPad Software, La Jolla, CA) and analyses were conducted using SAS software (Version 9.4 SAS Institute, Cary, NC).

Results

Patient ANCA bind $MPO_{447-461}$ most often at disease onset

Based on previous work in our lab that identified $MPO_{447-461}$ as a region of interest (*49*), we set out to assess patient ANCA reactivity to this region in a large cohort of patients. Fifty-three percent of tested patients (n=27/51) were positive for anti-$MPO_{447-461}$ autoantibodies at least once during their disease course (Figure 2.1A), most often at disease onset (Figure 2.1B). To understand any potential impact of therapy on anti-$MPO_{447-461}$ reactivity, patients who were positive for anti-$MPO_{447-461}$ were compared to those who were negative for reactivity, and we found that negative samples had a higher incidence of treatment prior to sample collection (Figure 2.1C). We also compared patients who were positive for anti-$MPO_{447-461}$ ever to those who were negative for reactivity to $MPO_{447-461}$ and PR3 controls to identify any potentially confounding differences in cohort characteristics (Table 2.2). In addition to treatment differences shown in Figure 2.1C, there were some differences in organ involvement and duration of follow up between groups. Anti-$MPO_{447-461}$ positive ever patients had a longer duration of follow up and more upper respiratory and joint involvement compared to anti-$MPO_{447-461}$ never positive patients. Therefore, the true prevalence of anti-$MPO_{447-461}$ autoantibodies may be underrepresented in our cohort.

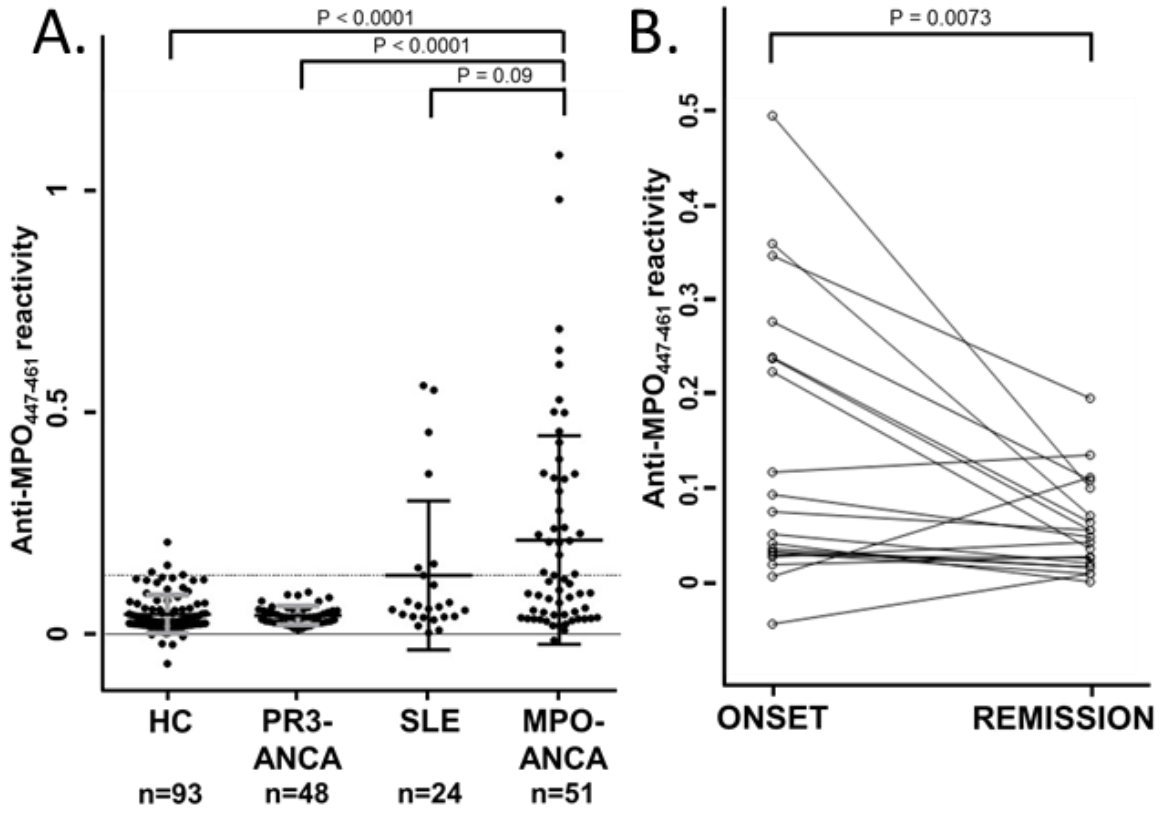

C.

	MPO(447-461)+ at onset (n=7)	MPO(447-461)- at onset (n=13)	P Value
Days from initiation of treatment (ave±st.Dev)	-6.86±14.66	12.46 ±20.76	0.0251

Figure 2.1. Anti-MPO$_{447-461}$ autoantibody is detectable in 53% of patients by ELISA most often at onset. (A) Measured serum or plasma anti-MPO$_{447-461}$ ELISA reactivity from healthy controls (HC, n=93), patients with PR3-ANCA vasculitis (n=48), patients with systemic lupus erythematous (SLE, n=24), and patients with MPO-ANCA vasculitis (n=51), normalized to a positive control. Threshold of positivity was determined by the average of healthy control samples plus two standard deviations and is indicated by the grey dashed line. (B) Reactivity of 20 samples collected at onset (active disease) paired with a remission sample from the same patient, normalized to a positive control. (C) Analysis of onset samples revealed that anti-MPO$_{447-461}$ negative samples had a higher prevalence of treatment prior to collection.

Characteristic	MPO-ANCA+ $MPO_{(447-461)}$+Ever (N=27)	MPO-ANCA+ $MPO_{(447-461)}$+Never (N=24)	PR3-ANCA+ (N=48)	P Value*
Age at disease onset *(years)*				
Median(IQR)	49(2,63)	58(50,69)	52(35,59)	0.0558
Gender				
Female	17 (63%)	12 (50%)	22 (46%)	0.3584
Ethnicity				
White	15 (56%)	19 (80%)	43 (90%)	0.0044
Duration of Follow-up *(years)*				
Median(IQR)	5(3,7)	2(1,3)	NA	<0.0001
Disease				
MPA	13 (48%)	13(54%)	21(48%)	
GPA	8 (30%)	4(17%)	21(48%)	0.0184
EGPA	1 (4%)	1(4%)	1(2%)	
Renal-limited	5 (19%)	6(25%)	1(2%)	
Organ involvement				
Lung	10 (37%)	11 (46%)	30 (63%)	0.0889
Upper Respiratory	12 (44%)	4 (17%)	24 (50%)	0.0185
Joints	12 (44%)	5 (21%)	28 (58%)	0.0091
GI	1 (4%)	0(0%)	3 (6%)	0.8058
Neuro	1 (4%)	3 (13%)	11 (23%)	0.0717
Derm	5 (19%)	4 (17%)	16 (33%)	0.2139
Kidney	24 (89%)	20 (83%)	38 (79%)	
Peak serum creatinine *(mg/dl)*				
Median(IQR)	2(1,3)	3(2,4)	2(1,3)	0.0121
MPO-ANCA peak titer[f] *(u/ml)*				
Median(IQR)	80(37,108)	60(33,117)	NA	0.7188
Medications				
Solumedrol	24 (89%)	18 (75%)	NA	0.2759
Prednisone	25 (93%)	22 (92%)	19 (40%)	<0.0001
Cyclophosphamide	23 (85%)	20 (83%)	4 (8%)	<0.0001
MMF	18 (67%)	5 (21%)	11 (23%)	<0.0001
Aza	16 (59%)	10 (42%)	7 (15%)	0.0002
Cyclosporine	4 (15%)	0(0%)	0(0%)	NA
Pravacl	1 (4%)	0(0%)	0(0%)	NA
Rituximab	23 (85%)	16 (67%)	9 (19%)	<0.0001
Plasmapheresis	10 (37%)	7 (29%)	4 (8%)	0.0069
Plaquenil	1 (4%)	1 (4%)	1 (2%)	1.0000
Methotrexate	3 (11%)	0(0%)	0(0%)	NA
Belimumab	1 (4%)	0(0%)	0(0%)	NA

* P values were calculated by Fisher Exact Test for categorical variables and Wilcoxon Two Sample Test for continuous variables.

Table 2.2. Comparison of ELISA Study Patient Demographics by anti-$MPO_{447-461}$ reactivity. Groups include $MPO_{447-461}$ positive ever, $MPO_{447-461}$ positive never, and PR3-ANCA vasculitis patient controls.

MPO-ANCA vasculitis patients in this cohort had serial serum samples that were used to assess correlation between anti-$MPO_{447-461}$ and disease activity. We identified a close correlation

between anti-$MPO_{447-461}$ reactivity and disease activity in a portion of patients (results from illustrative patient shown in Figure 2.2A), while others demonstrated anti-$MPO_{447-461}$ reactivity only at disease onset (Figure 2.2B).

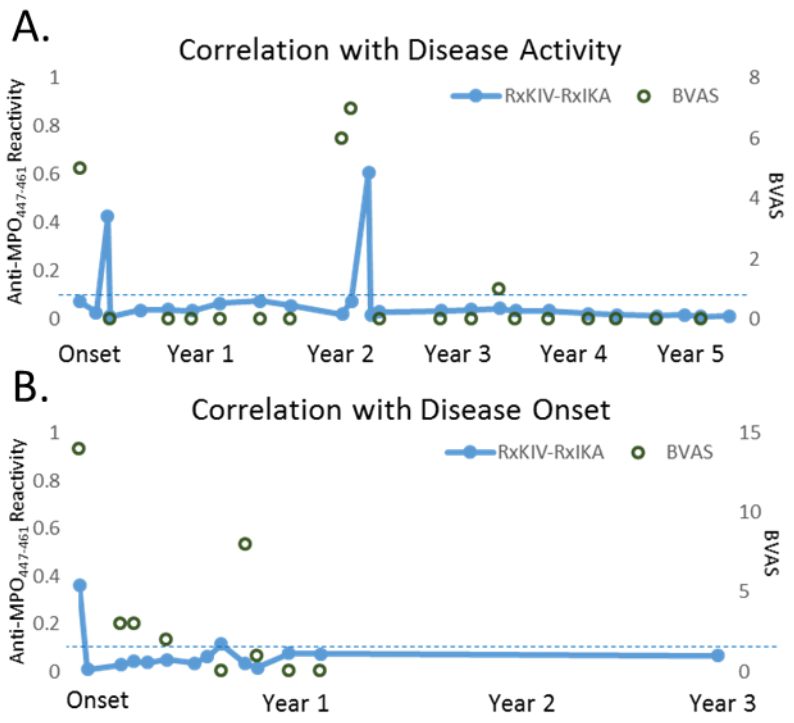

Figure 2.2. Anti-$MPO_{447-461}$ reactivity correlates with disease activity or disease onset in patients. Temporal analysis of patient $MPO_{447-461}$ ELISA reactivity compared to BVAS scores. (A) Patient anti-$MPO_{447-461}$ reactivity correlates with disease activity assessed by BVAS score. (B) Patient anti-$MPO_{447-461}$ reactivity correlates with disease onset, not disease activity assessed by BVAS score. Plotted $MPO_{447-461}$ reactivity values are reflective of $MPO_{447-461}$ (RxKIV) values minus corresponding Anti-$MPO_{447-461scramble}$ (RxIKA) negative control reactivity to normalize between samples.

Furthermore, there was no correlation between ANCA reactivity to whole MPO and $MPO_{447-461}$ (Figure 2.3) suggesting that ANCA reactivity to the B cell epitope $MPO_{447-461}$ is specific, not just a readout for ANCA reactivity to whole MPO.

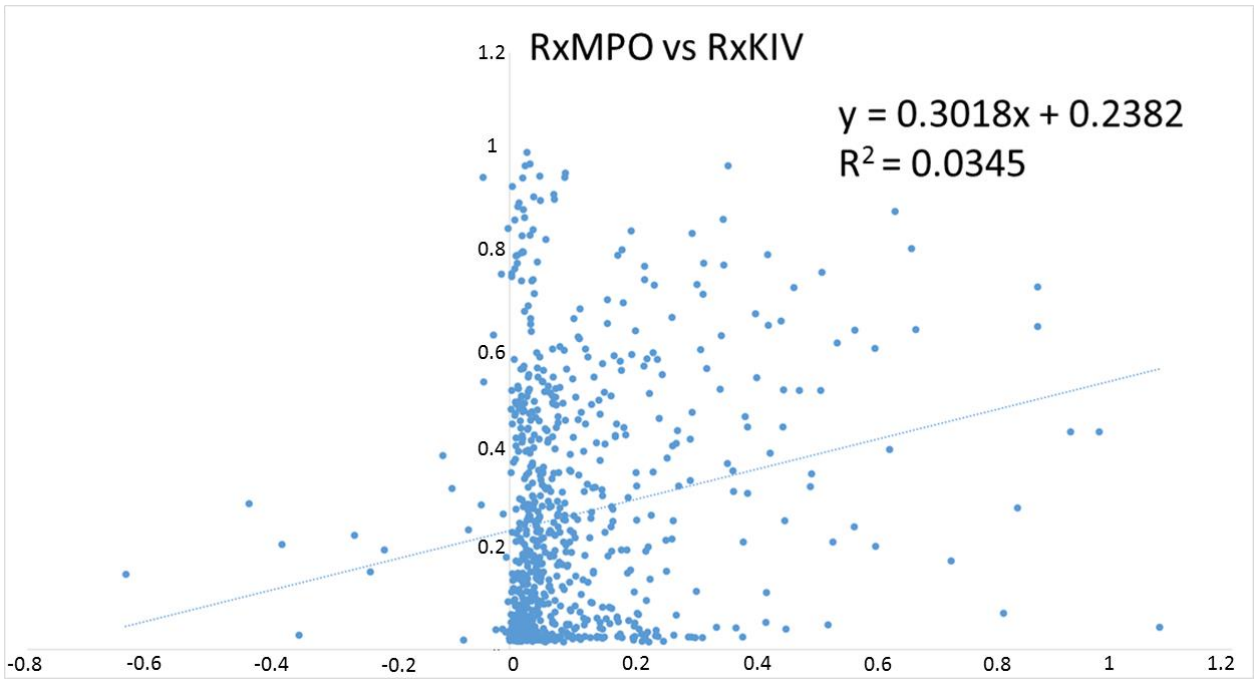

Figure 2.3. Anti-MPO$_{447\text{-}461}$ reactivity to MPO$_{447\text{-}461}$ does not correlate with reactivity to whole MPO. Correlation between whole MPO reactivity and MPO$_{447\text{-}461}$ reactivity for all samples tested (n =766 samples from 66 patients).

MPO$_{447\text{-}461}$ is buried and MPO$_{435\text{-}454}$ is exposed to solvent

We sought to understand the dynamics of how B and CD4$^+$ T cells are able to interact with these epitopes. Utilizing the crystal structure of human MPO, we found that MPO$_{435\text{-}454}$ and MPO$_{447\text{-}461}$ are adjacently located on the same alpha helix (Figure 2.4A & 2.4B). Solvent accessibility predictions were then made based on the crystal structure of MPO using the 'rolling ball' algorithm and GETAREA software (Figure 2.4C).

The solvent exposure analysis confirmed that the B cell epitope MPO$_{447\text{-}461}$ is buried inside MPO. Although we would expect both epitopes to be exposed to solvent and therefore to patient ANCA (allowing antibody reactivity), antigenic epitopes buried inside self-proteins have been previously reported (*140*). In contrast, and as we would expect, the T cell epitope MPO$_{435\text{-}454}$ has residues that are exposed to solvent. Collectively, the data demonstrate that the majority

of this region $MPO_{435-461}$ is buried within MPO (illustrated in figure 2.5), which would preclude immune recognition of the B cell epitope under normal conditions.

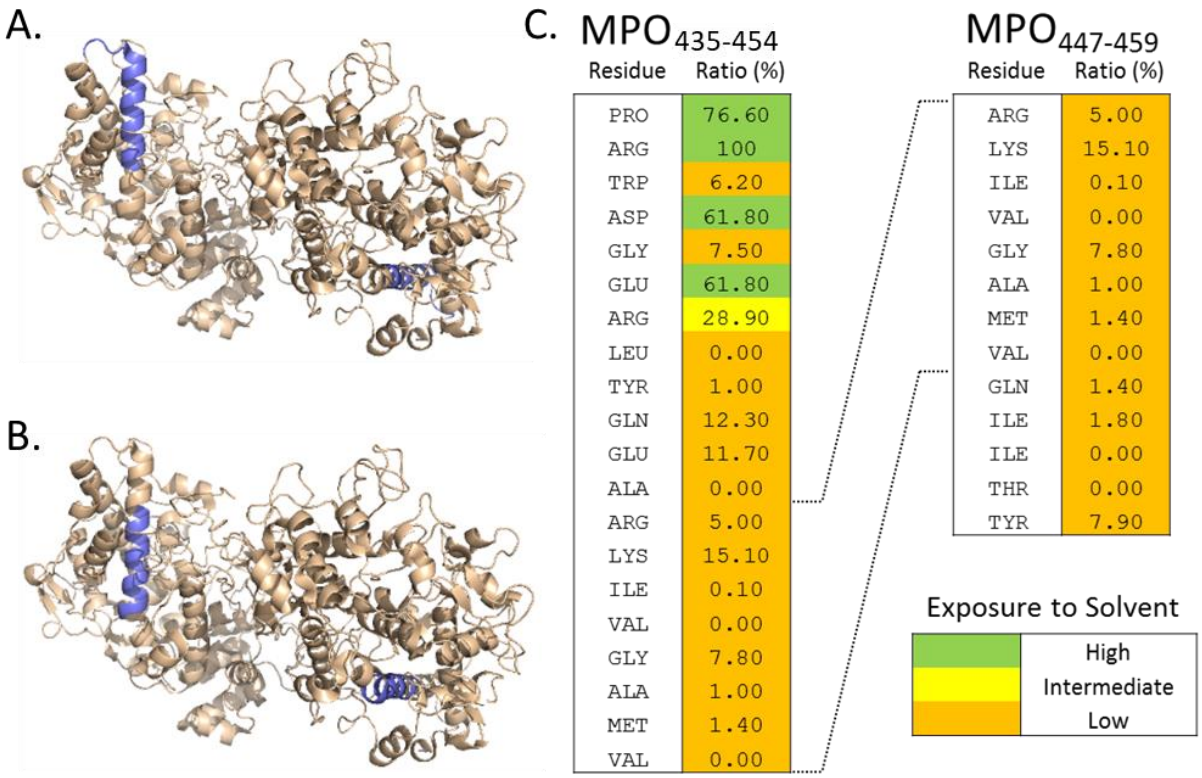

Figure 2.4. $MPO_{435-461}$ is located on an alpha helix that is mostly buried within MPO. Cartoon models of (A) $MPO_{447-461}$ and (B) $MPO_{435-454}$ highlighted in blue demonstrate alpha-helical structure of the region. Models were generated using Pymol and human MPO crystral structure (PDBID:5FIW). (C) $MPO_{447-461}$ is buried, while part of $MPO_{435-454}$ is exposed to solvent. Accessibility to solvent of each amino acid determined using human MPO crystal structure (PDBID:1CXP). Residues are considered to be solvent exposed if ratio value > 50%, and buried if the ratio value < 20%.

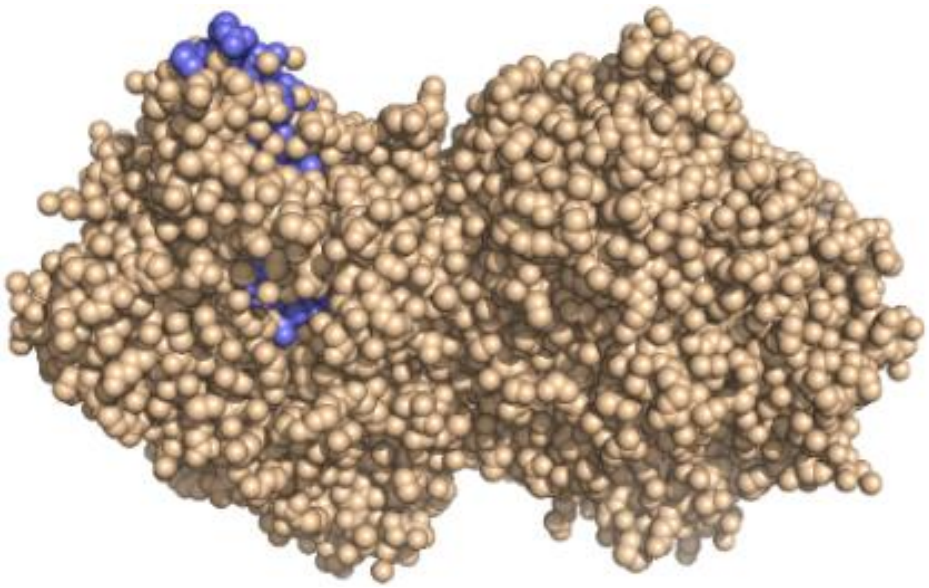

Figure 2.5. Sphere model demonstrating exposed portions of region $MPO_{435-459}$ based on crystal structure. Blue color demonstrates location of $MPO_{435-459}$ region. Model was generated using crystal structure (PDBID:5FIW) and Pymol software.

Lysine$_{448}$ and Isoleucine$_{456}$ are required for ANCA binding to MPO$_{447-461}$

Considering that buried epitopes require conformational changes to become exposed to the immune system, we further investigated the B cell epitope $MPO_{447-461}$. These studies were designed to identify the critical amino acids that mediate binding of anti-MPO ANCA to $MPO_{447-461}$ with alanine scanning experiments. Peptides for $MPO_{447-461}$ were generated using sequential substitutions of alanine for each amino acid in the peptide. Sera from eight anti-$MPO_{447-461}$ positive patients were used to assess reactivity to each peptide. These experiments revealed that peptides with alanine substitutions for Lysine$_{448}$ and Isoleucine$_{456}$ demonstrate significantly decreased serum reactivity to the peptide (Figure 2.6). At neutral pH lysine is hydrophobic, polar, and positively charged and therefore plays an important role in structure. Alanine replacement of this amino acid is likely to disturb the structure of $MPO_{447-461}$ due to its non-polar and mildly hydrophobic nature. Also hydrophobic, isoleucine is limited by bulkiness near the protein backbone that limits conformation and is very non-reactive. Perhaps the small

size of the alanine replacement is enough to disturb $MPO_{447-461}$ structure and inhibit ANCA binding.

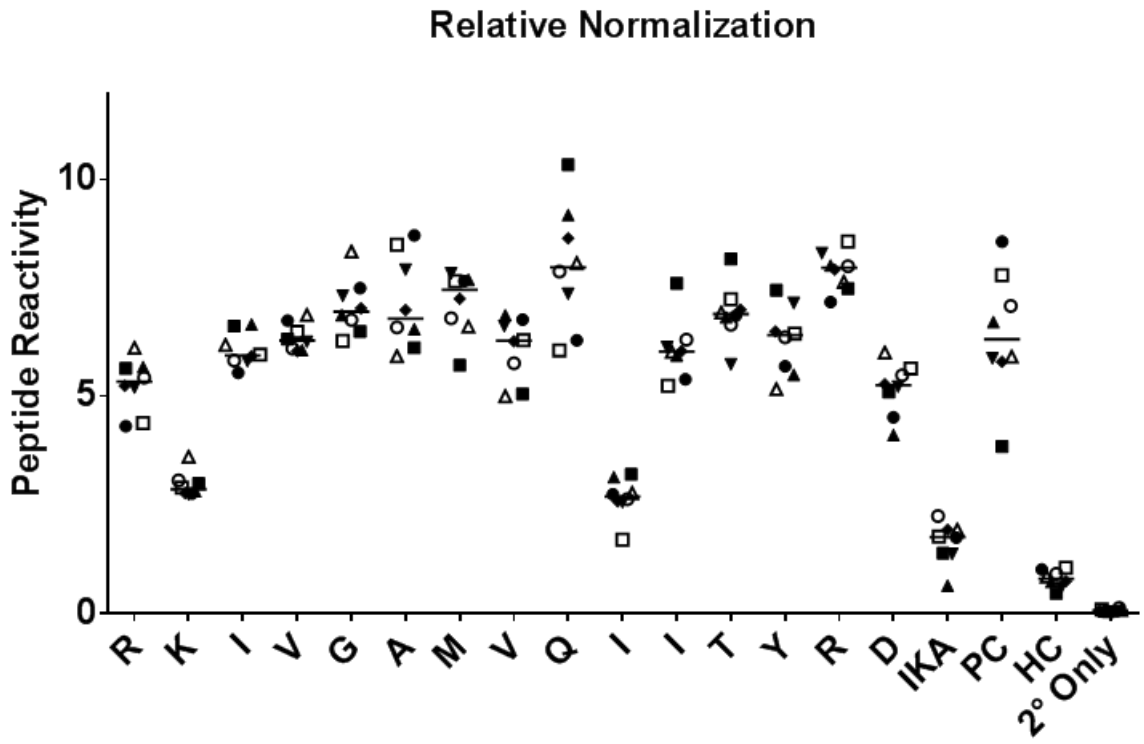

Figure 2.6. Alanine scanning of $MPO_{447-461}$ reveals $Lysine_{448}$ or $Isoleucine_{456}$ are required for binding to patient ANCA. Experiments were performed in triplicate with eight previously positive patients by ELISA for $MPO_{447-461}$. The positive control (PC) was the same highly positive serum included on every plate and the same healthy control (HC) was included on every plate. IKA is an $MPO_{447-461}$ scrambled control and a secondary antibody only (2° Only) control was also used.

The alpha helix structure of $MPO_{447-461}$ is required for ANCA binding

Amino acid substitutions often cause changes in the secondary structure; therefore, circular dichroism experiments were performed to examine any resulting structural changes. These experiments revealed that alanine substitutions for $Lysine_{448}$ or $Isoleucine_{456}$ resulted in a disrupted alpha helical structure, which likely explains the altered autoantibody binding (Figure 2.7). This same alpha helix disruption was observed for the $MPO_{447-461scramble}$ epitope used as a control throughout numerous experiments. Therefore, these data indicate that linear epitope

$MPO_{447\text{-}461}$ is buried within the molecule and that patient ANCA binding to this epitope is dependent on the alpha-helix structure.

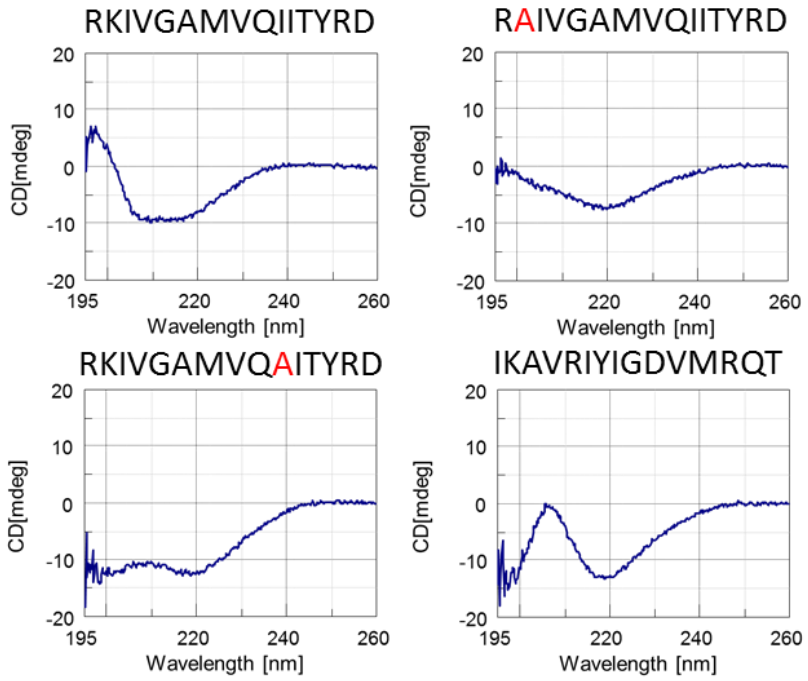

Figure 2.7. Circular dichroism experiments reveal loss of alpha-helical structure with alanine substitutions at K_{448} or I_{456}. RKIVGAMVQIITYRD is the amino acid sequence for $MPO_{447\text{-}461}$ and IKAVRIYIGDVMRQT is the sequence for $MPO_{447\text{-}461scramble}$. Spectra were the average of four scans obtained by collecting data at 0.2 nm intervals from 260 to 190 nm, with a response time of 2 seconds and a bandwidth of 1 nm.

Patient HLA alleles are predicted to bind regions of MPO

In addition to patient ANCA reactivity to specific regions of MPO, we wanted to study T cell binding to MPO. Due to the specificity of antigen recognition by TCRs, we first needed to investigate the ability of patient HLA encoded MHC II alleles to bind MPO epitopes of interest. Unbiased *in silico* binding predictions from the Immune Epitope Database identified five putative MPO epitopes (15 amino acids in length based on algorithm limitations) with their respective HLA binding partner(s) and identified HLA-DRB4*01:01 as the predicted binding partner for our previously identified B cell epitope $MPO_{447\text{-}461}$ (Table 2.3). Additionally, a 15 amino acid long section of the mouse immunodominant MPO epitope published in Ooi et al.

(2012) was included in this analysis (mouse $MPO_{413-427}$), and was predicted to bind HLA-DRB5*01:01.

Protein	Peptide	AUC	Predicted Percentile Rank	Most Frequent Allele in Positives	Most Frequent Allele in Negatives
Mouse MPO	$MPO_{413-427}$ (GEKLYQEARKIVGAM)	0.40	12.19	HLA-DRB5*01:01	HLA-DRB1*03:01
Human MPO	$MPO_{447-461}$ (RKIVGAMVQIITYRD)	0.51	2.83	HLA-DRB4*01:01	HLA-DRB4*01:01
Human MPO	$MPO_{105-119}$ (PVAATRTAVRAADYL)	0.37	10.88	HLA-DQA1*05:01/ DQB1*02:01	HLA-DQA1*05:01/ DQB1*02:01
Human MPO	$MPO_{488-502}$ (PRIANVFTNAFRYGH)	0.39	7.82	HLA-DRB5*01:01	HLA-DRB5*01:01
Human MPO	$MPO_{245-259}$ (DQERSLMFMQWGQLL)	0.64	1.84	HLA-DPA1*01:03/ DPB1*04:02	HLA-DPA1*01:03/ DPB1*04:02
Human MPO	$MPO_{545-559}$ (PILRGLMATPAKLNR)	0.62	2.48	HLA-DRB1*04:04	HLA-DRB5*01:01
Human MPO	$MPO_{409-423}$ (MPELTSMHTLLLREH)	0.62	3.05	HLA-DPA1*01/ DPB1*04:01	HLA-DPA1*01/ DPB1*04:01

Table 2.3. MPO epitopes and *in silico* predicted HLA binding partners. AUC is Area Under the Curve and Predicted Percentile Rank is calculated based on how the predicted affinity of that peptide for that allele ranks in a very large set of peptides randomly extracted from UniProt.

HLA-DPB1*04:01 and HLA-DRB4*01:01 bind $MPO_{447-461}$ and $MPO_{435-454}$ *in vitro*

The seven epitopes from *in silico* prediction, in addition to the previously identified T cell epitope $MPO_{435-454}$ and scrambled control epitope $MPO_{447-461scramble}$ were assessed for binding to HLA using an *in vitro* competitive binding assay. The B cell epitope $MPO_{447-461}$ and control epitope $MPO_{447-461scramble}$ bound both HLA-DPB1*04:01 and HLA-DRB4*01:01 with high affinity (Table 2.4). In contrast, the T cell epitope $MPO_{435-454}$ bound HLA-DRB4*01:01 with high affinity, while binding affinity to HLA-DPB1*04:01 was lower (Table 2.4).

Protein	Peptide	HLA-DPA1*01:03/ HLA-DPB1*04:01	HLA-DPA1*01:03/ HLA-DPB1*04:02	HLA-DQB1*02:01/ *02:02	HLA-DRB1*03:04/ *03:07	HLA-DRB1*04:01-*04:13	HLA-DRB4*01:01/ *01:03	HLA-DRB5*01:01/ *01:02/ *02:02
Mouse MPO	$MPO_{413-427}$ (GEKLYQEARKIVGAM)	53700	19400	56400	31100	933	9350	1440
Human MPO	$MPO_{447-461}$ (RKIVGAMVQIITYRD)	98	74	615	13900	46	240	1210
Human MPO	$MPO_{105-119}$ (PVAATRTAVRAADYL)	7120	6165	285	14500	433	876	321
Human MPO	$MPO_{488-502}$ (PRIANVFTNAFRYGH)	5620	1345	1000	2970	2	725	5
Human MPO	$MPO_{245-259}$ (DQERSLMFMQWGQLL)	1090	910	7050	70000	4140	381	1180
Human MPO	$MPO_{545-559}$ (PILRGLMATPAKLNR)	12000	2475	2550	32800	8	68	29
Human MPO	$MPO_{409-423}$ (MPELTSMHTLLLREH)	409	826	1210	11000	16	217	81
Human MPO	$MPO_{435-454}$ (PRWDGERLYQEAYRKIVGAMV)	1050	N.D.	N.D.	N.D.	N.D.	253	N.D.
Human MPO	$MPO_{447-461scramble}$ (IKAVRIYIGDVMRQT)	38	N.D.	N.D.	N.D.	N.D.	17	N.D.
*HLA-DRB1*03:01, *03:02, and *03:03 also react with DR3 to a lesser extent than *03:04 and *03:07.								

Table 2.4. MPO epitopes and *in vitro* HLA binding partners. IC50 values under 100 are indicative of high affinity binding to HLA, values between 100 and 1000 represent good binding pairs, and values greater than 1000 indicate lack of binding to the HLA.

Discussion

Immune recognition of self-proteins plays an important role in the early pathogenesis of autoimmune disease. Identifying specific epitopes within these self-proteins that immune cells react to is critical not only to further elucidate disease pathogenesis, but also for the development of new therapies for patients. Additionally, we may be able to identify patterns of epitope autoreactivity that will lead to the identification of previously unrecognized autoantigens. Our analysis of previously reported regions of MPO revealed the buried nature of B cell epitope $MPO_{447\text{-}461}$, residues required for binding of patient ANCA, the alpha helical structure of $MPO_{435\text{-}461}$, and the ability of patient HLA to bind and present both the B cell and T cell epitopes.

Although the buried nature of $MPO_{447\text{-}461}$ is surprising, it is not unprecedented. An epitope identified by anti-glomerular basement membrane (GBM) antibodies is also buried and requires conformational changes of the antigen to be revealed (*146*). The buried nature of these epitopes implicates a substantial disruption to normal protein structure to reveal the antigenic epitopes. The possibility of buried antigenic peptides is also supported by several proposed mechanisms for the breakdown in peripheral tolerance that allow adaptive immune system recognition of self-proteins. These mechanisms include conformational changes that reveal new epitopes, overproduction of the self-antigen, post-translational modifications, or cellular mislocation of proteins (*147, 148*).

The Immune Epitope Database was used to predict regions of MPO and their HLA binding partners. As expected, not all of the epitopes identified by *in silico* predictions bound effectively to HLA during *in vitro* binding experiments, however both $MPO_{447\text{-}461}$ and $MPO_{435\text{-}454}$ had moderate to strong binding affinity for HLA-DPB1*04:01 and HLA-DRB4*01:01. These two epitopes were particularly interesting based on prior reports from both human and mouse

studies. Mouse $MPO_{409-428}$, which corresponds to human $MPO_{435-454}$, was reported as an immunodominant $CD4^+$ T cell epitope, and mouse $MPO_{431-439}$ (human $MPO_{457-465}$) was reported as a pathogenic CD8+ T cell epitope (*50, 115, 139*). These two epitopes overlap with our previously published B-cell epitope ($MPO_{447-459}$), discovered by epitope excision mass spectrometry, by eight and three amino acids respectively (or eight and five amino acids with $MPO_{447-461}$ used for the studies reported herein, Figure 2.8).

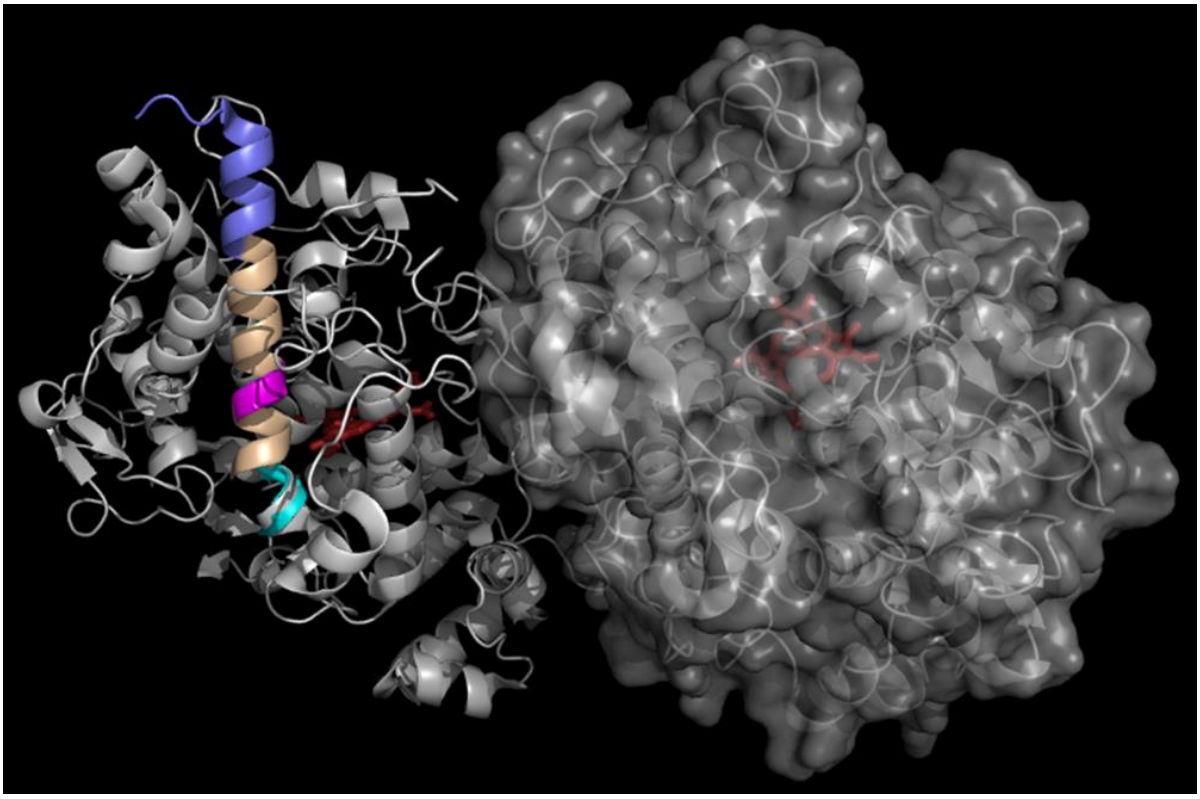

Figure 2.8. Human myeloperoxidase model based on crystal structure. (PDBID:5FIW) Highlighted regions are as follows; dark blue - $MPO_{435-454}$ (Ooi et al. 2012), purple- $MPO_{447-459}$ (Roth et al. 2013), light blue - $MPO_{457-465}$ (Chang et al. 2017), gold - overlap between highlighted regions. The active site heme of myeloperoxidase is colored red.

Further strengthening the importance of this region of MPO is a previous study, which utilized human-mouse chimeric MPO molecules. These studies demonstrated that sera from ten of fourteen patients bound the same region where these epitopes are located (*51*). However, there

are other MPO epitopes of interest on both the light (*52*) and heavy chains (*49, 51, 53-56*) that should be investigated using the methods described here.

Given patient autoantibody reactivity and MHC binding to previously identified epitopes, this region of MPO may be a strong candidate for reintroduction of immune tolerance. Mouse $MPO_{409-428}$ (corresponds to human $MPO_{435-454}$, our T cell epitope) has been used to reintroduce tolerance by nasal insufflation in a mouse model of focal necrotizing glomerulonephritis. Insufflation of this peptide afforded protection before onset of disease and partially ameliorated established autoimmune disease (*115*). This suggests that new antigen-specific therapies targeting this region of MPO may provide some relief for patients with MPO-ANCA vasculitis.

CHAPTER 3: AUTOREACTIVE CD4$^+$ T CELLS ARE PRO-INFLAMMATORY MEMORY CELLS THAT BIND MPO

Introduction

As mentioned in Chapter 2, despite convincing evidence that ANCA are pathogenic (*39*), the existence of naturally occurring anti-MPO antibodies in healthy individuals (*44*) and ANCA negative patients (*45*) complicate our understanding of ANCA vasculitis pathogenesis. Another possible explanation for this discrepancy is that T cells play an important role in disease pathogenesis beyond just B cell help via cytokine secretion. In addition to genetic associations with HLA, there is a significant body of work that implicates T cells in the pathogenesis of autoimmune diseases and ANCA vasculitis. First, T cells have been detected in the kidneys, lungs, and nasal biopsies in patients with ANCA vasculitis (*149*). Additionally, Sanders et al. showed an increase in soluble IL-2 and CD30 in the plasma of patients that correlated with disease activity (*150*), and Abdulahad et al. demonstrated an increase of circulating memory T cells in the urine of patients with active disease (*151*). Studies also suggest that CD4$^+$ T cells mediate MPO-ANCA production in patients (*152*). These findings represent just a snapshot of decades of research that make a clear case for the role of T cells in the pathogenesis of MPO ANCA vasculitis.

There is also a body of work that has suggested a pathogenic role for a pro-inflammatory subset of T cells, called Th17 cells, in glomerulonephritis (*153*). Numerous studies in mice have linked Th17 responses to organ specific autoimmune inflammation (*154*), rheumatoid arthritis (*155, 156*), and inflammatory bowel disease (IBD) (*157*), therefore they likely also play a role in ANCA vasculitis. Additionally, studies have demonstrated that immune dysregulation in

autoimmunity can be attributed to dysfunction of regulatory T cells (Treg) (*72*), hyperactivation of effector T cells (Teff) (*73*), or an imbalance of cell subsets (*158*). T cell studies in ANCA vasculitis report conflicting results of increased (*103*) and decreased Treg frequency (*104, 159*), as well as normal (*160*) and decreased Treg function (*103, 104, 159*). Additionally, effector T cell resistance to Treg suppression was reported in patients (*73*). Recent studies from our lab demonstrated increased but dysfunctional regulatory T cells in combination with an expanded pro-inflammatory, IL-17 producing, $CD25^{intermediate}$ population that is resistant to Treg cell suppression in patients (*105*).

Though most studies in ANCA vasculitis have focused on $CD4^+$ T cell subsets, CD8+ cytotoxic T cells have also been implicated in the pathogenesis of autoimmunity (*161*). Consistent with previous $CD4^+$ T cell findings, CD8+ T cells are more activated (*100, 162*), they have been identified in the kidney (*98, 163*), and their numbers correlate with eGFR at presentation in patients with ANCA vasculitis (*163*). Another study that performed transcriptional profiling of CD8+ T cells found an association between poor prognosis and expansion of a CD8+ memory T cell population in patients with ANCA vasculitis (*164*). Additionally, a mouse model of ANCA immunopathogenesis demonstrated that MPO specific CD8+ T cells exacerbated disease (*139*). However, CD8+ T cells differ from $CD4^+$ T cells in that they recognize peptides presented by MHC I instead of MHC II receptors, and they can kill cells directly via perforin and granzymes.

$CD4^+$ T cells identify antigens in tissue and peripheral blood via TCR binding to specific receptors on the surface of antigen presenting cells (APCs) called major histocompatibility complex (MHC). APCs bind antigen to form a peptide-MHC II complex that is presented to T cells and bound by the TCR. This binding is specific to the structure of the TCR, the antigen, and

the MHC molecule, and is the first step in the initiation of an immune cascade designed to destroy the pathogen. The rarity of autoreactive T cells, specificity and low affinity of these TCR-peptide-MHC interactions, and elusive autoantigens in many autoimmune diseases have hindered the study of this process in disease. However, recent enhancements to MHC II tetramers allow direct investigation of this interaction at a single cell level (*165*).

TCR sequencing is used to assess the clonality of T cells. Random gene rearrangement during development generates enormous TCR diversity within an individual, making it very unlikely that T cells with identical TCRs arise from independent T cell clones (*166, 167*). Clonal expansion of T cells occurs upon recognition of antigen and results in differentiation of clones with various effector and memory phenotypes to effectively fight pathogens. In autoimmunity, one recent study described a restricted TCR repertoire with public (shared) TCR alpha chains in a group of patients with type 1 diabetes (*168*), while another reported that the TCR repertoire in patient synovium is dominated by a small number of highly expanded clones in rheumatoid arthritis (*169*), suggesting clonal expansion of rare autoreactive T cells. Restricted clonality and the presence of public TCRs in autoimmunity suggest a role for an immunodominant epitope in the initial loss of immune tolerance. Additionally, identification of clonally expanded, autoreactive, public (shared) TCR sequences that are not found in non-pathogenic $CD4^+$ T cells may inform development of TCR directed therapy.

In Chapter 3, I investigated the ability of patient $CD4^+$ T cells to bind B cell epitope $MPO_{447\text{-}461}$ and T cell epitope $MPO_{435\text{-}454,}$ introduced in Chapter 2. We are predominantly interested in $CD4^+$ helper T cells because of previously described GWAS and HLA sequencing studies that implicated HLA alleles that encode MHC II receptors (HLA-DP and HLA-DQ alleles) in disease. I tested the hypothesis that autoreactive $CD4^+$ T cells in MPO-ANCA

vasculitis are $CD25^{intermediate}$ pro-inflammatory cells that bind specific regions of the respective autoantigen (B cell epitope $MPO_{447-461}$ and/or T cell epitope $MPO_{435-454}$), that these cells are clonally restricted compared to control T cells, and that there are some public or shared TCRs between patients. Using MHC II tetramers, flow cytometry, and TCR sequencing, I attempted to identify a signature of $CD4^+$ T cell autoreactivity that distinguishes these cells from non-pathogenic $CD4^+$ T cells. The ability to precisely identify autoreactive cells will inform the use of chimeric antigen receptor techniques to selectively target autoreactive cells, or design antigen specific regulatory T cells to replace the faulty Tregs in patients (*119*). Furthermore, if this T cell autoreactivity signature includes unique surface marker expression, apheresis may be used to selectively remove pathogenic cells (*170*).

Materials and Methods

Study Design

The objective of these experiments was to understand the interaction between MPO epitopes $MPO_{447-461}$ and $MPO_{435-454}$ and patient $CD4^+$ T cells. Patients with ANCA vasculitis were enrolled at University of North Carolina at Chapel Hill clinics and followed in the Glomerular Disease Collaborative Network (*127, 128*). Patients and healthy controls were recruited according to the guidelines of the Institutional Review Board (study no. 97–0523) by the University of North Carolina Office of Human Research Ethics. Study subjects gave informed, written consent and participated according to University review board guidelines.

Patient Cohort

Patients were diagnosed according to the Chapel Hill Consensus Conference (*18, 129*). Patient charts were reviewed by clinicians to confirm disease activity status, periods of relapse, periods of remission, and serotype prior to analysis. ANCA serotypes were assessed by indirect immunofluorescence and antigen-specific PR3 and MPO enzyme-linked immune-absorbent

assays (ELISA) (*130*). Disease activity was determined by the 2003 Birmingham Vasculitis Activity Score (BVAS) in conjunction with clinical signs of activity. In this study, patients with a BVAS of 0 and no clinical or laboratory evidence of active disease were considered to be in remission. Active disease was defined as a BVAS >0 with clinical and/or laboratory evidence of disease (*131*). Patients with suspected or confirmed drug-induced forms of AAV or overlapping disease were excluded. Patients that were ANCA negative by ELISA and healthy controls were used as comparator groups.

Demographic features of the study subjects (Table 3.1). For tetramer studies, patients were chosen based on HLA sequencing status as carriers of HLA-DPB1*04:01 and HLA-DRB4*01:01. Our patient cohort consisted of homozygous (n=4 for HLA-DRB4*01:01, n=6 for HLA-DPB1*04:01), heterozygous (n=8 for HLA-DRB4*01:01 and n=8 for HLA-DPB1*04:01), and null (n=5 for HLA-DRB4*01:01 and n= 4 for HLA-DPB1*04:01) patients for each HLA. Non-HLA-DPB1*04:01 alleles for heterozygous and null patients are included in Table 3.2. Patients that carried both HLA were tested with both sets of tetramers. Healthy controls with (n=2 for HLA-DRB4*01:01, n=4 for HLA-DPB1*04:01) and without (n=3 for HLA-DRB4*01:01, n=1 for HLA-DPB1*04:01) the HLA alleles of interest, and heterozygous ANCA negative patients (n=3) were tested as controls.

Characteristic		Tetramer Cohort (N=23)	IL-17 Functional Studies Cohort (N=8)	Healthy control (N=5)
Age (years)				
	Mean ± SD	60 ± 19	68±18	49± 13
	Median(IQR)	60(48, 74)	68(63, 81)	54(37, 55)
Sex				
	Female	13(57%)	3(38%)	3(60%)
	Male	10(43%)	5(63%)	2(40%)
Ethnicity				
	White	19(83%)	7(88%)	5(100%)
	Black	3(13%)	0(0%)	0(0%)
	Hispanic	1(4%)	0(0%)	0(0%)
	Unknown	0(0%)	1(13%)	0(0%)
Serology				
	KIV	2(9%)	0(0%)	NA
	MPO	20(87%)	8(100%)	NA
	NEG	1(4%)	0(0%)	NA
Diagnosis				
	EGPA	2(9%)	0(0%)	NA
	GPA	6(26%)	3(38%)	NA
	GPA-PULM LIM	1(4%)	0(0%)	NA
	Lim	4(17%)	2(25%)	NA
	MPA	10(43%)	3(37%)	NA
BVAS *				
	Mean ± SD	2 ± 3	1 ± 3	NA
	Median(IQR)	0(0, 3)	0(0,0)	NA
***Disease Duration** (months)*				
	Mean ± SD	113± 52	100 ± 67	NA
	Median(IQR)	107(75, 140)	89(48, 74)	NA
Medication 6 months prior to sample				
	AZA/Imuran	3(13%)	0(0%)	NA
	MMF/Cellcept/Prednisone	1(4%)	0(0%)	NA
	Rituximab/MMF/Cellcept	1(4%)	1(13%)	NA
	no meds	12(52%)	2(25%)	NA
	not DB	1(4%)	1(13%)	NA
	Prednisone	2(9%)	2(25%)	NA
	Rituximab	1(4%)	1(13%)	NA
	Rituximab/prednisone	2(9%)	1(13%)	NA

Table 3.1. Demographics summary for tetramer studies cohort. Healthy controls were reasonably well matched to patients on age, gender, and race. *There were three missing values for BVAS.

Allele	Carriers
01:01	2
02:01	5
03:01	1
04:02	5
05:01	1
06:01	1
10:01	1
13:01	1
14:01	1

Table 3.2. Non-HLA-DPB1*04:01 alleles in tetramer studies cohort. List of alleles other than *04:01 of null (n=5) and heterozygous (n=8) patients included in tetramer studies.

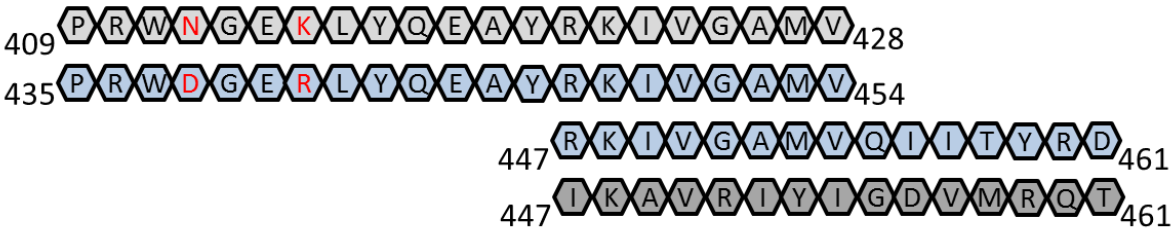

Figure 3.1. Amino acid sequence alignment of mouse and human myeloperoxidase. Mouse $MPO_{409-428}$ (light grey), human $MPO_{435-454}$ (blue), human $MPO_{447-461}$ (blue), and human $MPO_{447-461scramble}$ (dark grey). Amino acid differences between mouse and human epitopes shown in red.

MHC II Tetramer Studies

Tetramers were generated (Benaroya Institute, CA) for both HLA-DPB1*04:01 and HLA-DRB4*01:01 as previously described (*171*) by exogenously loading recombinant protein with the following MPO epitopes: $MPO_{447-461}$ (RKIVGAMVQIITYRD) and $MPO_{435-454}$ (PRWDGERLYQEARKIVGAMV). Tetramers created with $MPO_{447-461}$ scramble (IKAVRIYIGDVMRQT) were used as a control for both HLA alleles. To assess specificity of reactivity to the peptide, tetramers with both HLA-DPB1*04:01, HLA-DRB4*01:01, and

corresponding mouse $MPO_{409-428}$ (PRWNGEKLYQEAYRKIVGAMV) were created (Figure 3.1).

Patient peripheral blood mononuclear cells (PBMCs) were isolated from cell preparation tubes (CPT, BD Biosciences), washed twice with phosphate buffered saline (PBS, Life Technologies) and stored in 1mL RPMI with 10% FBS at 4°C overnight. Cells were then counted and resuspended at $5x10^6$/mL in RPMI with 10% FBS, blocked (Human TruStain FcX, Biolegend) for 10 minutes at 37°C. $5x10^5$ cells per condition were incubated with either no tetramer, or 2uL of one of the following tetramers: DPB1*04:01-$MPO_{447-461}$, DPB1*04:01-$MPO_{435-454}$, DPB1*04:01-$MPO_{447-461}$ scramble, DRB4*01:01-$MPO_{447-461}$, DRB4*01:01-$MPO_{435-454}$, or DRB4*01:01-$MPO_{447-461}$ scramble for 1 hour at 37°C. Cells were then washed, stained with a panel including CD4 (BioLegend, clone RPA-T4), CD8 (BioLegend, clone HIT8a), CD14 (BioLegend, clone 63D3), CD19 (Life Technologies, clone SJ25-C1), CD25 (BioLegend, clone BC96), and CD127 (BioLegend, clone A019D5) or a panel including CD4 (BioLegend, clone RPA-T4), CD8 (BioLegend, clone HIT8a), and CD45RO (BioLegend, clone UCHL1). Cells were acquired on an LSRII flow cytometer (BD), and analyzed using FlowJo software (Tree Star). Tetramer positive cells were detected after exclusion of doublets, followed by gating on lymphocytes, then $CD4^+$/CD8- cells, and tetramer positivity was set according to a no tetramer control for each patient (Figure 3.2).

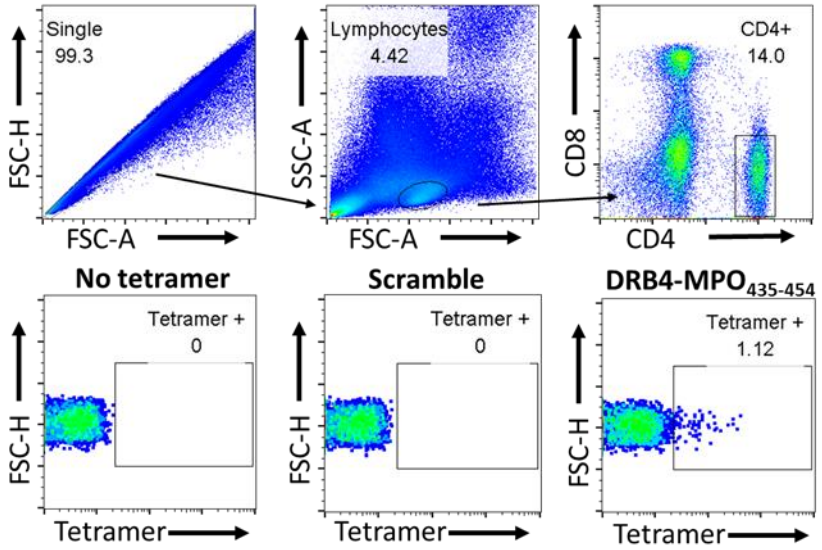

Figure 3.2. Strategy for gating tetramer$^+$ CD4$^+$ lymphocytes. Gating includes no tetramer control, $MPO_{447-461}$ scramble control, and HLA-DRB4 $MPO_{435-454}$. Tetramer positivity gate for each individual was set based on the corresponding no-tetramer control.

Cytokine Capture for IL-17A

Cytokine capture experiments for IL-17A production were also performed on patient PBMCs. Staining was performed following the kit protocol (IL-17A secretion assay PE, Miltenyi Biotec). Briefly, cells were stained with tetramer, incubated with CytoStim (human, Miltenyi Biotec) for 4 hours at 37 degrees, and then stained with capture and detection antibodies, CD4, CD8, CD25, and CD127 before fixation and analysis on a LSRII flow cytometer (BD), and analyzed using FlowJo software (Tree Star). IL-17A secreting cells were detected after exclusion of doublets, followed by gating on lymphocytes, and CD4$^+$/CD8$^-$ cells (Figure 3.2). Controls samples without stimulation and without IL-17A antibody were used to set positive thresholds for each patient (Figure 3.3).

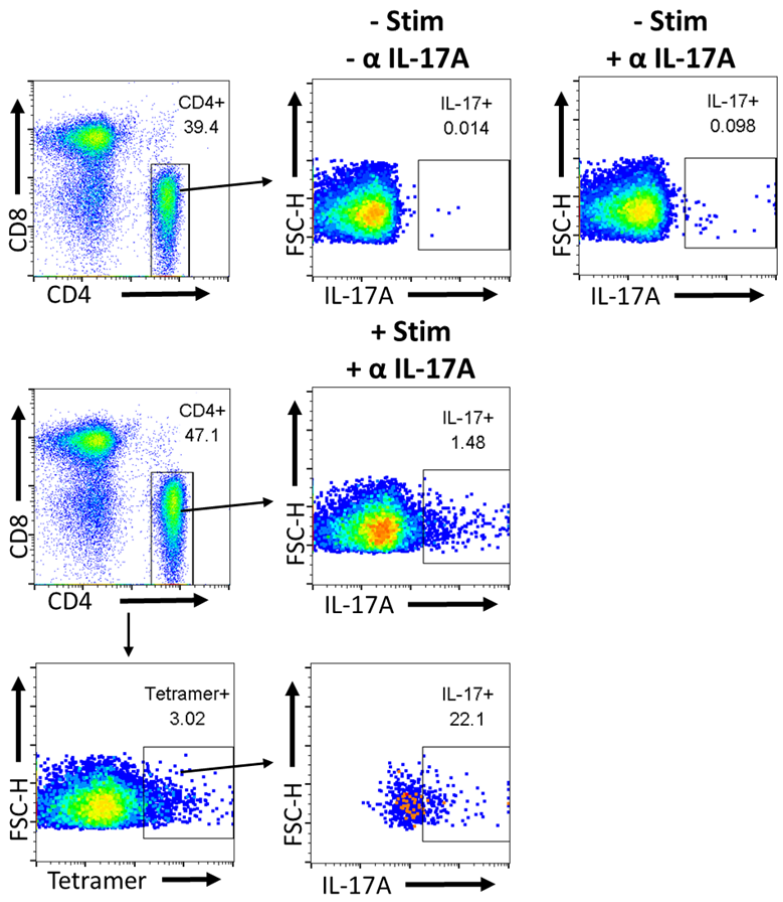

Figure 3.3. Gating strategy for IL-17A positivity. Representative plot shows gating scheme for determining percentage of IL-17A secreting cells for all $CD4^+$ and tetramer positive cells in patients compared to no stimulation and no antibody (α IL-17A) controls.

Flow Sorting

Samples were prepared for flow sorting as follows; patient peripheral blood mononuclear cells (PBMCs) were isolated from cell preparation tubes (CPT, BD Biosciences), washed twice with phosphate buffered saline (PBS), counted, resuspended at $50x10^6$/mL in RPMI with 10% FBS, and blocked (Human TruStain FcX, Biolegend) for 10 minutes at 37°C. PBMCs were then incubated with 3uL of DRB4*01:01-$MPO_{435-454}$ per $30x10^6$ cells for 1 hour at 37°C. Cells were then washed, stained with a panel including CD4 (BioLegend, clone RPA-T4), CD8 (BioLegend, clone HIT8a), CD14 (BioLegend, clone 63D3), CD19 (Life Technologies, clone SJ25-C1),

CD25 (BioLegend, clone BC96), and CD127 (BioLegend, clone A019D5). Cells were sorted into PBS using a Becton Dickinson FACSAria II (BSL-2) flow cytometer with a 70µm nozzle.

RNA Isolation

Immediately after flow sorting, RNA was isolated from sorted T cell populations using RNAqueous Micro Total RNA Isolation Kit (TermoFisher Scientific), and frozen at -80°C until library preparation.

TCR Sequencing

T cell receptor beta repertoire profiling was done with repertoire diversity measures adjusted for differential read coverage done as previously described (*172, 173*). Briefly, RNA quantity was assessed by bioanalyzer before processing with the SMARTer ® Human TCR a/b Profiling Kit (kit lot # 1512025A). Post library prep, library concentration was measured by Qubit 2.0 Fluorometer using the dsDNA HS Assay Kit (lot# 1910791). Qubit was calibrated using the dsDNA HS standards #1 and #2 (0ng/ul and 10ng/ul respectively), then samples were diluted 1ul in 199ul of the assay buffer and run on Qubit after the standards. Samples were then run on an Agilent Technologies 2200 Tapestation to determine library size in base pairs using the High Sensitivity D1000 screentape and associated buffer (2ul buffer:2ul sample). Samples were then diluted to 10nM with SMARTer ® Human TCR a/b Profiling Kit elution buffer, based on Qubit concentrations and pooled in equal volumes. Qubit and tapestation were repeated on the final pool. The pool was loaded it on to a MiSeq at the UNC High Throughput Sequencing Facility at 13.5pM.

Statistical Analysis

GraphPad Prism was used to generate figures (Version 7, GraphPad Software, La Jolla, CA). For T cell receptor Beta (TRB) analysis, amplicon read quality was assessed using FastQC, indicating read counts and Phred scores were comparable for all samples with all samples having

over 250K reads. TRB clones were aligned and assembled using MiXCR 2.1.9 (*174*) with imgt library version 201802-5 (*175*). Diveristy metrics were calculated on the nucleotide sequnce of Complementarity-Determining Region 3 (CDR3) of productive clones. Uncorrected diversity metrics included Abundance (read counts for a clone), Richness (number of unique clones), Shannon Entropy (calculated in R (*176*) using vegan::diversity (*177*) and Evenness (Shannon Entropy / Log Richness). The following normalized diversity metrics were calculated using VDJTools (*178*) to bootstrap counts 100x to the lowest number of aligned reads for all samples: Observed Diversity, Shannon-Wiener, Normalized Shannon-Wiener and d50. VDJTools was also used to exprapolate species number out to the highest read count (ChaoE) and asymptotic diversity (Chao1 and Efron-Thisted). Diversity metrics were compared using a T-Test for two group comparison and an ANOVA for more than two groups. Patient Identity was taken into account for these comparisons. False Discovery Rate corrections were done using the Benjamini-Hochberg method (*179*) using R ((*176*); stats::p.adjust). Morisita Horn Similarity Indices were performed on the amino acid CDR3 sequence of productive clones using the 'horn' method (*180*) of vegan::vegdist (*177*). The Morisita-Horn Dissimilarity Indices were subtracted from one to get the Similarity Indices presented. T-Tests were used to compare differences in these Indices between groups. Graphs were made using ggplot2 (*181*).

Results

MHC II tetramers identify patient autoreactive $CD4^+$ T cells

MHC II tetramers were used to investigate epitope specificity of autoreactive $CD4^+$ T cells in patients with MPO-ANCA vasculitis. While some patients had low responses across all tetramers (Figures 3.4A-3.4F), greater reactivity was demonstrated in response to $MPO_{435-454}$ with both HLA-DPB1*04:01 and HLA-DRB4*01:01 (Figure 3.4A & 3.4D), and a decreased, but still positive, response to $MPO_{447-461}$ in the HLA-DPB1*04:01 tetramer (Figure 3.4E) compared

to controls. Overall, healthy controls and patients who do not carry the corresponding HLA had low or undetectable tetramer binding (Figure 3.4A-F, HLA-DPB1 alleles other than *04:01 for null and heterozygous patients shown in Table 3.2).

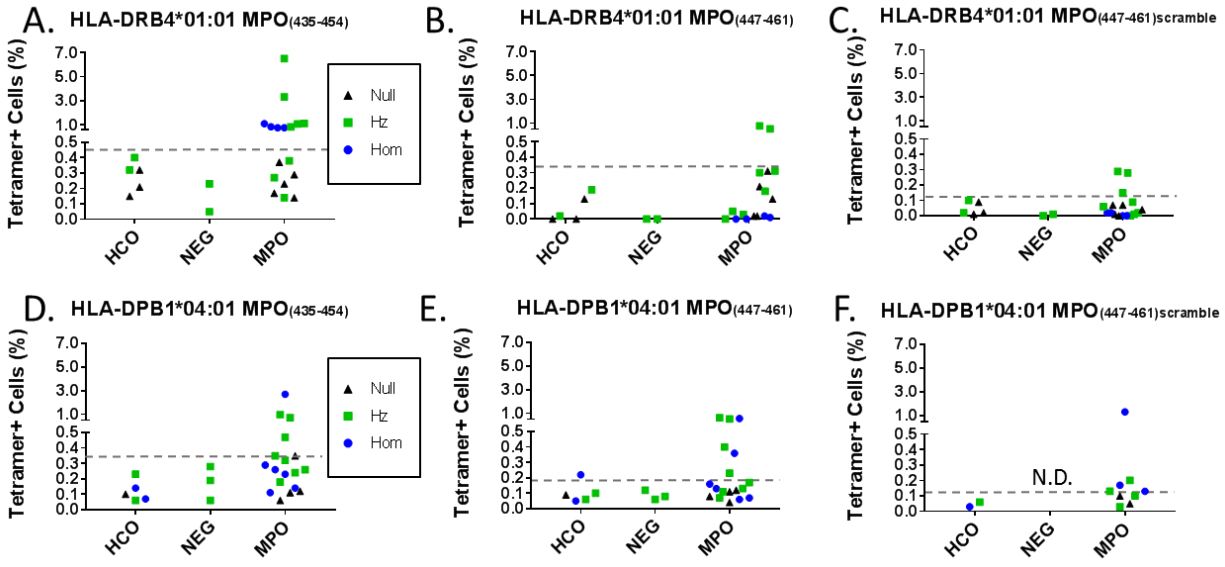

Figure 3.4. Patients demonstrate HLA and epitope specific tetramer recognition by $CD4^+$ T cells. (A-F) $CD4^+$ T cell recognition of tetramers in MPO-ANCA patients (n=20), ANCA negative patients (n=3), and healthy controls (n=5). Dashed grey line indicates threshold of positivity determined by the average plus two standard deviations of healthy control and null patient tetramer positivity. (A) HLA-DRB4*01:01 tetramer carrying $MPO_{435-454}$ (B) HLA-DRB4*01:01 tetramers carrying $MPO_{447-461}$ (C) HLA-DRB4*01:01 tetramer carrying $MPO_{447-461}$ scramble control. (D) HLA-DPB1*04:01 tetramer carrying $MPO_{435-454}$ (E) HLA-DPB1*04:01 tetramer carrying $MPO_{447-461}$ (F) HLA-DPB1*04:01 tetramer carrying $MPO_{447-461}$ scramble control.

When comparing reactivity of patient $CD4^+$ T cells to human $MPO_{435-454}$ and mouse $MPO_{409-428}$ using HLA-DPB1*04:01 tetramers, we found consistently higher reactivity to the human epitope (Figure 3.5A). In contrast, some patients demonstrate more $CD4^+$ T cell reactivity to HLA-DRB4*01:01 tetramers carrying mouse $MPO_{409-428}$ than human $MPO_{435-454}$, while others had minimal reactivity to both tetramers (Figure 3.5B). This again demonstrates that $CD4^+$ T cell reactivity to MPO is both epitope and MHC dependent.

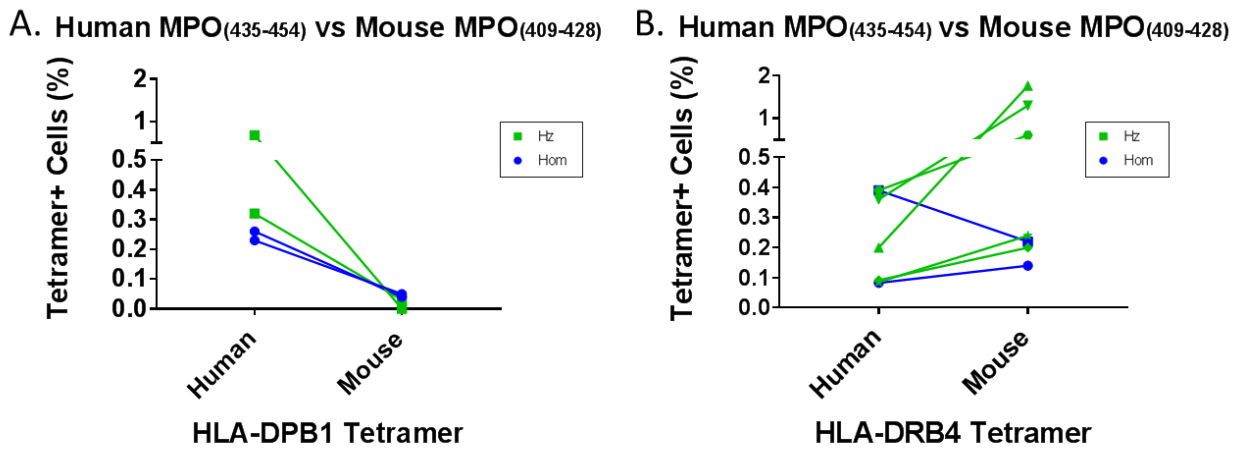

Figure 3.5. Epitope specificity of Patient $CD4^+$ tetramer binding. Patient $CD4^+$ T cells preferentially bind human $MPO_{435-454}$ over mouse MPO $MPO_{409-428}$ when presented with HLA-DPB1*04:01, but not with HLA-DRB4*01:01. (A) Comparison of patient (n=4) $CD4^+$ T cell recognition of HLA-DPB1*04:01 tetramers carrying human $MPO_{435-454}$ or mouse $MPO_{409-428}$. (B) Comparison of patient (n=7) $CD4^+$ T cell recognition of HLA-DRB4*01:01 tetramers carrying human $MPO_{435-454}$ or mouse $MPO_{409-428}$.

To further investigate the specificity of tetramer binding, dual tetramer staining was performed with the B cell epitope (DPB1*04:01-PE-$MPO_{447-461}$) and the T cell epitope (DPB1*04:01-PE/Cy5-$MPO_{435-454}$) loaded in the same HLA. We found that nearly all tetramer positive cells were positive for both tetramers (Figure 3.6), suggesting that the overlapping region of these epitopes may be required for binding to HLA. This supposition is also supported by the open binding pocket structure of MHC II receptors that allows for variable length epitope binding but relies on nine core residues (*182*).

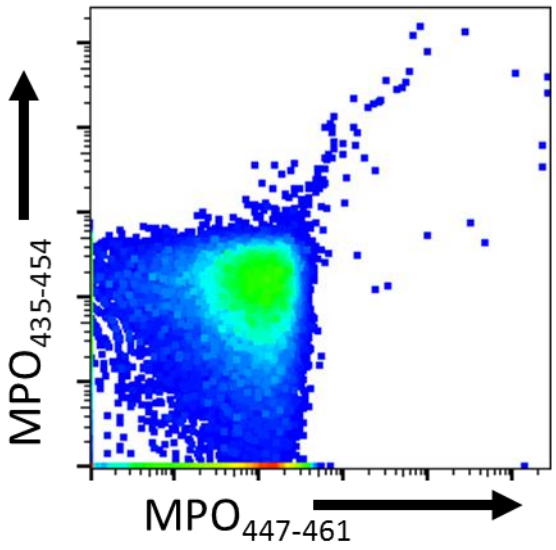

Figure 3.6. Dual staining reveals dual binding ability of patient CD4$^+$ T cells. Dual staining with DPB1*04:01 PE-MPO$_{447-461}$ and PE Cy5-MPO$_{434-454}$ tetramers day 1 ex-vivo. Plot shows n=4 patients concatenated due to low tetramer positivity of patient CD4$^+$ T cells.

Autoreactive CD4$^+$ T cells are enriched for CD25^{intermediate} memory effector cells

Tetramer positive CD4$^+$ T cells were further characterized for CD25 and CD127 expression and a significant portion of tetramer positive cells were CD25^{intermediate}CD127$^+$ cells (13.3%-77.4% across all tetramers, 44.7% average for MPO$_{447-461}$, 49.6% average for MPO$_{435-454}$), as previously described (Figure 3.7) (*105*).

Tetramer positive cells were also assessed for the presence of memory marker CD45RO on their surface. Consistently greater than 50% of the tetramer positive population expressed memory marker CD45RO (60% average across all tetramers). This is consistent with a previous report from our group that characterized CD25^{intermediate} cells as memory cells (*105*).

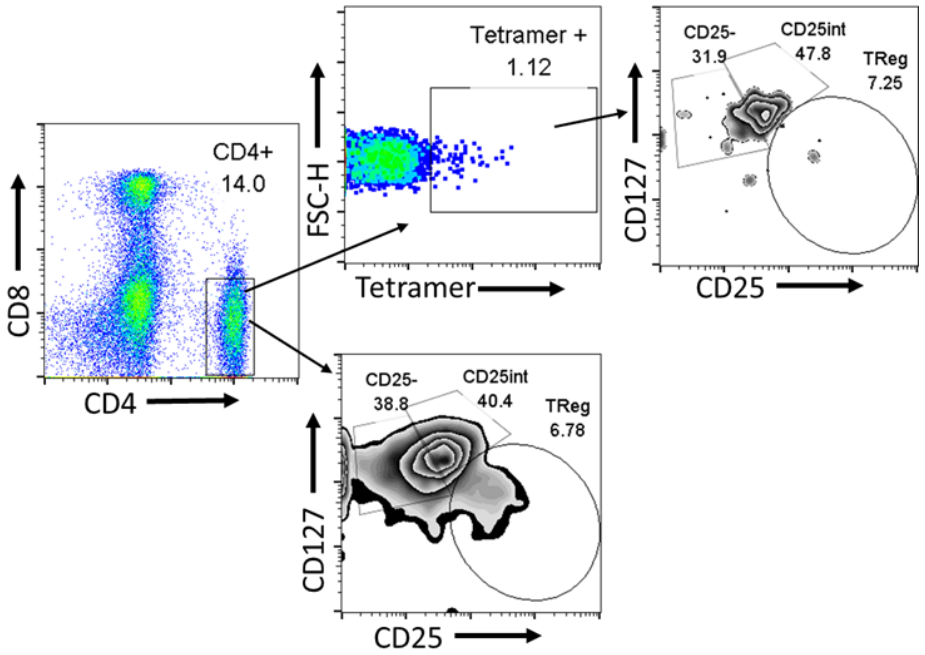

Figure 3.7. Patient $CD4^+$ T cells that bind tetramers are enriched for $CD25^{intermediate}$ cells. (A) Gating strategy for $CD25^{intermediate}$ cells using a representative patient. Consistently half of tetramer positive cells were $CD25^{intermediate}$ T cells (n=14).

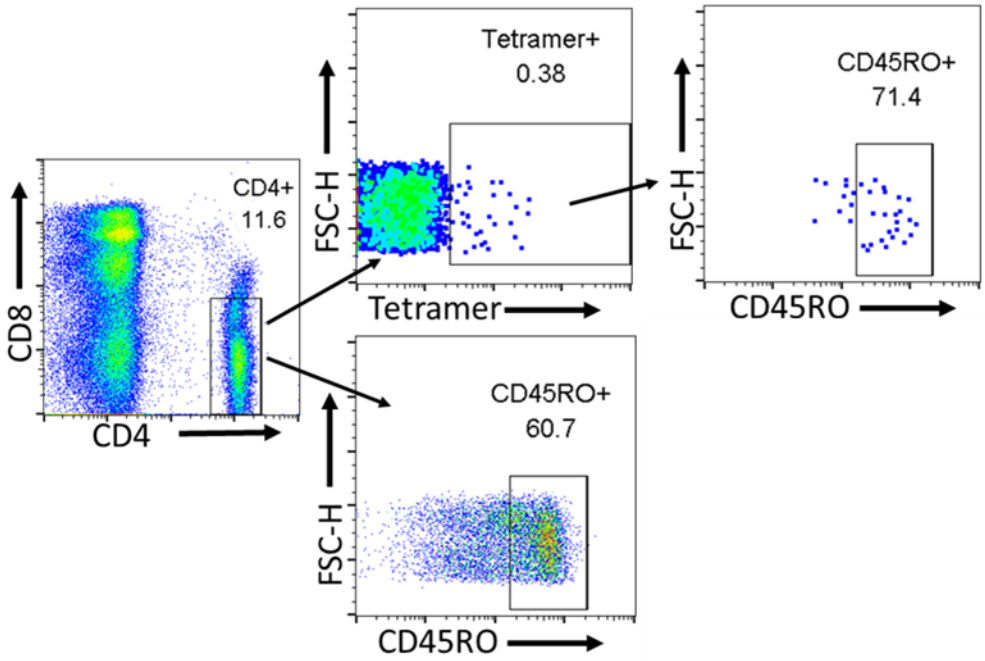

Figure 3.8. Patient $CD4^+$ T cells that bind tetramers are enriched for memory marker CD45RO. Representative plot demonstrating that the expression of $CD45RO^+$ was slightly higher in tetramer positive cells than overall $CD4^+$ T cells.

Autoreactive CD4$^+$ T cells secrete IL-17A

Based on previous reports of cytokine secretion in autoimmunity and ANCA vasculitis, we investigated the ability of patient autoreactive CD4$^+$ T cells to secrete IL-17A (*105, 156, 157*). We compared IL-17A secretion of tetramer positive CD4$^+$ T cells to IL-17A secretion by total CD4$^+$ T cells in each patient. For these studies, tetramers with both HLA-DPB1 and HLA-DRB4 carrying the T cell epitope $MPO_{435-454}$ were used. A higher proportion of tetramer positive cells secreted IL-17A in response to stimulation than total CD4$^+$ T cells for each patient regardless of HLA restriction, confirming the pro-inflammatory ability of the autoreactive CD4$^+$ T cells (Figure 3.9).

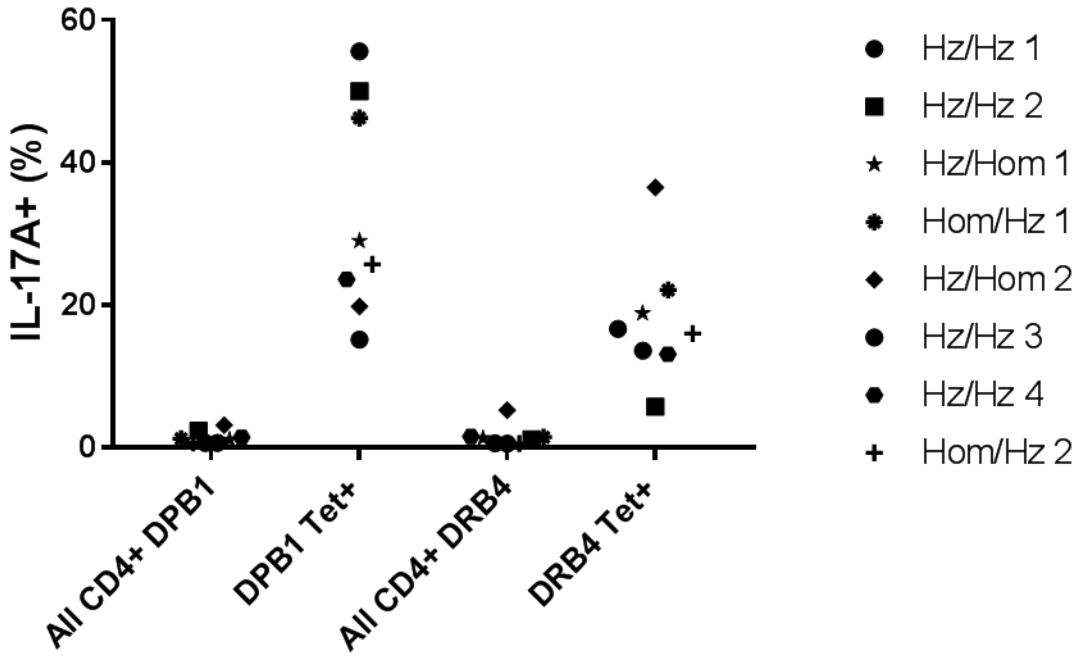

Figure 3.9. Patient CD4$^+$ T cells that bind tetramers are pro-inflammatory cells that secrete IL-17A. Compared to all CD4$^+$ T cells, a higher proportion of tetramer positive CD4$^+$ T cells secrete IL-17A in patients for both HLA-DPB1*04:01 and HLA-DRB4*01:01 (n=8). Patients included in experiments were either Hom = homozygous, Hz = heterozygous for HLA-DPB1*04:01/HLA-DRB4*01:01.

Autoreactive $CD4^+$ T cells are clonally restricted compared to controls

We next sought to understand whether $MPO_{435-454}$ specific T cells showed evidence of clonal expansion relative to the tetramer negative, $CD25^{intermediate}$, $CD25^-$, and regulatory T cell populations. Utilizing the MiSeq platform, we analyzed the TCR repertoires of four FACS sorted T cell populations ($tetramer^+$, $CD25^{intermediate}$, $CD25^-$, and Tregs). The HLA-DRB4*01:01 tetramer carrying $MPO_{435-454}$ was used exclusively for these experiments based on consistent patient reactivity to it (Figure 1D), to collect as many cells as possible from the rare tetramer positive population. HLA-DRB4*01:01-$MPO_{435-454}$ specific T cell receptor repertoires showed decreased species richness, Shannon entropy, and d50 indices, consistent with diminished T cell receptor repertoire diversity in the antigen-specific T cell population compared to all controls (Figure 3.10A). Interestingly, we also observed a decrease in TCR repertoire diversity in the $CD25^{intermediate}$ memory effector cells compared to naïve $CD25^-$ T cells. Treg diversity was not different from memory $CD25^{intermediate}$ T cells, but was decreased compared to $CD25^-$ naïve T cells. Importantly, matched uncorrected (Abundance, Richness, Shannon Entropy, Evenness, Figure 3.10B) and matched extrapolated (ChaoE, Chao1, Efron Thisted, Figure 3.10C) diversity measures replicated the same patterns of diversity between populations as the matched bootstrapped diversity measures. These results suggest increased clonal expansion of MPO reactive $CD4^+$ T cells compared to unselected $CD25^{intermediate}$ memory, $CD25^-$ naïve, and regulatory T cell populations, supporting chronic antigen exposure in these patients.

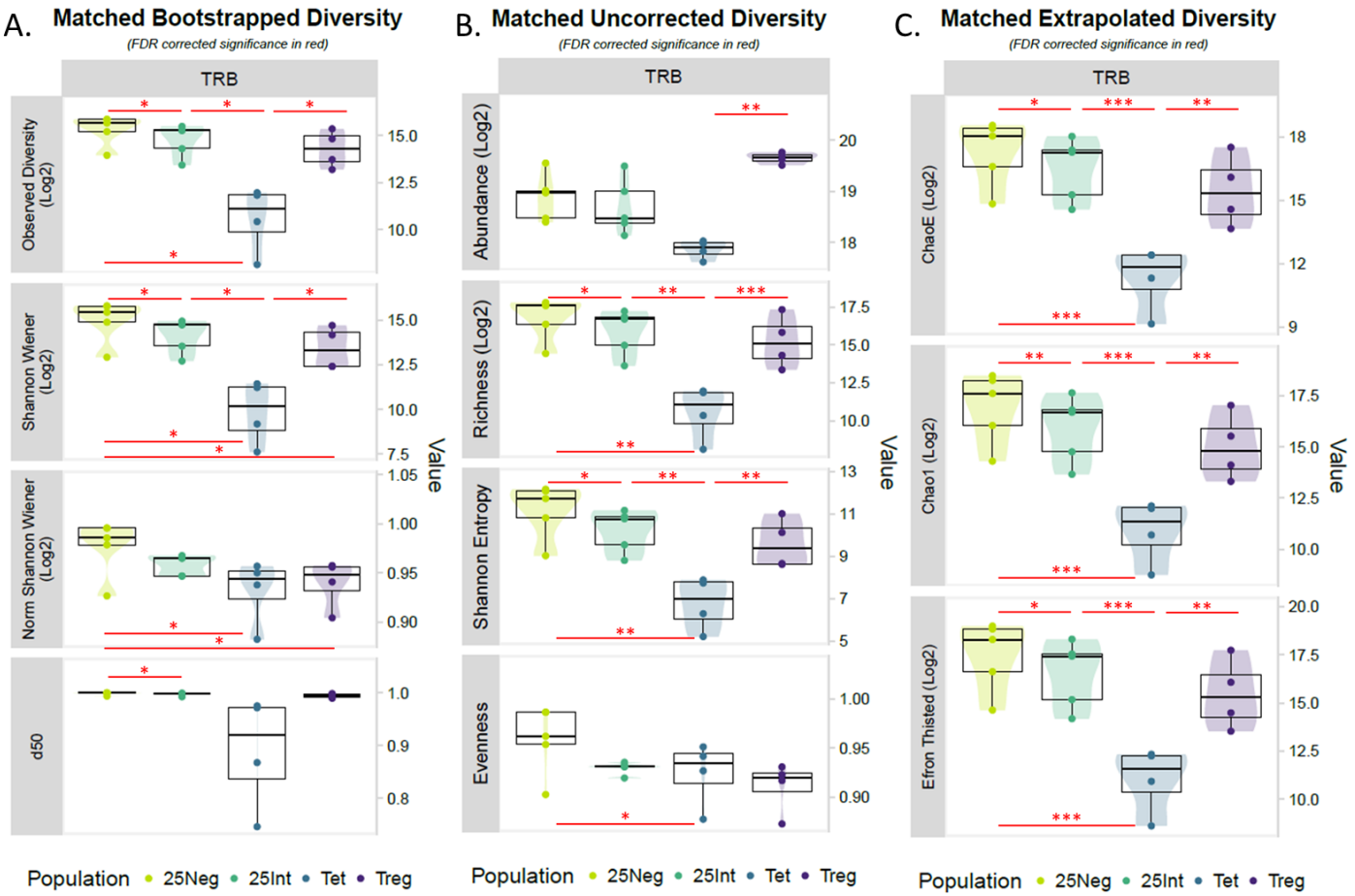

Figure 3.10. Patient tetramer positive cells demonstrate decreased TCR diversity compared to controls. Decreased diversity of $MPO_{435-454}$ specific T cells relative to unselected $CD25^{intermediate}$, $CD25^{-}$, and regulatory T cells. (A) Matched bootstrapped diversity indices including species richness, Shannon entropy, and d50 (B) Matched uncorrected diversity indices including Abundance, Richness, Shannon Entropy, and Evenness and (C) Matched Extrapolated Diversity indices including ChaoE, Chao1, and Efron Thisted derived from T cell receptor beta profiling (patient n=5) and corrected for false discovery rate (FDR). Patients missing $tetramer^{+}$ and Treg samples (n=1 each) were excluded from matched pairwise comparisons involving these populations. * $p<0.05$, ** $p<0.01$, ***$p<0.001$.

TCR sequencing reveals some public TCR clones

We also investigated T cell receptor Beta (TRB) clonotype similarity between patients to identify any public TCR clones. Although we do not see any TCR sharing between the antigen selected tetramer positive cell populations in patients as we predicted (Figure 3.11), we do see some TCR sharing within the $CD25^-$ naïve T cell populations of two patients (Figure 3.11A). Similarly, we see less but still some TCR sharing between two different patients within the $CD25^{intermediate}$ population (Figure 3.11B). Considering that these cells were not selected for antigen reactivity, the vast diversity of possible TCR arrangements, and that both patients have MPO-ANCA vasculitis, it is highly unlikely that these public TCRs are due to chance. These results suggest T cell dysregulation in patients beyond MPO antigen specificity of TCRs.

In addition to pairwise TRB colonotype similarity comparisons, we performed population comparisons for TRB subunit frequency. T cell receptor beta variable (TRBV) analysis reveals a trend toward decreased TRBV6-2 subunit usage in both tetramer positive and Treg populations, and increased TRBV6-3 subunit usage in both tetramer positive and Treg populations compared to $CD25^-$ naive and $CD25^{intermediate}$ T cell populations (Figure 3.12). It is possible that these differences indicate a shift from TRBV6-2 to TRBV6-3 usage in the tetramer positive and regulatory T cell populations in patients with MPO-ANCA vasculitis. We also assessed T cell receptor beta joining (TRBJ) subunit frequency and found no differences between tetramer positive cells and control T cell populations (Figure 3.13). This result is not surprising given the limited number of joining (J) gene segments.

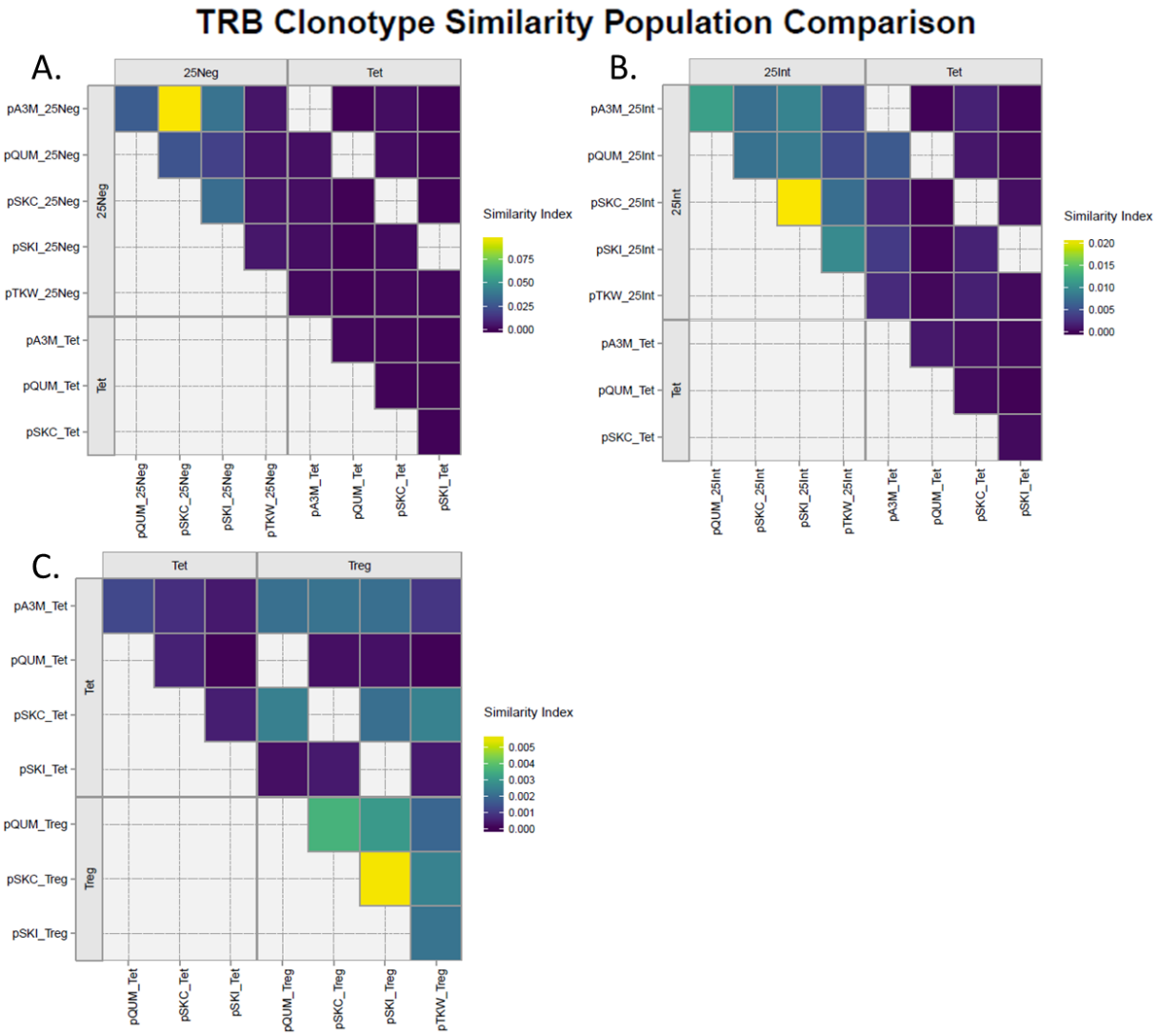

Figure 3.11. Clonotype population comparison reveals CD25^{-} naive and CD25^{intermediate} memory T cell clones shared between two patients. Comparison of tetramer positive and control T cell clonotype populations in n=5 patients (n=4 for tetramer and Treg samples). (A) comparison of tetramer positive and CD25^{-} naive T cell clonotypes (B) comparison of tetramer positive and CD25^{intermediate} memory T cell clonotypes and (C) comparison of tetramer positive and regulatory T cell clonotypes. Note that similarity index colors are consistent between plots while similarity index values change.

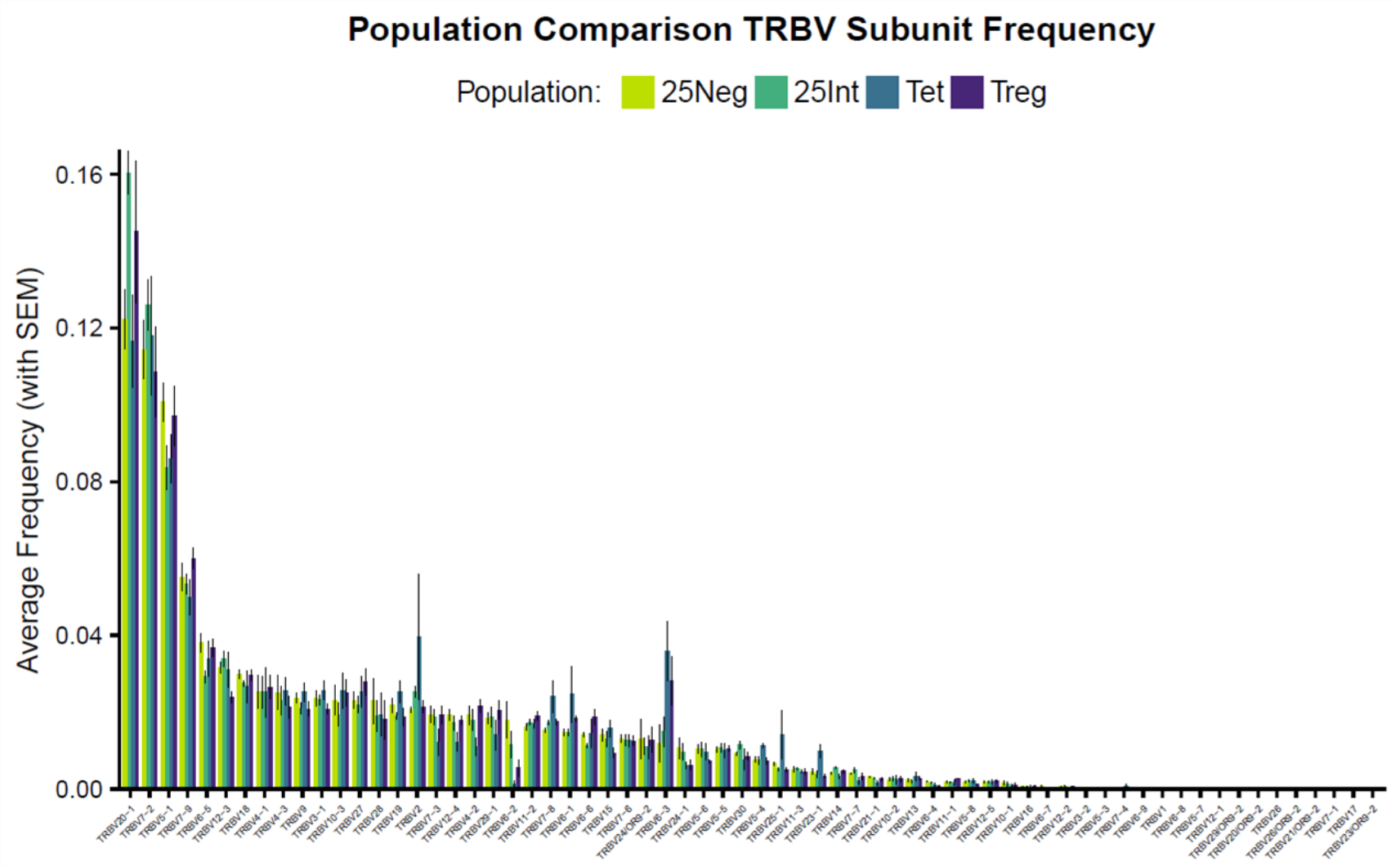

Figure 3.12. TRBV subunit frequency analysis reveals differences in TRBV-6 subunit usage between tetramer positive cells and control T cell populations. None of the differences were statistically significant (n=5 patients, n=4 for tetramer and Treg samples).

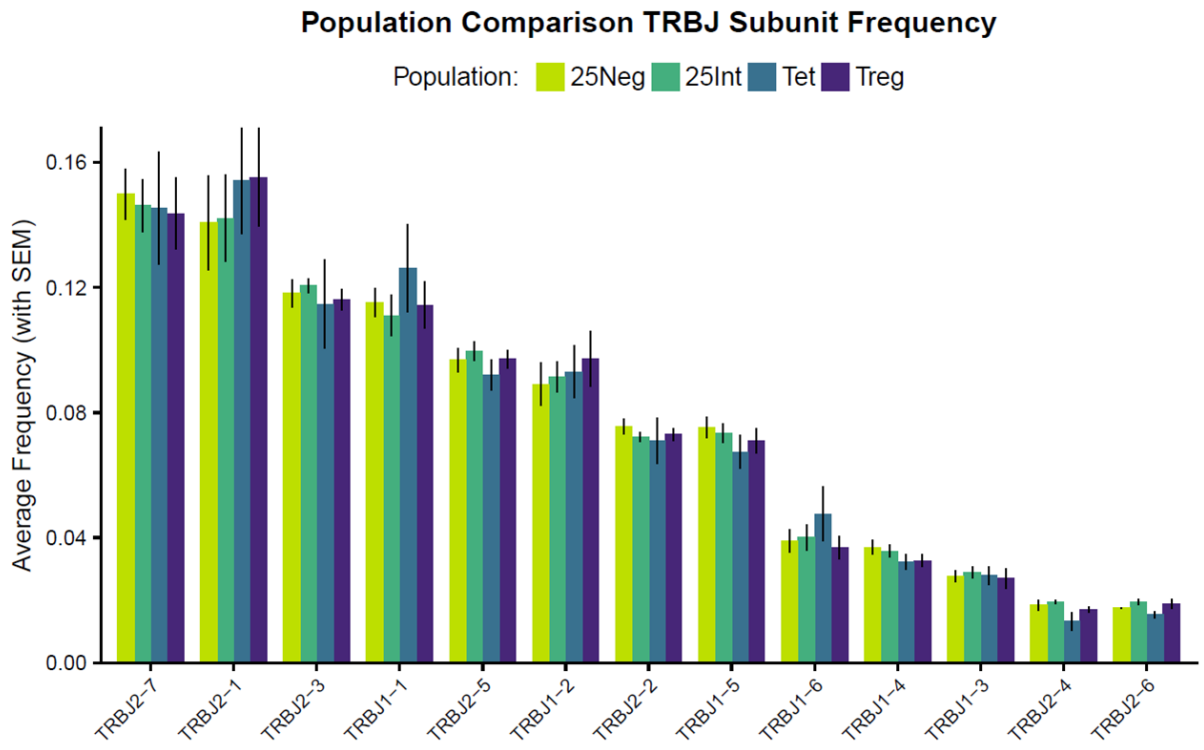

Figure 3.13. TRBJ subunit frequency analysis reveals no differences in joining subunit usage between tetramer positive cells and control T cell populations.

Discussion

Studies using MHC class II tetramers demonstrated that patients with HLA-DPB1*04:01, HLA-DRB4*01:01, or both, have $CD4^+$ T cells that recognize and bind specific regions of MPO (specifically B cell epitope $MPO_{447\text{-}461}$ and/or T cell epitope $MPO_{435\text{-}454}$) when stained directly *ex vivo* without stimulation. HLA-DPB1*04:01 and HLA-DRB4*01:01 were chosen for tetramer analysis based on binding to the epitopes of interest during *in vitro* studies and their prevalence in our patient cohort. Our ability to detect measurable frequencies of tetramer positive $CD4^+$ T cells directly *ex vivo* suggests chronic autoantigen exposure *in vivo* to maintain these autoreactive cells at detectable levels.

Approximately half of the tetramer positive $CD4^+$ T cells were $CD25^{intermediate}$CD127+ cells, which suggests that these may be activated effector memory cells, a conclusion further

supported by positivity for memory marker CD45RO. We also assessed IL-17A secretion of patient T cells based on results from previous work that demonstrated increased IL-17A, increased IL-4, and unchanged interferon gamma (IFN-γ) secretion from $CD25^{intermediate}$ cells compared to control $CD4^+$ T cells in patients (*105*). When compared to overall $CD4^+$ T cells, a higher proportion of tetramer positive cells secrete IL-17A upon stimulation suggesting that these autoreactive cells are primed and poised to respond in a pro-inflammatory manner. Together, these results suggest that tetramer positive $CD25^{intermediate}$ T cells are autoreactive cells that play a role in the immunopathogenesis of MPO-ANCA vasculitis.

Additionally, dual positivity of the HLA-DPB1*04:01 tetramers suggests the overlapping region between these two epitopes may contain the most important residues for immune recognition in patients with HLA-DPB1*04:01. It is also possible that this dual staining is explained by non-specific binding of these tetramers, though the difference in T cell binding to HLA-DPB1*04:01 tetramers with the mouse and human versions of the T cell epitope (Figure 3.5A) makes this explanation less likely.

TCR sequencing revealed decreased diversity of the autoreactive $CD4^+$ TCR repertoire compared to $CD25^{intermediate}$, $CD25^-$, and regulatory T cell controls, which supports chronic antigen exposure leading to clonal expansion of the autoreactive cells in patients. This stepwise decrease in diversity from $CD25^-$ naïve cells, to $CD25^{intermediate}$ memory cells, to our $MPO_{435-454}$ reactive cells underscores the specificity of this $CD4^+$ T cell response to MPO. Interestingly, the regulatory T cell population is most similar to $CD25^{intermediate}$ cells with regard to TCR diversity. Population TCR comparisons revealed some receptor sharing between patients, though not in the tetramer positive population of cells. One explanation is that we are missing existing tetramer positive cells with public TCR clones located at sites of inflammation because we are sampling

$CD4^+$ T cells from peripheral blood. Another possible explanation is that patient autoreactive $CD4^+$ T cells start as a diverse population of cells with shared clones between patients, but that different cells end up clonally expanding in different patients, narrowing the repertoire and masking any sharing upon analysis. Finally, TRBV analysis reveals a shift in TRBV6-2 to TRBV6-3 subunit usage in $tetramer^+$ and regulatory T cells, but not in $CD25^-$ naïve or $CD25^{intermediate}$ T cell populations. Though not significant, if this shift is present in additional patients, it may reveal a role for TRBV subunit usage in that pathogenesis of MPO-ANCA vasculitis.

These surface staining and TCR sequencing experiments reveal some markers of $CD4^+$ T cell autoreactivity in patients, though they do not identify a unique autoreactivity signature. Additional experiments including RNA sequencing of tetramer positive cells and control populations may reveal other markers in this signature. Eventually, this signature can be used to develop CAR T cells that specifically target autoreactive cells. For now, this work provides new insight into the interactions between HLA, antigenic peptides, and the CD4+ T cell-mediated adaptive immune response that will inform the development of these new therapies for patients with MPO-ANCA vasculitis and other autoimmune diseases.

Summary

The presented body of work focused on the interactions between autoreactive cells and pathogenic epitopes in ANCA vasculitis. Chapter 1 assessed HLA sequence based typing of a large cohort (n=249) of patients with ANCA vasculitis and revealed, contrary to previous reports, that carriage of HLA-DPB1*04:01 does not increase risk of relapse in a combined (MPO and PR3-ANCA) cohort. Additionally, this analysis identified HLA-DPB1*04:01 and HLA-DRB4*01:01 as highly represented alleles in our cohort of MPO-ANCA vasculitis patients. This chapter also included a discussion of the differences between MPO and PR3 ANCA-vasculitis

and reasons for studying pathogenic epitopes and autoreactive cells for each serotype independently.

Chapter 2 investigated previously identified epitopes $MPO_{447\text{-}461}$ and $MPO_{435\text{-}454}$ for patient autoantibody reactivity, binding to MHC receptors, structural characteristics, and solvent exposure. These studies showed that $MPO_{447\text{-}461}$ and $MPO_{435\text{-}454}$ are located on the same alpha helix, that this alpha helical structure is required for anti-$MPO_{447\text{-}461}$ binding, and that $MPO_{447\text{-}461}$ is buried while $MPO_{435\text{-}454}$ is exposed to solvent. Additionally, ELISA studies revealed that 53% of patients have anti-$MPO_{447\text{-}461}$ antibodies, most often at onset. Finally, *in vitro* binding studies confirmed the ability of $MPO_{447\text{-}461}$, $MPO_{435\text{-}454}$, and a scrambled control epitope to bind HLA-DPB1*04:01 and HLA-DRB4*01:01.

Chapter 3 combined knowledge from chapters 1 and 2 to create HLA-DPB1*04:01 and HLA-DRB4*01:01 tetramers carrying $MPO_{447\text{-}461}$ and $MPO_{435\text{-}454}$ and a scrambled control. Studies using these tetramers identified autoreactive $CD4^+$ T cells in patients that were pro-inflammatory (IL-17 secretion), memory (CD45RO expression), $CD25^{intermediate}$ cells. TCR sequencing revealed increased clonal expansion of tetramer positive autoreactive cells compared to naïve and memory T cell controls from the same patient. TRB analysis also revealed some shared clones between patient $CD25^-$ and $CD25^{intermediate}$ T cell populations and altered TRBV subunit frequency in $tetramer^+$ and regulatory $CD4^+$ T cell populations. These data further implicate $CD4^+$ T cells in the etiology and pathogenesis of MPO-ANCA vasculitis and provide targets for the development new therapies.

Taken together, these results elucidate the specific interaction between B and $CD4^+$ T cells and MPO epitopes in patients with MPO-ANCA vasculitis. We characterized each piece of

the cell-mediated adaptive immune response including MHC receptor, peptide, and TCR to better understand the loss of immune tolerance in our patients. Ideally, these discoveries will pave the way to antigen-specific therapies and improved quality of life for patients suffering from ANCA vasculitis and other autoimmune conditions.

EPILOGUE: RESTRICTED EPITOPE RECOGNITION IN PATIENTS WITH MPO-ANCA VASCULITIS

Considering the significant homology between human and mouse whole MPO (86.5% identical, 94.4% similar), the minor amino acid differences between this region in mouse and human MPO supports the hypothesis that autoantigens reside in highly conserved domains (*183*). This region of MPO also fits the hypothesis that many important autoantigens are enzymes engaged in important biological functions, and that the immune response is often directed at the active/catalytic site of the antigen (*184*). While this region of interest does not fall directly adjacent to the active site of MPO, based on the crystal structure of human MPO, $MPO_{447\text{-}461}$ is adjacent to an alpha helix that stabilizes the active site and interacts with the implicated alpha helix via a hydrogen bond and hydrophobic residues (Figure E.1).

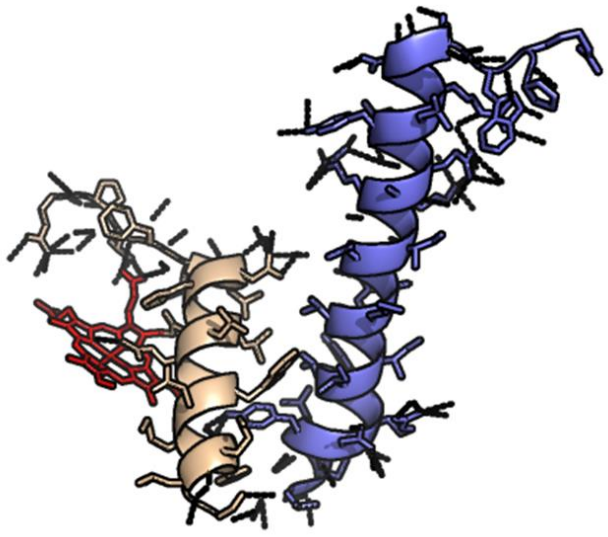

Figure E.1. $MPO_{435\text{-}461}$ in relation to the active site of MPO. Interactions between $MPO_{435\text{-}461}$ (blue) and the neighboring alpha helix that stabilizes the active site (red) include multiple hydrogen bonds and hydrophobic contacts (highlighted in red) PRWDGERLYQEAYRKIVGAMVQIITYRDYL.

Given that the B cell epitope $MPO_{447-461}$ is buried within MPO, the structure of MPO must be substantially disrupted to facilitate an IgG-directed immune response to this epitope in patients. The location of this epitope in proximity to the active site of MPO suggests that a substantial structural disruption that would make $MPO_{447-461}$ accessible to the immune system would likely also disturb the active site. The events leading to this disruption of MPO that reveal buried epitopes to the immune system may be equally as important for the autoimmune process as the presence of autoreactive cells. Possible explanations for this structural disruption include misfolding and/or protease cleavage of MPO, possibly due to overexpression in patient neutrophils. This is an intriguing possibility because the epitope for anti-glomerular basement membrane (GBM) antibodies is also buried and requires conformational changes of the antigen to be revealed (*146*).

Of the twelve patients included in both tetramer and ELISA studies, half with ANCA reactivity to $MPO_{447-461}$ by ELISA also demonstrated tetramer reactivity to at least one peptide from the same MPO region. Therefore, this region of MPO contains overlapping B and T cell epitopes. This is important to consider for the development of future therapies designed to induce tolerance using T cell epitopes as they may lead to an unintentional autoantibody response in patients. While overlapping B and T cell epitopes have been reported in infection (*185, 186*), other studies have reported that separate, although often adjacent, epitopes are required for efficient B and T cell collaboration (*187*). These data combined with previously reported immunogenicity in mice suggest an important role for overlapping MPO epitopes in the coordination of both the B cell and T cell components of adaptive immunity in MPO-ANCA vasculitis.

While it is clear that the region of MPO we chose to assess is involved in disease immunopathogenesis, there may be other pathogenic regions. Previous studies demonstrated autoantibody reactivity to other regions of MPO on both the light (*52*) and heavy chains (*49, 51, 53-55*). One study, Fujii et al., used recombinant deletion mutations within specific regions of MPO to identify B and T cell epitopes and found some recognition of this region (Hc; $MPO_{409-474}$), but higher reactivity to other regions of the heavy chain of MPO (Ha; $MPO_{279-341}$, Hb; $MPO_{341-409}$, and Hg; $MPO_{598-745}$) (*56*). Although epitopes within the region $MPO_{435-461}$ have been implicated in disease immunopathogenesis for some patients, there may be a combinatorial effect with other HLA-peptide combinations, and some patients may have reactivity to other regions of MPO exclusively. It is also possible that patients have T cell autoreactivity to conformational (non-continuous) epitopes, though identification and confirmation of these epitopes is technically very challenging. Importantly, one group has demonstrated evidence that nasal insufflation of an epitope in this region induced tolerance to whole MPO in a mouse model of ANCA vasculitis (*115*), so it is possible to restore immune tolerance to an entire autoantigen with the use of a single pathogenic epitope.

Future Directions

The studies reported here examine immune reactivity to one very specific piece of MPO. As described above, other regions of MPO have been implicated in disease and should be investigated. Additionally, the studies presented here reveal additional HLA-peptide combinations of interest that should be investigated. For example, HLA-DQ alleles have been associated with MPO-ANCA vasculitis in multiple GWAS studies (*59, 70*) and our *in silico* and *in vitro* binding studies identified $MPO_{105-119}$ as a potential binding partner. However, it is clear that $MPO_{435-461}$ plays a role in disease pathogenesis. The results presented here inform the design of antigen specific therapies using epitopes in this region to reintroduce tolerance in disease. Gan

et al. demonstrated disease amelioration with nasal insufflation of a peptide in this region in a mouse model of ANCA vasculitis immunopathogenesis (*115*). Additionally, tolerogenic dendritic cell therapies are now in clinical trials for some autoimmune diseases (*120, 121*). New treatments that harness nanoparticle presentation of antigen, tolerogenic dendritic cell presentation of antigen, or antigen targeted cells should be pursued using this region of MPO in pursuit of better therapies for patients with MPO-ANCA vasculitis.

Another aspect of the autoimmune response in ANCA vasculitis that we have yet to investigate is the role of CD8+ cytotoxic lymphocytes. Similar *in silico* binding predictions, *in vitro* binding studies, and tetramer studies may be performed using MHC I tetramers to identify antigenic regions of MPO that patient CD8+ T cells are recognizing. Studies in mice have demonstrated the pathogenic potential of CD8+ T cells in a model of anti-MPO glomerulonephritis and identified a pathogenic CD8+ T cell epitope $MPO_{431-439}$, which corresponds to human $MPO_{457-465}$ and overlaps with our B cell epitope $MPO_{447-461}$ (*139*). It is definitely worth investigating patient CD8+ T cell reactivity to this region in patients with MPO-ANCA vasculitis.

These studies do not address the relationship between T cell autoreactivity to $MPO_{435-461}$ and disease activity. This may be addressed in future studies using paired samples from patients at times of active disease and remission, or cross-sectionally with a large cohort including patients in disease remission and with active disease. These studies also raise the question of how immunosuppressive medication alters the presence of autoreactive cells. While some of the patients in our cohort were in remission and untreated for a year or more, every patient used for the tetramer studies has a history of at least some immunosuppressive therapy. Although performing these studies in new onset ANCA vasculitis patients prior to therapy is ideal, the

need for high-resolution HLA typing information makes tetramer experiments technically unattainable unless patients have been typed prior to disease onset and tetramers are available. Studies to assess the effects of common immunosuppressive medication on tetramer reactivity may be informative in this case.

Flow cytometry is a powerful tool that has greatly increased our understanding of immune cell subsets since it was first developed. However, the technique is limited by fluorophore spectral overlap, which restricts the number of markers that can be assessed at any given time in one population of cells. It is also a targeted method where surface markers of interest are determined before doing the experiment. In contrast, RNA sequencing of cells provides an unbiased look at the expression of all genes within specific populations of cells. The sheer number of cells that needed to be sequenced for informative gene expression data once limited the practicality of this method, but technological advancements now allow efficient sequencing of rare cell populations. RNA sequencing can reveal heterogeneity within cell populations that share the same surface markers but have different gene expression profiles, or it can be used to identify similarities between seemingly diverse populations of cells. For example, this technique identified a signature that distinguishes populations of Th17 cells, which can be pathogenic or non-pathogenic depending on cytokines in the environment during cell polarization (*188*). In this case, we can use this technique to identify similarities within a potentially diverse population of autoreactive cells. Defining a unique "autoreactive signature" will increase our understanding of how and why autoreactive $CD4^+$ T cells escape regulation in the periphery of patients.

Finally, studies of PR3-ANCA vasculitis have been hindered by a lack of animal models of disease (*138*). Ultimately analysis of MHC-peptide-TCR interactions described in this

dissertation should be performed for previously identified regions of both PR3 and complementary PR3. If patient $CD4^+$ T cells react to specific regions of complementary PR3, it may help narrow the search for the proposed infectious molecular mimic that causes disease induction. Given GWAS and HLA sequencing identification of HLA-DPB1*04:01 as a risk allele for patients with PR3-ANCA vasculitis (*1, 59, 69, 70*), and our results from chapter 1 that suggest carrier risk for PR3-ANCA vasculitis patients, pursuing epitopes predicted to bind this HLA will likely yield epitopes of interest. Due to the epitope specificity in most patients, therapies designed to reintroduce tolerance in patients with MPO-ANCA vasculitis will likely not be effective for patients with PR3-ANCA vasculitis, though the same methods may be effective for both. Therefore, it is imperative to identify pathogenic regions of PR3 that will inform development of new antigen specific therapies for patients with PR3-ANCA vasculitis.

Conclusions

This field is rapidly moving toward the use of antigen-specific therapies that either reintroduce immune tolerance using pathogenic autoantigen epitopes, or target antigen specific autoreactive cells. However, embarking on this quest requires a thorough understanding of the interaction between HLA, autoantigen peptides, and autoreactive B and T cells for each autoimmune disease. Here I identified and characterized the specific interactions between MHC II receptors, MPO epitopes, and $CD4^+$ TCRs that occur in patients with MPO-ANCA vasculitis. This work directly informs the design of new antigen-specific therapies for our patients.

REFERENCES

1. M. Hilhorst *et al.*, HLA-DPB1 as a Risk Factor for Relapse in Antineutrophil Cytoplasmic Antibody-Associated Vasculitis: A Cohort Study. *Arthritis & rheumatology (Hoboken, N.J.)* **68**, 1721-1730 (2016).

2. E. M. Tan, H. G. Kunkel, Characteristics of a soluble nuclear antigen precipitating with sera of patients with systemic lupus erythematosus. *Journal of immunology (Baltimore, Md. : 1950)* **96**, 464-471 (1966).

3. G. M. Edelman, H. G. Kunkel, E. C. Franklin, Interaction of the rheumatoid factor with antigen-antibody complexes and aggregated gamma globulin. *The Journal of experimental medicine* **108**, 105-120 (1958).

4. E. S. Lander, N. J. Schork, Genetic dissection of complex traits. *Science (New York, N.Y.)* **265**, 2037-2048 (1994).

5. K. W. Wucherpfennig, Structural basis of molecular mimicry. *Journal of autoimmunity* **16**, 293-302 (2001).

6. J. F. Bach, The hygiene hypothesis in autoimmunity: the role of pathogens and commensals. *Nature reviews. Immunology* **18**, 105-120 (2018).

7. G. A. Rook, R. Martinelli, L. R. Brunet, Innate immune responses to mycobacteria and the downregulation of atopic responses. *Current opinion in allergy and clinical immunology* **3**, 337-342 (2003).

8. F. M. Strickland, B. C. Richardson, Epigenetics in human autoimmunity. Epigenetics in autoimmunity - DNA methylation in systemic lupus erythematosus and beyond. *Autoimmunity* **41**, 278-286 (2008).

9. E. Maverakis *et al.*, Glycans in the immune system and The Altered Glycan Theory of Autoimmunity: a critical review. *Journal of autoimmunity* **57**, 1-13 (2015).

10. A. A. R. D. Association. (2017).

11. D. Jansen *et al.*, Flow Cytometric Clinical Immunomonitoring Using Peptide-MHC Class II Tetramers: Optimization of Methods and Protocol Development. *Frontiers in immunology* **9**, 8 (2018).

12. U. S. D. o. H. a. H. Services, "Autoimmune Diseases Research Plan," (National Institutes of Health).

13. M. D. Rosenblum, I. K. Gratz, J. S. Paw, A. K. Abbas, Treating human autoimmunity: current practice and future prospects. *Science translational medicine* **4**, 125sr121 (2012).

14. D. Liu *et al.*, A practical guide to the monitoring and management of the complications of systemic corticosteroid therapy. *Allergy, asthma, and clinical immunology : official journal of the Canadian Society of Allergy and Clinical Immunology* **9**, 30 (2013).

15. A. A. R. D. Association, "The Cost Burden of Autoimmune Disease: The Latest Front in the War on Healthcare Spending," (2011).

16. R. A. Watts *et al.*, Classification, epidemiology and clinical subgrouping of antineutrophil cytoplasmic antibody (ANCA)-associated vasculitis. *Nephrology, dialysis, transplantation : official publication of the European Dialysis and Transplant Association - European Renal Association* **30 Suppl 1**, i14-22 (2015).

17. D. L. Hirsch, P. Ponda, Antigen-based immunotherapy for autoimmune disease: current status. *ImmunoTargets and therapy* **4**, 1-11 (2015).

18. J. Jennette *et al.*, 2012 Revised International Chapel Hill Consensus Conference Nomenclature of Vasculitides. *Arthritis & Rheumatism* **65**, 1-11 (2013).

19. J. C. Jennette *et al.*, 2012 revised International Chapel Hill Consensus Conference Nomenclature of Vasculitides. *Arthritis and rheumatism* **65**, 1-11 (2013).

20. I. A. Mansi, A. Opran, F. Rosner, ANCA-associated small-vessel vasculitis. *American family physician* **65**, 1615-1620 (2002).

21. M. Walsh *et al.*, Risk factors for relapse of antineutrophil cytoplasmic antibody-associated vasculitis. *Arthritis and rheumatism* **64**, 542-548 (2012).

22. M. A. Little *et al.*, Early mortality in systemic vasculitis: relative contribution of adverse events and active vasculitis. *Annals of the rheumatic diseases* **69**, 1036-1043 (2010).

23. M. Faurschou *et al.*, Increased morbidity from ischemic heart disease in patients with Wegener's granulomatosis. *Arthritis and rheumatism* **60**, 1187-1192 (2009).

24. J. Robson *et al.*, Damage in the anca-associated vasculitides: long-term data from the European vasculitis study group (EUVAS) therapeutic trials. *Annals of the rheumatic diseases* **74**, 177-184 (2015).

25. R. Kettritz, J. C. Jennette, R. J. Falk, Crosslinking of ANCA-antigens stimulates superoxide release by human neutrophils. *Journal of the American Society of Nephrology : JASN* **8**, 386-394 (1997).

26. R. J. Falk, R. S. Terrell, L. A. Charles, J. C. Jennette, Anti-neutrophil cytoplasmic autoantibodies induce neutrophils to degranulate and produce oxygen radicals in vitro. *Proceedings of the National Academy of Sciences of the United States of America* **87**, 4115-4119 (1990).

27. A. J. Porges *et al.*, Anti-neutrophil cytoplasmic antibodies engage and activate human neutrophils via Fc gamma RIIa. *Journal of immunology (Baltimore, Md. : 1950)* **153**, 1271-1280 (1994).

28. N. Lepse, W. H. Abdulahad, C. G. Kallenberg, P. Heeringa, Immune regulatory mechanisms in ANCA-associated vasculitides. *Autoimmunity reviews* **11**, 77-83 (2011).

29. H. Xiao, P. Hu, R. J. Falk, J. C. Jennette, Overview of the Pathogenesis of ANCA-Associated Vasculitis. *Kidney diseases (Basel, Switzerland)* **1**, 205-215 (2016).

30. L. A. Charles, M. L. Caldas, R. J. Falk, R. S. Terrell, J. C. Jennette, Antibodies against granule proteins activate neutrophils in vitro. *Journal of leukocyte biology* **50**, 539-546 (1991).

31. B. H. Ewert, J. C. Jennette, R. J. Falk, Anti-myeloperoxidase antibodies stimulate neutrophils to damage human endothelial cells. *Kidney international* **41**, 375-383 (1992).

32. C. O. Savage, B. E. Pottinger, G. Gaskin, C. D. Pusey, J. D. Pearson, Autoantibodies developing to myeloperoxidase and proteinase 3 in systemic vasculitis stimulate neutrophil cytotoxicity toward cultured endothelial cells. *The American journal of pathology* **141**, 335-342 (1992).

33. J. Charles Jennette, R. J. Falk, L1. Pathogenesis of ANCA-associated vasculitis: observations, theories and speculations. *Presse medicale (Paris, France : 1983)* **42**, 493-498 (2013).

34. A. Wikman *et al.*, Antineutrophil cytoplasmic antibodies induce decreased CD62L expression and enhanced metabolic activity in monocytes. *Scandinavian journal of immunology* **57**, 179-184 (2003).

35. S. Weidner, W. Neupert, M. Goppelt-Struebe, H. D. Rupprecht, Antineutrophil cytoplasmic antibodies induce human monocytes to produce oxygen radicals in vitro. *Arthritis and rheumatism* **44**, 1698-1706 (2001).

36. R. Nowack, K. Schwalbe, L. F. Flores-Suarez, B. Yard, F. J. van der Woude, Upregulation of CD14 and CD18 on monocytes In vitro by antineutrophil cytoplasmic autoantibodies. *Journal of the American Society of Nephrology : JASN* **11**, 1639-1646 (2000).

37. R. J. Falk, J. C. Jennette, Anti-neutrophil cytoplasmic autoantibodies with specificity for myeloperoxidase in patients with systemic vasculitis and idiopathic necrotizing and crescentic glomerulonephritis. *The New England journal of medicine* **318**, 1651-1657 (1988).

38. J. L. Niles, R. T. McCluskey, M. F. Ahmad, M. A. Arnaout, Wegener's granulomatosis autoantigen is a novel neutrophil serine proteinase. *Blood* **74**, 1888-1893 (1989).

39. R. J. Falk, J. C. Jennette, ANCA are pathogenic--oh yes they are! *Journal of the American Society of Nephrology : JASN* **13**, 1977-1979 (2002).

40. J. C. Jennette, R. J. Falk, ANCAs are also antimonocyte cytoplasmic autoantibodies. *Clinical journal of the American Society of Nephrology : CJASN* **10**, 4-6 (2015).

41. H. Xiao *et al.*, Antineutrophil cytoplasmic autoantibodies specific for myeloperoxidase cause glomerulonephritis and vasculitis in mice. *The Journal of clinical investigation* **110**, 955-963 (2002).

42. F. Brunini, T. H. Page, M. Gallieni, C. D. Pusey, The role of monocytes in ANCA-associated vasculitides. *Autoimmunity reviews* **15**, 1046-1053 (2016).

43. G. S. Kerr *et al.*, Limited prognostic value of changes in antineutrophil cytoplasmic antibody titer in patients with Wegener's granulomatosis. *Arthritis and rheumatism* **36**, 365-371 (1993).

44. Z. Cui, M. H. Zhao, M. Segelmark, T. Hellmark, Natural autoantibodies to myeloperoxidase, proteinase 3, and the glomerular basement membrane are present in normal individuals. *Kidney international* **78**, 590-597 (2010).

45. M. Chen, C. G. Kallenberg, M. H. Zhao, ANCA-negative pauci-immune crescentic glomerulonephritis. *Nature reviews. Nephrology* **5**, 313-318 (2009).

46. F. J. van der Woude *et al.*, Autoantibodies against neutrophils and monocytes: tool for diagnosis and marker of disease activity in Wegener's granulomatosis. *Lancet (London, England)* **1**, 425-429 (1985).

47. X. Bossuyt *et al.*, Position paper: Revised 2017 international consensus on testing of ANCAs in granulomatosis with polyangiitis and microscopic polyangiitis. *Nature reviews. Rheumatology* **13**, 683-692 (2017).

48. S. J. Klebanoff, Myeloperoxidase: friend and foe. *Journal of leukocyte biology* **77**, 598-625 (2005).

49. A. J. Roth *et al.*, Epitope specificity determines pathogenicity and detectability in ANCA-associated vasculitis. *The Journal of clinical investigation* **123**, 1773-1783 (2013).

50. J. D. Ooi *et al.*, The immunodominant myeloperoxidase T-cell epitope induces local cell-mediated injury in antimyeloperoxidase glomerulonephritis. *Proceedings of the National Academy of Sciences of the United States of America* **109**, E2615-2624 (2012).

51. U. Erdbrugger *et al.*, Mapping of myeloperoxidase epitopes recognized by MPO-ANCA using human-mouse MPO chimers. *Kidney international* **69**, 1799-1805 (2006).

52. E. Pedrollo, L. Bleil, F. A. Bautz, J. R. Kalden, E. K. Bautz, Antineutrophil cytoplasmic autoantibodies (ANCA) recognizing a recombinant myeloperoxidase subunit. *Advances in experimental medicine and biology* **336**, 87-92 (1993).

53. K. Tomizawa *et al.*, A panel set for epitope analysis of myeloperoxidase (MPO)-specific antineutrophil cytoplasmic antibody MPO-ANCA using recombinant hexamer histidine-tagged MPO deletion mutants. *Journal of clinical immunology* **18**, 142-152 (1998).

54. K. Suzuki *et al.*, Analysis of risk epitopes of anti-neutrophil antibody MPO-ANCA in vasculitis in Japanese population. *Microbiology and immunology* **51**, 1215-1220 (2007).

55. B. F. Bruner, E. S. Vista, D. M. Wynn, J. A. James, Epitope specificity of myeloperoxidase antibodies: identification of candidate human immunodominant epitopes. *Clinical and experimental immunology* **164**, 330-336 (2011).

56. A. Fujii *et al.*, Epitope analysis of myeloperoxidase (MPO) specific anti-neutrophil cytoplasmic autoantibodies (ANCA) in MPO-ANCA-associated glomerulonephritis. *Clinical nephrology* **53**, 242-252 (2000).

57. D. J. Bautz *et al.*, Antibodies with dual reactivity to plasminogen and complementary PR3 in PR3-ANCA vasculitis. *Journal of the American Society of Nephrology : JASN* **19**, 2421-2429 (2008).

58. W. F. Pendergraft, 3rd, B. M. Pressler, J. C. Jennette, R. J. Falk, G. A. Preston, Autoantigen complementarity: a new theory implicating complementary proteins as initiators of autoimmune disease. *Journal of molecular medicine (Berlin, Germany)* **83**, 12-25 (2005).

59. P. A. Merkel *et al.*, Identification of functional and expression polymorphisms associated with risk for anti-neutrophil cytoplasmic autoantibody-associated vasculitis. *Arthritis & rheumatology (Hoboken, N.J.)*, (2016).

60. J. J. Yang *et al.*, Circumvention of normal constraints on granule protein gene expression in peripheral blood neutrophils and monocytes of patients with antineutrophil cytoplasmic autoantibody-associated glomerulonephritis. *Journal of the American Society of Nephrology : JASN* **15**, 2103-2114 (2004).

61. S. Ohlsson *et al.*, Increased monocyte transcription of the proteinase 3 gene in small vessel vasculitis. *Clinical and experimental immunology* **141**, 174-182 (2005).

62. E. A. McInnis *et al.*, Dysregulation of autoantigen genes in ANCA-associated vasculitis involves alternative transcripts and new protein synthesis. *Journal of the American Society of Nephrology : JASN* **26**, 390-399 (2015).

63. D. J. Ciavatta *et al.*, Epigenetic basis for aberrant upregulation of autoantigen genes in humans with ANCA vasculitis. *The Journal of clinical investigation* **120**, 3209-3219 (2010).

64. B. E. Jones *et al.*, Gene-Specific DNA Methylation Changes Predict Remission in Patients with ANCA-Associated Vasculitis. *Journal of the American Society of Nephrology : JASN* **28**, 1175-1187 (2017).

65. J. M. Vyas, A. G. Van der Veen, H. L. Ploegh, The known unknowns of antigen processing and presentation. *Nature reviews. Immunology* **8**, 607-618 (2008).

66. C. Kurts, B. W. Robinson, P. A. Knolle, Cross-priming in health and disease. *Nature reviews. Immunology* **10**, 403-414 (2010).

67. V. L. Crotzer, J. S. Blum, Autophagy and adaptive immunity. *Immunology* **131**, 9-17 (2010).

68. D. Schmid, M. Pypaert, C. Munz, Antigen-loading compartments for major histocompatibility complex class II molecules continuously receive input from autophagosomes. *Immunity* **26**, 79-92 (2007).

69. G. Xie *et al.*, Association of granulomatosis with polyangiitis (Wegener's) with HLA-DPB1*04 and SEMA6A gene variants: evidence from genome-wide analysis. *Arthritis and rheumatism* **65**, 2457-2468 (2013).

70. P. A. Lyons *et al.*, Genetically distinct subsets within ANCA-associated vasculitis. *The New England journal of medicine* **367**, 214-223 (2012).

71. J. Neefjes, M. L. Jongsma, P. Paul, O. Bakke, Towards a systems understanding of MHC class I and MHC class II antigen presentation. *Nature reviews. Immunology* **11**, 823-836 (2011).

72. S. A. Long, J. H. Buckner, CD4+FOXP3+ T regulatory cells in human autoimmunity: more than a numbers game. *Journal of immunology (Baltimore, Md. : 1950)* **187**, 2061-2066 (2011).

73. A. Schneider *et al.*, The effector T cells of diabetic subjects are resistant to regulation via CD4+ FOXP3+ regulatory T cells. *Journal of immunology (Baltimore, Md. : 1950)* **181**, 7350-7355 (2008).

74. M. J. Shlomchik, Sites and stages of autoreactive B cell activation and regulation. *Immunity* **28**, 18-28 (2008).

75. L. Klein, M. Hinterberger, G. Wirnsberger, B. Kyewski, Antigen presentation in the thymus for positive selection and central tolerance induction. *Nature reviews. Immunology* **9**, 833-844 (2009).

76. M. S. Anderson *et al.*, The cellular mechanism of Aire control of T cell tolerance. *Immunity* **23**, 227-239 (2005).

77. M. S. Anderson *et al.*, Projection of an immunological self shadow within the thymus by the aire protein. *Science (New York, N.Y.)* **298**, 1395-1401 (2002).

78. M. Yano *et al.*, Aire controls the differentiation program of thymic epithelial cells in the medulla for the establishment of self-tolerance. *The Journal of experimental medicine* **205**, 2827-2838 (2008).

79. J. Derbinski *et al.*, Promiscuous gene expression in thymic epithelial cells is regulated at multiple levels. *The Journal of experimental medicine* **202**, 33-45 (2005).

80. E. M. Shevach, CD4+ CD25+ suppressor T cells: more questions than answers. *Nature reviews. Immunology* **2**, 389-400 (2002).

81. D. S. Tan *et al.*, Thymic deletion and regulatory T cells prevent antimyeloperoxidase GN. *Journal of the American Society of Nephrology : JASN* **24**, 573-585 (2013).

82. F. McQueen, A B cell explanation for autoimmune disease: the forbidden clone returns. *Postgraduate medical journal* **88**, 226-233 (2012).

83. J. E. Lewis, S. M. Fu, F. Gaskin, Autoimmunity, end organ damage, and the origin of autoantibodies and autoreactive T cells in systemic lupus erythematosus. *Discovery medicine* **15**, 85-92 (2013).

84. O. T. Chan, M. P. Madaio, M. J. Shlomchik, The central and multiple roles of B cells in lupus pathogenesis. *Immunological reviews* **169**, 107-121 (1999).

85. R. Varela-Calvino, C. Calvino-Sampedro, I. Gomez-Tourino, O. J. Cordero, Apportioning Blame: Autoreactive CD4+ and CD8+ T Cells in Type 1 Diabetes. *Archivum immunologiae et therapiae experimentalis*, (2017).

86. C. Y. Hu *et al.*, Treatment with CD20-specific antibody prevents and reverses autoimmune diabetes in mice. *The Journal of clinical investigation* **117**, 3857-3867 (2007).

87. D. Wang, Y. Li, Y. Liu, G. Shi, The role of autoreactive T cell in the pathogenesis of rheumatoid arthritis and implications for T cell targeted vaccine therapy. *Minerva medica* **106**, 157-167 (2015).

88. J. C. Edwards *et al.*, Efficacy of B-cell-targeted therapy with rituximab in patients with rheumatoid arthritis. *The New England journal of medicine* **350**, 2572-2581 (2004).

89. J. H. Stone *et al.*, Rituximab versus cyclophosphamide for ANCA-associated vasculitis. *The New England journal of medicine* **363**, 221-232 (2010).

90. L. T. Aybar *et al.*, Reduced CD5(+) CD24(hi) CD38(hi) and interleukin-10(+) regulatory B cells in active anti-neutrophil cytoplasmic autoantibody-associated vasculitis permit increased circulating autoantibodies. *Clinical and experimental immunology* **180**, 178-188 (2015).

91. D. O. Bunch *et al.*, Gleaning relapse risk from B cell phenotype: decreased CD5+ B cells portend a shorter time to relapse after B cell depletion in patients with ANCA-associated vasculitis. *Annals of the rheumatic diseases* **74**, 1784-1786 (2015).

92. N. Dumoitier, B. Terrier, J. London, S. Lofek, L. Mouthon, Implication of B lymphocytes in the pathogenesis of ANCA-associated vasculitides. *Autoimmunity reviews* **14**, 996-1004 (2015).

93. S. K. Todd *et al.*, Regulatory B cells are numerically but not functionally deficient in anti-neutrophil cytoplasm antibody-associated vasculitis. *Rheumatology (Oxford, England)* **53**, 1693-1703 (2014).

94. M. A. Little *et al.*, Anti-proteinase 3 anti-neutrophil cytoplasm autoantibodies recapitulate systemic vasculitis in mice with a humanized immune system. *PloS one* **7**, e28626 (2012).

95. W. H. Abdulahad, Y. M. van der Geld, C. A. Stegeman, C. G. Kallenberg, Persistent expansion of CD4+ effector memory T cells in Wegener's granulomatosis. *Kidney international* **70**, 938-947 (2006).

96. P. Lamprecht *et al.*, CD28 negative T cells are enriched in granulomatous lesions of the respiratory tract in Wegener's granulomatosis. *Thorax* **56**, 751-757 (2001).

97. A. Komocsi *et al.*, Peripheral blood and granuloma CD4(+)CD28(-) T cells are a major source of interferon-gamma and tumor necrosis factor-alpha in Wegener's granulomatosis. *The American journal of pathology* **160**, 1717-1724 (2002).

98. A. E. Berden *et al.*, Cellular immunity in Wegener's granulomatosis: characterizing T lymphocytes. *Arthritis and rheumatism* **60**, 1578-1587 (2009).

99. E. Brouwer *et al.*, Predominance of IgG1 and IgG4 subclasses of anti-neutrophil cytoplasmic autoantibodies (ANCA) in patients with Wegener's granulomatosis and clinically related disorders. *Clinical and experimental immunology* **83**, 379-386 (1991).

100. M. Schlesier, T. Kaspar, J. Gutfleisch, G. Wolff-Vorbeck, H. H. Peter, Activated CD4+ and CD8+ T-cell subsets in Wegener's granulomatosis. *Rheumatology international* **14**, 213-219 (1995).

101. J. Gutfleisch *et al.*, Increased expression of CD25 and adhesion molecules on peripheral blood lymphocytes of patients with Wegener's granulomatosis (WG) and ANCA positive vasculitides. *Advances in experimental medicine and biology* **336**, 397-404 (1993).

102. E. R. Popa, C. A. Stegeman, N. A. Bos, C. G. Kallenberg, J. W. Tervaert, Differential B- and T-cell activation in Wegener's granulomatosis. *The Journal of allergy and clinical immunology* **103**, 885-894 (1999).

103. W. H. Abdulahad *et al.*, Functional defect of circulating regulatory CD4+ T cells in patients with Wegener's granulomatosis in remission. *Arthritis and rheumatism* **56**, 2080-2091 (2007).

104. M. D. Morgan *et al.*, Patients with Wegener's granulomatosis demonstrate a relative deficiency and functional impairment of T-regulatory cells. *Immunology* **130**, 64-73 (2010).

105. M. E. Free *et al.*, Patients with antineutrophil cytoplasmic antibody-associated vasculitis have defective Treg cell function exacerbated by the presence of a suppression-resistant effector cell population. *Arthritis and rheumatism* **65**, 1922-1933 (2013).

106. L. Wang, F. S. Wang, M. E. Gershwin, Human autoimmune diseases: a comprehensive update. *Journal of internal medicine* **278**, 369-395 (2015).

107. E. L. Sauer, N. C. Cloake, J. M. Greer, Taming the TCR: antigen-specific immunotherapeutic agents for autoimmune diseases. *International reviews of immunology* **34**, 460-485 (2015).

108. P. Zhang, Q. Lu, Genetic and epigenetic influences on the loss of tolerance in autoimmunity. *Cellular & molecular immunology*, (2018).

109. L. S. Walker, A. K. Abbas, The enemy within: keeping self-reactive T cells at bay in the periphery. *Nature reviews. Immunology* **2**, 11-19 (2002).

110. N. A. Danke, D. M. Koelle, C. Yee, S. Beheray, W. W. Kwok, Autoreactive T cells in healthy individuals. *Journal of immunology (Baltimore, Md. : 1950)* **172**, 5967-5972 (2004).

111. T. Lohmann, R. D. Leslie, M. Londei, T cell clones to epitopes of glutamic acid decarboxylase 65 raised from normal subjects and patients with insulin-dependent diabetes. *Journal of autoimmunity* **9**, 385-389 (1996).

112. G. Semana, R. Gausling, R. A. Jackson, D. A. Hafler, T cell autoreactivity to proinsulin epitopes in diabetic patients and healthy subjects. *Journal of autoimmunity* **12**, 259-267 (1999).

113. C. Bouneaud, P. Kourilsky, P. Bousso, Impact of negative selection on the T cell repertoire reactive to a self-peptide: a large fraction of T cell clones escapes clonal deletion. *Immunity* **13**, 829-840 (2000).

114. X. Clemente-Casares *et al.*, Expanding antigen-specific regulatory networks to treat autoimmunity. *Nature* **530**, 434-440 (2016).

115. P. Y. Gan *et al.*, Myeloperoxidase Peptide-Based Nasal Tolerance in Experimental ANCA-Associated GN. *Journal of the American Society of Nephrology : JASN* **27**, 385-391 (2016).

116. S. Prasad *et al.*, Tolerogenic Ag-PLG nanoparticles induce tregs to suppress activated diabetogenic CD4 and CD8 T cells. *Journal of autoimmunity*, (2017).

117. S. Fourlanos *et al.*, Evidence that nasal insulin induces immune tolerance to insulin in adults with autoimmune diabetes. *Diabetes* **60**, 1237-1245 (2011).

118. C. T. Ellebrecht *et al.*, Reengineering chimeric antigen receptor T cells for targeted therapy of autoimmune disease. *Science (New York, N.Y.)* **353**, 179-184 (2016).

119. P. R. Adair, Y. C. Kim, A. H. Zhang, J. Yoon, D. W. Scott, Human Tregs Made Antigen Specific by Gene Modification: The Power to Treat Autoimmunity and Antidrug Antibodies with Precision. *Frontiers in immunology* **8**, 1117 (2017).

120. N. Giannoukakis, B. Phillips, D. Finegold, J. Harnaha, M. Trucco, Phase I (safety) study of autologous tolerogenic dendritic cells in type 1 diabetic patients. *Diabetes care* **34**, 2026-2032 (2011).

121. H. Benham *et al.*, Citrullinated peptide dendritic cell immunotherapy in HLA risk genotype-positive rheumatoid arthritis patients. *Science translational medicine* **7**, 290ra287 (2015).

122. Y. Cao *et al.*, DRB1*15 allele is a risk factor for PR3-ANCA disease in African Americans. *Journal of the American Society of Nephrology : JASN* **22**, 1161-1167 (2011).

123. T. Stratmann *et al.*, Susceptible MHC alleles, not background genes, select an autoimmune T cell reactivity. *The Journal of clinical investigation* **112**, 902-914 (2003).

124. S. Bjorck, C. Brundin, E. Lorinc, K. F. Lynch, D. Agardh, Screening detects a high proportion of celiac disease in young HLA-genotyped children. *Journal of pediatric gastroenterology and nutrition* **50**, 49-53 (2010).

125. D. L. Morris *et al.*, Unraveling multiple MHC gene associations with systemic lupus erythematosus: model choice indicates a role for HLA alleles and non-HLA genes in Europeans. *American journal of human genetics* **91**, 778-793 (2012).

126. L. A. Fussner *et al.*, Factors Determining the Clinical Utility of Serial Measurements of Antineutrophil Cytoplasmic Antibodies Targeting Proteinase 3. *Arthritis & rheumatology (Hoboken, N.J.)* **68**, 1700-1710 (2016).

127. S. L. Hogan *et al.*, Predictors of relapse and treatment resistance in antineutrophil cytoplasmic antibody-associated small-vessel vasculitis. *Annals of internal medicine* **143**, 621-631 (2005).

128. C. Pagnoux *et al.*, Predictors of treatment resistance and relapse in antineutrophil cytoplasmic antibody-associated small-vessel vasculitis: comparison of two independent cohorts. *Arthritis and rheumatism* **58**, 2908-2918 (2008).

129. R. J. Falk *et al.*, Granulomatosis with polyangiitis (Wegener's): an alternative name for Wegener's granulomatosis. *Annals of the Rheumatic Diseases* **70**, 704-704 (2011).

130. E. C. Hagen, B. Ballieux, L. Van Es, M. Daha, F. Van Der Woude, Antineutrophil cytoplasmic autoantibodies: a review of the antigens involved, the assays, and the clinical and possible pathogenetic consequences. *Blood* **81**, 1996-2002 (1993).

131. R. Luqmani *et al.*, Birmingham vasculitis activity score (BVAS) in system necrotizinig vasculitis. *QJM* **87**, 671-678 (1994).

132. D. Cornec, E. Cornec-Le Gall, F. C. Fervenza, U. Specks, ANCA-associated vasculitis - clinical utility of using ANCA specificity to classify patients. *Nature reviews. Rheumatology* **12**, 570-579 (2016).

133. R. J. Falk, J. C. Jennette, ANCA disease: where is this field heading? *Journal of the American Society of Nephrology : JASN* **21**, 745-752 (2010).

134. R. A. Watts, D. G. Scott, ANCA vasculitis: to lump or split? Why we should study MPA and GPA separately. *Rheumatology (Oxford, England)* **51**, 2115-2117 (2012).

135. W. F. Pendergraft, 3rd *et al.*, Autoimmunity is triggered by cPR-3(105-201), a protein complementary to human autoantigen proteinase-3. *Nature medicine* **10**, 72-79 (2004).

136. S. L. Hogan *et al.*, Association of silica exposure with anti-neutrophil cytoplasmic autoantibody small-vessel vasculitis: a population-based, case-control study. *Clinical journal of the American Society of Nephrology : CJASN* **2**, 290-299 (2007).

137. S. Lionaki *et al.*, Association between thyroid disease and its treatment with ANCA small-vessel vasculitis: a case-control study. *Nephrology, dialysis, transplantation : official publication of the European Dialysis and Transplant Association - European Renal Association* **22**, 3508-3515 (2007).

138. A. D. Salama, M. A. Little, Animal models of antineutrophil cytoplasm antibody-associated vasculitis. *Current opinion in rheumatology* **24**, 1-7 (2012).

139. J. Chang *et al.*, CD8+ T Cells Effect Glomerular Injury in Experimental Anti-Myeloperoxidase GN. *Journal of the American Society of Nephrology : JASN* **28**, 47-55 (2017).

140. A. Shrake, J. A. Rupley, Environment and exposure to solvent of protein atoms. Lysozyme and insulin. *Journal of molecular biology* **79**, 351-371 (1973).

141. J. Sidney *et al.*, Quantitative peptide binding motifs for 19 human and mouse MHC class I molecules derived using positional scanning combinatorial peptide libraries. *Immunome research* **4**, 2 (2008).

142. J. Sidney *et al.*, Majority of peptides binding HLA-A*0201 with high affinity crossreact with other A2-supertype molecules. *Hum Immunol* **62**, 1200-1216 (2001).

143. J. Sidney *et al.*, Measurement of MHC/peptide interactions by gel filtration or monoclonal antibody capture. *Current protocols in immunology / edited by John E. Coligan ... [et al.]* **Chapter 18**, Unit 18 13 (2013).

144. K. Gulukota, J. Sidney, A. Sette, C. DeLisi, Two complementary methods for predicting peptides binding major histocompatibility complex molecules. *Journal of molecular biology* **267**, 1258-1267 (1997).

145. Y. Cheng, W. H. Prusoff, Relationship between the inhibition constant (K1) and the concentration of inhibitor which causes 50 per cent inhibition (I50) of an enzymatic reaction. *Biochemical pharmacology* **22**, 3099-3108 (1973).

146. V. Pedchenko *et al.*, Molecular architecture of the Goodpasture autoantigen in anti-GBM nephritis. *The New England journal of medicine* **363**, 343-354 (2010).

147. G. Gammon, E. Sercarz, How some T cells escape tolerance induction. *Nature* **342**, 183-185 (1989).

148. E. R. Unanue, V. Turk, J. Neefjes, Variations in MHC Class II Antigen Processing and Presentation in Health and Disease. *Annual review of immunology* **34**, 265-297 (2016).

149. S. Weidner, M. Carl, R. Riess, H. D. Rupprecht, Histologic analysis of renal leukocyte infiltration in antineutrophil cytoplasmic antibody-associated vasculitis: importance of monocyte and neutrophil infiltration in tissue damage. *Arthritis and rheumatism* **50**, 3651-3657 (2004).

150. J. S. Sanders, M. G. Huitma, C. G. Kallenberg, C. A. Stegeman, Plasma levels of soluble interleukin 2 receptor, soluble CD30, interleukin 10 and B cell activator of the tumour necrosis factor family during follow-up in vasculitis associated with proteinase 3-antineutrophil cytoplasmic antibodies: associations with disease activity and relapse. *Annals of the rheumatic diseases* **65**, 1484-1489 (2006).

151. W. H. Abdulahad, C. G. Kallenberg, P. C. Limburg, C. A. Stegeman, Urinary CD4+ effector memory T cells reflect renal disease activity in antineutrophil cytoplasmic antibody-associated vasculitis. *Arthritis and rheumatism* **60**, 2830-2838 (2009).

152. M. Yoshida *et al.*, In vitro production of myeloperoxidase anti-neutrophil cytoplasmic antibody and establishment of Th1-type T cell lines from peripheral blood lymphocytes of patients. *Clinical and experimental rheumatology* **23**, 227-230 (2005).

153. J. D. Ooi, A. R. Kitching, S. R. Holdsworth, Review: T helper 17 cells: their role in glomerulonephritis. *Nephrology (Carlton, Vic.)* **15**, 513-521 (2010).

154. C. L. Langrish *et al.*, IL-23 drives a pathogenic T cell population that induces autoimmune inflammation. *The Journal of experimental medicine* **201**, 233-240 (2005).

155. K. Hirota *et al.*, Preferential recruitment of CCR6-expressing Th17 cells to inflamed joints via CCL20 in rheumatoid arthritis and its animal model. *The Journal of experimental medicine* **204**, 2803-2812 (2007).

156. S. Nakae *et al.*, IL-17 production from activated T cells is required for the spontaneous development of destructive arthritis in mice deficient in IL-1 receptor antagonist. *Proceedings of the National Academy of Sciences of the United States of America* **100**, 5986-5990 (2003).

157. D. Yen *et al.*, IL-23 is essential for T cell-mediated colitis and promotes inflammation via IL-17 and IL-6. *The Journal of clinical investigation* **116**, 1310-1316 (2006).

158. T. Korn *et al.*, Myelin-specific regulatory T cells accumulate in the CNS but fail to control autoimmune inflammation. *Nature medicine* **13**, 423-431 (2007).

159. M. Rimbert *et al.*, Decreased numbers of blood dendritic cells and defective function of regulatory T cells in antineutrophil cytoplasmic antibody-associated vasculitis. *PloS one* **6**, e18734 (2011).

160. K. M. Chavele *et al.*, Regulation of myeloperoxidase-specific T cell responses during disease remission in antineutrophil cytoplasmic antibody-associated vasculitis: the role of Treg cells and tryptophan degradation. *Arthritis and rheumatism* **62**, 1539-1548 (2010).

161. S. Tsai, A. Shameli, P. Santamaria, CD8+ T cells in type 1 diabetes. *Advances in immunology* **100**, 79-124 (2008).

162. C. Iking-Konert *et al.*, T lymphocytes in patients with primary vasculitis: expansion of CD8+ T cells with the propensity to activate polymorphonuclear neutrophils. *Rheumatology (Oxford, England)* **47**, 609-616 (2008).

163. K. M. O'Sullivan *et al.*, Renal participation of myeloperoxidase in antineutrophil cytoplasmic antibody (ANCA)-associated glomerulonephritis. *Kidney international* **88**, 1030-1046 (2015).

164. E. F. McKinney *et al.*, A CD8+ T cell transcription signature predicts prognosis in autoimmune disease. *Nature medicine* **16**, 586-591, 581p following 591 (2010).

165. S. Sims, C. Willberg, P. Klenerman, MHC-peptide tetramers for the analysis of antigen-specific T cells. *Expert review of vaccines* **9**, 765-774 (2010).

166. M. J. Stubbington *et al.*, T cell fate and clonality inference from single-cell transcriptomes. *Nature methods* **13**, 329-332 (2016).

167. A. Han, J. Glanville, L. Hansmann, M. M. Davis, Linking T-cell receptor sequence to functional phenotype at the single-cell level. *Nature biotechnology* **32**, 684-692 (2014).

168. Y. F. Fuchs *et al.*, CD8+ T cells specific for the islet autoantigen IGRP are restricted in their T cell receptor chain usage. *Scientific reports* **7**, 44661 (2017).

169. P. L. Klarenbeek *et al.*, Inflamed target tissue provides a specific niche for highly expanded T-cell clones in early human autoimmune disease. *Annals of the rheumatic diseases* **71**, 1088-1093 (2012).

170. K. Golab *et al.*, Utilization of leukapheresis and CD4 positive selection in Treg isolation and the ex-vivo expansion for a clinical application in transplantation and autoimmune disorders. *Oncotarget* **7**, 79474-79484 (2016).

171. E. J. Novak, A. W. Liu, G. T. Nepom, W. W. Kwok, MHC class II tetramers identify peptide-specific human CD4(+) T cells proliferating in response to influenza A antigen. *The Journal of clinical investigation* **104**, R63-67 (1999).

172. B. Vincent *et al.*, iWAS--A novel approach to analyzing Next Generation Sequence data for immunology. *Cellular immunology* **299**, 6-13 (2016).

173. V. Venturi, K. Kedzierska, S. J. Turner, P. C. Doherty, M. P. Davenport, Methods for comparing the diversity of samples of the T cell receptor repertoire. *Journal of immunological methods* **321**, 182-195 (2007).

174. D. A. Bolotin *et al.*, MiXCR: software for comprehensive adaptive immunity profiling. *Nature methods* **12**, 380-381 (2015).

175. M. P. Lefranc *et al.*, IMGT-ONTOLOGY for immunogenetics and immunoinformatics. *In silico biology* **4**, 17-29 (2004).

176. R. C. Team. (R Foundation for Statistical Computing, Vienna, Austria, 2017).

177. F. G. B. Jari Oksanen, Michael Friendly, Roeland Kindt, Pierre Legendre, Dan McGlinn, Peter R. Minchin, R. B. O'Hara, Gavin L. Simpson, Peter Solymos, M. Henry H. Stevens, Eduard Szoecs and Helene Wagner. (2017).

178. M. Shugay *et al.*, VDJtools: Unifying Post-analysis of T Cell Receptor Repertoires. *PLoS computational biology* **11**, e1004503 (2015).

179. Y. Klipper-Aurbach *et al.*, Mathematical formulae for the prediction of the residual beta cell function during the first two years of disease in children and adolescents with insulin-dependent diabetes mellitus. *Medical hypotheses* **45**, 486-490 (1995).

180. H. S. Horn, Measurement of "Overlap" in Comparative Ecological Studies. *The American Naturalist* **100**, 419-424 (1966).

181. H. Wickham, *ggplot2: Elegant Graphics for Data Analysis*. (Springer-Verlag, New York, 2009).

182. C. Meydan, H. H. Otu, O. U. Sezerman, Prediction of peptides binding to MHC class I and II alleles by temporal motif mining. *BMC bioinformatics* **14 Suppl 2**, S13 (2013).

183. E. K. Chan, E. M. Tan, Human autoantibody-reactive epitopes of SS-B/La are highly conserved in comparison with epitopes recognized by murine monoclonal antibodies. *The Journal of experimental medicine* **166**, 1627-1640 (1987).

184. E. M. Tan, E. K. Chan, K. F. Sullivan, R. L. Rubin, Antinuclear antibodies (ANAs): diagnostically specific immune markers and clues toward the understanding of systemic autoimmunity. *Clinical immunology and immunopathology* **47**, 121-141 (1988).

185. M. Terajima, J. A. Babon, M. D. Co, F. A. Ennis, Cross-reactive human B cell and T cell epitopes between influenza A and B viruses. *Virology journal* **10**, 244 (2013).

186. M. Lehtinen, M. H. Hibma, G. Stellato, T. Kuoppala, J. Paavonen, Human T helper cell epitopes overlap B cell and putative cytotoxic T cell epitopes in the E2 protein of human papillomavirus type 16. *Biochemical and biophysical research communications* **209**, 541-546 (1995).

187. T. Sakurai *et al.*, Cryptic B cell determinant in a short peptide: T cells do not induce antibody response of B cells when their determinants entirely overlap each other. *International immunology* **5**, 793-800 (1993).

188. L. Bird, T cells: Seq-ing out the 'bad' guys. *Nature reviews. Immunology* **16**, 3 (2016).